CONTROL OF QUANTUM PHENOMENA

CONSTANTIN BRIF,[1] RAJ CHAKRABARTI,[2] and HERSCHEL RABITZ[1]

[1]*Department of Chemistry, Princeton University, Princeton, NJ 08544, USA*
[2]*School of Chemical Engineering, Purdue University, West Lafayette, IN 47907, USA*

CONTENTS

Advances in Chemical Physics, Volume 148, First Edition. Edited by Stuart A. Rice and Aaron R. Dinner.

I. INTRODUCTION

During the past two decades, considerable effort has been devoted to the control of physical and chemical phenomena at the atomic and molecular scale governed by the laws of quantum mechanics [1–11]. Quantum control offers the ability to not just observe but also actively manipulate the course of processes on this scale, thereby providing hitherto unattainable means to explore quantum dynamics and opening the way for a multitude of practical applications [8, 9, 12–23]. Owing to the tremendous growth of research in this area, it would be impossible to cover in one chapter all the advances. Therefore, this chapter is not intended to be a complete review of quantum control, but rather will focus on a number of important topics, including controllability of quantum systems, quantum optimal control theory (QOCT), adaptive feedback control (AFC) of quantum phenomena in the laboratory, and the theory of quantum control landscapes (QCLs).

The origins of quantum control can be traced back to early attempts at the use of lasers for the selective breaking of bonds in molecules. The concept was based on the application of monochromatic laser radiation tuned to the particular vibrational frequency that would excite and, ultimately, break the targeted chemical bond. However, numerous attempts to implement this strategy [24–26] were largely unsuccessful due to intramolecular vibrational redistribution of the deposited energy that rapidly dissipated the initial local excitation and thus generally prevented selective bond breaking [27–29].

Important advances toward selective quantum control of chemical and physical processes were made in the late 1980s, when the role of quantum interference in optical control of molecular systems was identified [30–40]. In particular, Brumer and Shapiro [30–33] proposed to use two monochromatic laser beams with commensurate frequencies and tunable intensities and phases for creating

quantum interference between two reaction pathways. In this approach, control over branching ratios of molecular reactions, in principle, can be achieved by tuning the phase difference between the two laser fields [41–43]. The method of coherent control via two-pathway quantum interference was experimentally demonstrated in a number of applications in atomic, molecular, and semiconductor systems [44–59]. Although the practical effectiveness of this method is limited (by a number of factors including the problem of identifying two particular pathways among a dense set of other transitions, the difficulty of matching excitation rates along the two pathways, and undesirable phase and amplitude locking of the two laser fields in optically dense media [60]), the concept of control via two-pathway quantum interference has played an important role in the historical development of the field [1, 6, 61, 62].

Another important step toward selective control of intramolecular reactions was made by Tannor, Kosloff, and Rice [34, 35], who proposed the method of pump–dump control, based on the use of two successive femtosecond laser pulses with a tunable time delay between them. In this approach, a vibrational wave packet generated by the first laser pulse (the "pump") evolves on the potential energy surface (PES) of an excited electronic state of the molecule until the second laser pulse (the "dump") transfers the population back to the ground-state PES into the desired product channel. Product selectivity can be achieved by using the time delay between the two pulses to control the location at which the wave packet is dumped to the ground-state PES [3, 5]. The pump–dump control method was applied in a number of experiments [63–67]. A useful feature of pump–dump control experiments is the possibility of qualitatively interpreting the control mechanism by developing a simple and intuitive picture of the system dynamics in the time domain. Moreover, the pump–dump scheme also can be used as a time-resolved spectroscopy technique to explore transient molecular states and thus obtain information about the molecular dynamics at various stages of a reaction [68–75]. While the employment of transform-limited laser pulses in the pump–dump method can be satisfactory for some applications [3, 5, 14], the effectiveness of this technique as a practical control tool can be immensely increased by optimally shaping one or both the pulses.

There also exist other control methods employing pairs of time-delayed laser pulses; however, in contrast to pump–dump control, the goal of these methods is primarily to transfer population between discrete quantum states in atoms and molecules. In one approach, known as stimulated Raman adiabatic passage (STIRAP), two time-delayed laser pulses (typically, of nanosecond duration) are applied to a three-level Λ-type configuration to achieve complete population transfer between the two lower levels via the intermediate upper level [76–83]. The laser-induced coherence between the quantum states is controlled by tuning the time delay, in order to keep the transient population in the intermediate state almost at zero (thus avoiding losses by radiative decay). The applicability of the STIRAP

method is limited to control of population transfer between a few discrete states as arise in atoms and small diatomic and triatomic molecules; in larger polyatomic molecules, adiabatic passage is generally prevented by the very high density of levels [82, 83]. In another method, referred to as wave packet interferometry (WPI) [20], population transfer between bound states in atoms, molecules, and quantum dots is controlled by employing quantum interference of coherent wave packets excited by two laser pulses with a tunable time delay between them [84–96].

The possibility of significantly improving control capabilities by using specially shaped ultrafast laser pulses to produce desired quantum interference patterns in the controlled system was proposed in the late 1980s [36–40]. Independently, significant advances have been made in the technology of femtosecond laser pulse shaping [97–99]. In first applications of pulse shaping to optical control of quantum phenomena, only the linear chirp[1] was tuned. Linearly chirped ultrashort laser pulses were employed for control of various processes in atoms and molecules [100–122]. In particular, when applied to molecules with overlapping emission and absorption bands, pulses with negative and positive chirp excite vibrational modes predominately in the ground and excited electronic states, respectively (this effect was utilized for state-selective control of vibrational wave packets [100, 104–106]). Another useful property is the ability of negatively and positively chirped pulses to increase and decrease, respectively, the localization of optically excited vibrational wave packets in diatomic molecules [101–103] (the localization effect of negatively chirped pulses was employed to enhance selectivity in pump–dump control of photodissociation reactions [103] and protect vibrational wave packets against rotationally induced decoherence [123]).

The control approaches discussed above share the same fundamental mechanism based on quantum interference induced by laser fields in the controlled system. However, another common feature of these methods is the reliance on just one control parameter (e.g., the phase difference between two monochromatic laser fields, the time delay between two laser pulses, or the linear chirp rate), which is only a nascent step toward the full exploitation of control field resources for controlling quantum phenomena. While single-parameter control may be effective in some simple circumstances, more flexible and capable control resources are required for more complex systems and applications. The concept of control with specially tailored ultrafast laser pulses has unified and generalized the single-parameter control schemes. Rabitz and coworkers [36–38] and others [39, 40] proposed to steer quantum evolution toward a desired target by specifically designing and tailoring the time-dependent electric field of the laser pulse to the characteristics of the system and the control objective. In particular, QOCT

[1] The linear chirp represents an increase or decrease of the instantaneous frequency $\omega(t)$ as a function of time t under the pulse envelope: $\omega(t) = \omega_0 + 2bt$, where ω_0 is the carrier frequency and b is the chirp parameter that can be negative or positive.

[36–40, 124–129] has emerged as the leading theoretical tool to design and explore laser pulse shapes that are best suited for achieving the desired goal (see, for example, Refs. [3, 5, 11, 130, 131] for earlier reviews). An optimally shaped laser pulse typically has a complex form, in both time and frequency domains, in keeping with the rich dynamical capabilities of strongly coupled multiparticle quantum systems. In this fashion, the phases and amplitudes of the available spectral components of the field are optimized to excite an interference pattern among multiple quantum pathways to best achieve the control objective.

The fruitful synergistic influence of theoretical and experimental advances has played a central role in the development of the quantum control field. A combination of the conceptual insights described above and breakthroughs in ultrafast laser technology ultimately resulted in the establishment of the AFC laboratory procedure proposed by Judson and Rabitz [132]. AFC has proved to be the most effective and flexible practical tool for the vast majority of quantum control applications [4, 7–9, 12, 13, 19, 133–138]. In AFC experiments, femtosecond pulse-shaping technology is utilized to the fullest extent, guided by measurement-driven, closed-loop optimization to identify laser pulses that are optimally tailored to meet the needs of complex quantum dynamical objectives. Optimization in AFC uses a learning algorithm, with stochastic methods (e.g., genetic algorithms and evolutionary strategies) being especially effective due to their inherent robustness to noise and to operational uncertainties [4, 139, 140]. A sizeable body of experimental research has demonstrated the capability of AFC to manipulate the dynamics of a broad variety of quantum systems and explore the underlying physical mechanisms [8, 9]. Owing to modeling limitations, QOCT-based control designs are typically less effective in practice than solutions optimized via AFC directly in the laboratory for the actual quantum system. However, theoretical studies employing QOCT and other similar methods are extremely valuable for analyzing the feasibility of controlling new classes of quantum phenomena and providing a basic understanding of controlled quantum dynamics [141].

Theoretical research in the field of quantum control involves the exploration of several fundamental issues with important practical implications. One such issue is controllability that addresses the question whether a control field, in principle, exists that can drive the quantum system to the target goal [10, 134, 142, 143]. A related but distinct issue is concerned with the existence and multiplicity of optimal controls, that is, solutions that maximize the chosen objective functional [144, 145]. More generally, the objective as a function of the control variables forms the QCL [146, 147], and exploration of its entire structure is of fundamental importance. The study of QCL topology builds on controllability results. In turn, the characterization of the critical points[2] of the QCL forms a foundation for

[2] A critical point is a location on the landscape at which the gradient of the objective with respect to the control field is zero.

analyzing the complexity of finding optimal control solutions [148–151]. This theoretical analysis has direct practical implications as its results provide a basis to determine the ease of finding effective and robust controls in the laboratory [148] and can help identify the most suitable optimization algorithms for various applications of quantum control [152, 153].

This chapter is organized as follows. Controlled quantum dynamics is described in Section II, including a review of the basic notions of quantum theory needed for the remaining presentation. Controllability of closed and open quantum systems is discussed in Section III. QOCT is presented in Section IV, including the mathematical formalism of objective functionals and methods employed to find optimal control solutions, as well as a survey of applications. In section V, numerous laboratory implementations of AFC of quantum phenomena are reviewed. Section VI discusses the relationship of QOCT and AFC, along with the role of theoretical control designs in experimental realizations. Section VII is devoted to the theory of QCLs, including such topics as the characterization of critical points that determine the QCL topology, conditions of control optimality, Pareto optimality for multiobjective control, methods of homotopy trajectory control, and the practical implications of QCL analysis. A summary of this chapter is presented in Section VIII.

II. CONTROLLED QUANTUM DYNAMICS

In this section, we present basic results from quantum theory that are needed to describe the dynamics of closed and open quantum systems under the influence of external time-dependent controls. Coherent control of quantum phenomena involves the application of classical fields (e.g., laser pulses) to quantum systems (e.g., atoms, molecules, quantum dots, etc.). Consider first a coherently controlled closed quantum system (i.e., a system isolated from the environment during the control process) whose evolution is governed by the time-dependent Hamiltonian of the form

$$H(t) = H_0 + H_c(t) \tag{1}$$

Here, H_0 is the free Hamiltonian of the system and $H_c(t)$ is the control Hamiltonian (at time t) that represents the interaction of the system with the external field. In the mathematically oriented literature, the control Hamiltonian is usually formally written as $H_c(t) = \sum_m c_m(t) H_m$, where $\{c_m(t)\}$ are real-valued control functions at time t and $\{H_m\}$ are Hermitian operators through which the controls couple to the system. In physical and chemical applications, the control Hamiltonian is often given by

$$H_c(t) = -\varepsilon(t)\mu \tag{2}$$

where μ is the dipole operator and $\varepsilon(t)$ is the control field at time t. The Hamiltonian of the form given in Eq. (2) adequately describes the interaction of an atomic or molecular system with a laser electric field in the dipole approximation or the interaction of a spin system with a time-dependent magnetic field. However, other forms for $H_c(t)$ can arise including those nonlinear in $\varepsilon(t)$. For the control fields, we will use the notation $\varepsilon(\cdot) \in \mathbb{K}$ and $c_m(\cdot) \in \mathbb{K}$, where $\mathbb{K}$ is the space of locally bounded, sufficiently smooth, square integrable functions of time defined on some interval $[0, T]$, with T being the target time for achieving the desired control outcome.

The Hilbert space $\mathcal{H}$ of a quantum system is spanned by the eigenstates of the free Hamiltonian H_0. Let $\mathcal{T}(\mathcal{H})$ be the space of trace class operators on $\mathcal{H}$. For example, for an N-level quantum system, $\mathcal{H} = \mathbb{C}^N$ is the space of complex vectors of length N and $\mathcal{T}(\mathcal{H}) = \mathcal{M}_N$ is the space of $N \times N$ complex matrices. The set of admissible states of a quantum system, which are represented by density matrices on the Hilbert space $\mathcal{H}$, is denoted as $\mathcal{D}(\mathcal{H})$. Any density matrix $\rho \in \mathcal{D}(\mathcal{H})$ is a positive operator of trace one, that is, $\rho \geq 0$ and $\mathrm{Tr}(\rho) = 1$ (thus, $\mathcal{D}(\mathcal{H}) \subset \mathcal{T}(\mathcal{H})$). The density matrix of a pure state satisfies $\mathrm{Tr}(\rho^2) = 1$ and can be expressed as $\rho = |\psi\rangle\langle\psi|$, where $|\psi\rangle$ is a normalized complex vector in $\mathcal{H}$. Any quantum state that is not pure can be represented as a statistical mixture of pure states and therefore is called mixed; the density matrix of a mixed state satisfies $\mathrm{Tr}(\rho^2) < 1$.

The time evolution of a closed quantum system from $t = 0$ to t is given in the Schrödinger picture by

$$\rho(t) = U(t)\rho_0 U^\dagger(t) \tag{3}$$

where $\rho(t)$ is the density matrix of the system at time t, $\rho_0 = \rho(0)$ is the initial state, and $U(t)$ is the system's unitary evolution operator (for an N-level quantum system, $U(t)$ is an $N \times N$ unitary matrix). If the state is initially pure: $\rho_0 = |\psi_0\rangle\langle\psi_0|$, it will always remain pure under unitary evolution: $\rho(t) = |\psi(t)\rangle\langle\psi(t)|$, where

$$|\psi(t)\rangle = U(t)|\psi_0\rangle \tag{4}$$

The evolution operator satisfies the Schrödinger equation:

$$\frac{d}{dt}U(t) = -\frac{i}{\hbar}H(t)U(t), \quad U(0) = I \tag{5}$$

where I is the identity operator on $\mathcal{H}$. The corresponding evolution equation for the density matrix (called the von Neumann equation) is

$$\frac{d}{dt}\rho(t) = -\frac{i}{\hbar}[H(t), \rho(t)], \quad \rho(0) = \rho_0 \tag{6}$$

and the Schrödinger equation for a pure state is

$$\frac{d}{dt}|\psi(t)\rangle = -\frac{i}{\hbar}H(t)|\psi(t)\rangle, \quad |\psi(0)\rangle = |\psi_0\rangle \tag{7}$$

In practice, it is often necessary to take into account interactions between quantum systems (e.g., between molecules in a liquid or between electron spins and nuclear spins in a semiconductor material). If for a particular problem only one of the interacting subsystems is of interest (now referred to as the system), all other subsystems that surround it are collectively referred to as the environment. A quantum system coupled to an environment is called open [154]. A molecule in a solution or an atom coupled to the vacuum electromagnetic field are examples of open quantum systems. The interaction with the environment typically results in a process of decoherence, in which a coherent superposition state of an open quantum system is transformed into a statistical mixture (decoherence is often accompanied by dissipation of the initial excitation, although in some situations pure dephasing is possible; see Refs. [154, 155] for details). Generally, all quantum systems are open; however, whether environmentally induced processes are important depends on their rate relative to the rate of the coherent evolution. From a practical perspective, the importance of decoherence also depends on the control objective. In chemical applications such as control over the yield of a reaction product, environmental effects may play a significant role in the liquid phase where relaxation processes happen on the timescale of the order of one picosecond [8, 9, 156, 157]. On the other hand, decoherence induced by collisions in the gas phase can often be neglected (at least at low pressures), as the time between collisions is much longer than the characteristic period of vibronic dynamics controlled by femtosecond laser pulses [8]. In contrast, in quantum information processing, an unprecedented level of control accuracy is required to minimize quantum gate errors, and therefore decoherence needs to be taken into account for practically all physical realizations [158].

The state of an open quantum system is described by the reduced density matrix $\rho = \mathrm{Tr}_{\mathrm{env}}(\rho_{\mathrm{tot}})$, where ρ_{tot} represents the state of the system and environment taken together, and $\mathrm{Tr}_{\mathrm{env}}$ denotes the trace over the environment degrees of freedom. There are many models of open-system dynamics depending on the type of environment and character of the system–environment coupling [154, 155]. If the system and environment are initially uncoupled, $\rho_{\mathrm{tot}}(0) = \rho(0) \otimes \rho_{\mathrm{env}}$, then the evolution of the system's reduced density matrix from $t = 0$ to t is described by a completely positive, trace-preserving map Φ_t:

$$\rho(t) = \Phi_t \rho_0 \tag{8}$$

where $\rho_0 = \rho(0)$. A linear map $\Phi : \mathcal{T}(\mathcal{H}) \to \mathcal{T}(\mathcal{H})$ is called completely positive if the map $\Phi \otimes I_l : \mathcal{T}(\mathcal{H}) \otimes \mathcal{M}_l \to \mathcal{T}(\mathcal{H}) \otimes \mathcal{M}_l$ (where I_l is the identity map in $\mathcal{M}_l$)

is positive for any $l \in \mathbb{N}$. A map Φ is called trace preserving if $\mathrm{Tr}(\Phi\rho) = \mathrm{Tr}(\rho)$ for any $\rho \in \mathcal{T}(\mathcal{H})$. The map (8) can be defined for any time $t \geq 0$, and the entire time evolution of the open quantum system is described by a one-parameter family $\{\Phi_t \mid t \geq 0\}$ of dynamical maps (where Φ_0 is the identity map I).

Any completely positive, trace-preserving map has the Kraus operator-sum representation (OSR) [159–161]:

$$\rho(t) = \Phi_t \rho_0 = \sum_{j=1}^{n} K_j(t) \rho_0 K_j^{\dagger}(t) \tag{9}$$

where $\{K_j\}$ are the Kraus operators ($N \times N$ complex matrices for an N-level quantum system). The trace preservation is ensured by the condition

$$\sum_{j=1}^{n} K_j^{\dagger}(t) K_j(t) = I \tag{10}$$

Here, $n \in \mathbb{N}$ is the number of Kraus operators. We will refer to completely positive, trace-preserving maps simply as Kraus maps. Unitary transformations form a particular subset of Kraus maps corresponding to $n = 1$. There exist infinitely many OSRs (with different sets of Kraus operators) for the same Kraus map. For any Kraus map for an N-level quantum system, there always exists an OSR with a set of $n \leq N^2$ Kraus operators [161].

While the Kraus-map description of open-system dynamics is very general, it is often not the most convenient one for numerical calculations. With additional assumptions, various types of quantum master equations can be derived from the Kraus OSR [154, 155]. In particular, for a Markovian environment (i.e., when the memory time for the environment is zero), the set of Kraus maps $\{\Phi_t \mid t \geq 0\}$ is a semigroup, which means that any two maps in the set satisfy the condition [154]

$$\Phi_{t_1} \Phi_{t_2} = \Phi_{t_1 + t_2}, \quad t_1, t_2 \geq 0 \tag{11}$$

In this situation, the dynamics of an open quantum system is described by the quantum master equation of the form [154]

$$\frac{d}{dt}\rho(t) = -i\mathcal{L}\rho(t) \tag{12}$$

where the linear map $\mathcal{L}$ (also referred to as the Liouville superoperator) is the generator of the dynamical semigroup, that is, $\Phi_t = \exp(-i\mathcal{L}t)$. The evolution equation of the form (12) is often referred to as the Liouville–von Neumann equation. For an N-level quantum system coupled to a Markovian environment, the most general form of the map $\mathcal{L}$ can be constructed, resulting in the quantum master equation

of the Lindblad type [154, 155, 162]:

$$\frac{d}{dt}\rho(t) = -\frac{i}{\hbar}[H(t), \rho(t)] + \sum_{i=1}^{N^2-1} \gamma_i \left[L_i \rho(t) L_i^\dagger - \frac{1}{2} L_i^\dagger L_i \rho(t) - \frac{1}{2} \rho(t) L_i^\dagger L_i \right] \tag{13}$$

Here, $\{\gamma_i\}$ are nonnegative constants and $\{L_i\}$ are the Lindblad operators ($N \times N$ complex matrices) that form (together with the identity operator) an orthonormal operator basis on $\mathcal{H}$. By convention, $\{L_i\}$ are traceless. The first term in Eq. (13) represents the unitary part of the dynamics governed by the Hamiltonian H and the second (Lindblad) term represents the nonunitary effect of coupling to the environment. The constants $\{\gamma_i\}$ are given in terms of certain correlation functions of the environment and play the role of relaxation rates for different decay modes of the open system [154].

III. CONTROLLABILITY OF QUANTUM SYSTEMS

Before considering the design of a control or a control experiment, a basic issue to address is whether in principle a control exists to meet the desired objective. Assessing the system's controllability is an important issue from both fundamental and practical perspectives. A quantum system is called controllable in a set of configurations, $\mathcal{S} = \{\zeta\}$, if for any pair of configurations $\zeta_1 \in \mathcal{S}$ and $\zeta_2 \in \mathcal{S}$ there exists a control that can drive the system from the initial configuration ζ_1 to the final configuration ζ_2 in a finite time T.[3] Here, possible types of the configuration ζ include the system's state ρ, the expectation value $\mathrm{Tr}(\rho\Theta)$ of an observable (a Hermitian operator) Θ, the evolution operator U, and the Kraus map Φ, with the particular choice depending on the specific control problem.

First, consider the well-studied issue of controllability of closed quantum systems with unitary dynamics [142, 143, 163–179]. A closed quantum system is called kinematically controllable in a set $\mathcal{S}_\mathrm{K}$ of states if for any pair of states $\rho_1 \in \mathcal{S}_\mathrm{K}$ and $\rho_2 \in \mathcal{S}_\mathrm{K}$, there exists a unitary operator U, such that $\rho_2 = U\rho_1 U^\dagger$. Any two quantum states that belong to the same kinematically controllable set $\mathcal{S}_\mathrm{K}$ are called kinematically equivalent. As unitary evolution preserves the spectrum of a density matrix, two states ρ_1 and ρ_2 of a closed quantum system are kinematically equivalent if and only if they have the same eigenvalues [171, 172]. Therefore, all quantum states that belong to the same kinematically controllable set have the same density-matrix eigenvalues (and, correspondingly, the same von Neumann

[3] More generally, the definition of controllability can be extended by considering the asymptotic evolution in the limit $T \to \infty$. For the sake of simplicity, we will consider here only finite-time controllability.

entropy and purity [158]). For example, all pure states belong to the same kinematically controllable set. However, any pure state is not kinematically equivalent to any mixed state. For a closed quantum system, all states on the system's Hilbert space are separated into disconnected sets of kinematically equivalent states.

It is also possible to consider controllability in the dynamic picture. Assume that the Hamiltonian $H(t)$ that governs the dynamics of a closed quantum system through the Schrödinger equation (5) is a function of a set of time-dependent controls: $H(t) = H(c_1(t), \ldots, c_k(t))$. A closed quantum system is called dynamically controllable in a set $\mathcal{S}_{\mathrm{D}}$ of states if for any pair of states $\rho_1 \in \mathcal{S}_{\mathrm{D}}$ and $\rho_2 \in \mathcal{S}_{\mathrm{D}}$ there exist a finite time T and a set of controls $\{c_1(\cdot), \ldots, c_k(\cdot)\}$, such that the solution $U(T)$ of the Schrödinger equation (5) transforms ρ_1 into ρ_2: $\rho_2 = U(T)\rho_1 U^{\dagger}(T)$. Since a closed system is controllable only within a set of kinematically equivalent states, a dynamically controllable set of states $\mathcal{S}_{\mathrm{D}}$ is always a subset of the corresponding kinematically controllable set $\mathcal{S}_{\mathrm{K}}$. If the dynamically controllable set of pure states coincides with its kinematically controllable counterpart (i.e., the set of all pure states), the closed quantum system is called pure-state controllable. If for any pair of kinematically equivalent states ρ_1 and ρ_2 there exists a set of controls that drives ρ_1 into ρ_2 in finite time (i.e., if all dynamically controllable sets of states coincide with their kinematically controllable counterparts), the closed system is called density-matrix controllable.

It is also possible to consider controllability of closed quantum systems in the set of unitary evolution operators. A closed quantum system is called evolution-operator controllable if for any unitary operator W there exists a finite time T and a set of controls $\{c_1(\cdot), \ldots, c_k(\cdot)\}$, such that $W = U(T)$, where $U(T)$ is the solution of the Schrödinger equation (5) with $H(t) = H(c_1(t), \ldots, c_k(t))$. For an N-level closed quantum system, a necessary and sufficient condition for evolution-operator controllability is [143, 171–173] that the dynamical Lie group $\mathfrak{G}$ of the system (i.e., the Lie group generated by the system's Hamiltonian) be $\mathrm{U}(N)$ [or $\mathrm{SU}(N)$ for a traceless Hamiltonian]. It was also shown [171–173] that density-matrix controllability is equivalent to evolution-operator controllability. For specific classes of states, the requirements for controllability are weaker [165–167]. For example, pure-state controllability requires that the system's dynamical Lie group $\mathfrak{G}$ is transitive on the sphere $\mathbb{S}^{2N-1}$. For infinite-level quantum systems evolving on noncompact Lie groups, such as those arising in quantum optics, the conditions for controllability are more stringent [179, 180].

Controllability analysis was also extended to open quantum systems [181–188]. An open quantum system with Kraus-map evolution of the form (9) is called kinematically controllable in a set $\mathcal{S}_{\mathrm{K}}$ of states if for any pair of states $\rho_1 \in \mathcal{S}_{\mathrm{K}}$ and $\rho_2 \in \mathcal{S}_{\mathrm{K}}$ there exists a Kraus map Φ, such that $\rho_2 = \Phi\rho_1$. It was recently proved [186] that for a finite-level open quantum system with Kraus-map evolution, kinematic state controllability is complete, that is, the system is kinematically controllable in the set $\mathcal{S}_{\mathrm{K}} = \mathcal{D}(\mathcal{H})$ of all states ρ on the Hilbert space.

Moreover, for any target state $\rho_{\rm f}$ on the Hilbert space $\mathcal{H}$ of a finite-level open system, there exists a Kraus map Φ such that $\Phi\rho = \rho_{\rm f}$ for all states ρ on $\mathcal{H}$ [186].

The issue of dynamic state controllability of open quantum systems is yet to be fully explored. To analyze this problem, first it is necessary to specify dynamic capabilities, that is, the set of available controls. While unitary evolution of a closed quantum system can be induced only by coherent controls, Kraus-map evolution of an open system can involve both coherent and incoherent controls (the former act only through the Hamiltonian part of the dynamics, while the latter include interactions with other quantum systems and measurements). Let $\mathcal{C}$ be the set of all available finite-time controls, which may include coherent electromagnetic fields, an environment with a tunable distribution function [189], coupling to an auxiliary system [190–197], measurements [181, 198–203], and so on. Each particular set of controls, $\xi \in \mathcal{C}$, induces the corresponding time evolution of the system through the Kraus map $\Phi_{\xi,t}$ that transforms an initial state ρ_0 into the state $\rho(t) = \Phi_{\xi,t}\rho_0$ at time t. An open quantum system with Kraus-map evolution is called dynamically controllable in the set $\mathcal{S}_{\rm D}$ of states if for any pair of states $\rho_1 \in \mathcal{S}_{\rm D}$ and $\rho_2 \in \mathcal{S}_{\rm D}$, there exists a set of controls $\xi \in \mathcal{C}$ and a finite time T, such that the resulting Kraus map $\Phi_{\xi,T}$ transforms ρ_1 into ρ_2: $\rho_2 = \Phi_{\xi,T}\rho_1$. An open quantum system is called Kraus-map controllable if the set $\mathcal{C}$ of all available controls can generate any Kraus map Φ from the identity map I. It follows from these definitions and the result on kinematic state controllability described above that Kraus-map controllability is sufficient for an open quantum system to be dynamically controllable in the set $\mathcal{S}_{\rm D} = \mathcal{D}(\mathcal{H})$ of all states ρ on the Hilbert space [186]. In general, complete dynamic state controllability is a weaker property than Kraus-map controllability, since the former can be achieved even if the set of available controls generates only a particular subset of all possible Kraus maps [186].

In principle, there exist various methods to engineer arbitrary finite-time Kraus-map evolutions of open quantum systems. One method relies on the ability to coherently control both the system of interest and an ancilla (an auxiliary quantum system that serves as an effective environment). If a quantum system with Hilbert space dimension $N_{\rm s}$ is coupled to an ancilla with Hilbert space dimension $N_{\rm a}$, such that (1) $N_{\rm a} \geq N_{\rm s}^2$ and (2) the ancilla is initially prepared in a pure state, then evolution-operator controllability of the system and ancilla taken together is sufficient for Kraus-map controllability (and thus for complete dynamic state controllability) of the system [186]. Another method of Kraus-map engineering employs a combination of a measurement and a coherent control action in a feedback setup. Specifically, the ability to perform a single simple measurement on a quantum system, together with the ability to apply coherent control conditioned upon the measurement outcome, allows enacting an arbitrary finite-time Kraus-map evolution and thereby suffices for complete dynamic state controllability [181].

Analyses of controllability in closed and open quantum systems have important implications for the theory of QCLs, which in turn is the basis for understanding the optimization complexity of quantum control simulations and experiments. Specifically, controllability is one of the underlying assumptions required to establish the absence of regular critical points that are local traps in QCLs for several important types of quantum control objectives. This fundamental property of the QCL topology and its practical implications will be discussed in detail in Section VII.

IV. QUANTUM OPTIMAL CONTROL THEORY

In the majority of physical and chemical applications, the most effective way to coherently control complex dynamical processes in quantum systems is via the coordinated interaction between the system and the electromagnetic field whose temporal profile may be continuously altered throughout the control period. For a specified control objective, and with restrictions imposed by many possible constraints, the time-dependent field required to manipulate the system in a desired way can be designed using QOCT [11, 130, 131]. This general formulation encompasses both weak and strong field limits and incorporates as special cases the single-parameter methods such as control via two-pathway quantum interference and pump–dump control.

A. Control Objective Functionals

The formulation of a quantum control problem necessarily includes the definition of a quantitative control objective. Consider a coherently controlled N-level closed quantum system, with the Hamiltonian

$$H(t) = H_0 - \varepsilon(t)\mu \tag{14}$$

and the unitary evolution operator $U(t) \in \mathrm{U}(N)$ that obeys the Schrödinger equation (5). In QOCT, the control objective for such a system can be a functional of the set of evolution operators $U(\cdot) = \{U(t) \mid t \in [0, T]\}$, where T is the target time, as well as of the control fields $\varepsilon(\cdot)$. The general class of control objective functionals (also referred to as cost functionals) can be written as

$$J[U(\cdot), \varepsilon(\cdot)] = F(U(T)) + \int_0^T G(U(t), \varepsilon(t))dt \tag{15}$$

where F is a continuously differentiable function on $\mathrm{U}(N)$, and G is a continuously differentiable function on $\mathrm{U}(N) \times \mathbb{R}$. Usually, the first term in (15) represents the main physical goal, while the second term is used to incorporate various constraints

on the dynamics and control fields. The optimal control problem may be stated as the search for

$$J_{\text{opt}} = \max_{\varepsilon(\cdot)} J[U(\cdot), \varepsilon(\cdot)] \tag{16}$$

subject to the dynamical constraint (5). For the sake of consistency, throughout this chapter we will consider only maximization of cost functionals; any control problem can be easily reformulated from minimization to maximization and vice versa by changing the sign of the functional. The cost functional of the form (15) is said to be of the Bolza type. If only the term $\int_0^T G(U(t), \varepsilon(t))dt$ is present, the cost functional is said to be of the Lagrange type, whereas if only the term $F(U(T))$ is present, the functional is said to be of the Mayer type [204]. Three classes of problems corresponding to different choices of $F(U(T))$ have received the most attention in the quantum control community to date: (i) evolution-operator control, (ii) state control, and (iii) observable control.

For evolution-operator control, the goal is to generate $U(T)$ such that it is as close as possible to the target unitary transformation W. The Mayer-type cost functional in this case can be generally expressed as

$$F_1(U(T)) = 1 - \|W - U(T)\| \tag{17}$$

where $\|\cdot\|$ is an appropriate normalized matrix norm; that is, $F_1(U(T))$ is maximized when the distance between $U(T)$ and W is minimized. This type of objective is common in quantum computing applications [158], where $F_1(U(T))$ is the fidelity of a quantum gate [205, 206]. One frequently used form of the objective functional $F_1(U(T))$ is obtained utilizing the squared Hilbert–Schmidt norm [207] in (17) with an appropriate normalization (i.e., $\|X\| = (2N)^{-1}\text{Tr}(X^\dagger X)$) [208–210]:

$$F_1(U(T)) = \frac{1}{N}\text{Re}\left\{\text{Tr}\left[W^\dagger U(T)\right]\right\} \tag{18}$$

Other forms of the objective functional, which employ different matrix norms in (17), are possible as well [210–213]. For example, a modification of (18)

$$F_1(U(T)) = N^{-1}\left|\text{Tr}\left[W^\dagger U(T)\right]\right| \tag{19}$$

which is independent of the global phase of $U(T)$, can be used. Note that $F_1(U(T))$ is independent of the initial state, as the quantum gate must produce the same unitary transformation for any input state of the qubit system [158].

For state control, the goal is to transform the initial state ρ_0 into a final state $\rho(T) = U(T)\rho_0 U^\dagger(T)$ that is as close as possible to the target state ρ_f. The

corresponding Mayer-type cost functional is

$$F_2(U(T)) = 1 - \|U(T)\rho_0 U^\dagger(T) - \rho_f\| \tag{20}$$

where $\|\cdot\|$ is an appropriate normalized matrix norm (e.g., the Hilbert–Schmidt norm can be used) [145, 214–216].

For observable control, the goal is typically to maximize the expectation value of a target quantum observable Θ (represented by a Hermitian operator). The corresponding Mayer-type cost functional is [124, 217–220]

$$F_3(U(T)) = \mathrm{Tr}\left[U(T)\rho_0 U^\dagger(T)\Theta\right] \tag{21}$$

An important special case is state transition control (also known as population transfer control), for which $\rho_0 = |\psi_i\rangle\langle\psi_i|$ and $\Theta = |\psi_f\rangle\langle\psi_f|$, where $|\psi_i\rangle$ and $|\psi_f\rangle$ are eigenstates of the free Hamiltonian H_0. In this case, the objective functional (21) has the form

$$F_3(U(T)) = P_{i\to f} = |\langle\psi_f|U(T)|\psi_i\rangle|^2 \tag{22}$$

which is the probability of transition (i.e., the population transfer yield) between the energy levels of the quantum system [146, 221]. In many chemical and physical applications of quantum control, absolute yields are not known, and therefore maximizing the expectation value of an observable (e.g., the population transfer yield) is a more appropriate laboratory goal than minimizing the distance to a target expectation value.

Also, in quantum control experiments (see Section V), measuring the expectation value of an observable is much easier than estimating the quantum state or evolution operator. Existing methods of quantum state and evolution-operator estimation rely on tomographic techniques [222–229] that are extremely expensive in terms of the number of required measurements (e.g., in quantum computing applications, standard methods of state and process tomography require numbers of measurements that scale exponentially in the number of qubits [158, 229–233]). Therefore, virtually all quantum control experiments so far have used observable control with objective functionals of the form (21) or (22). For example, in an AFC experiment [123], in which the goal was to maximize the degree of coherence, the expectation value of an observable representing the degree of quantum state localization was used as a coherence "surrogate," instead of state purity or von Neumann entropy, which are nonlinear functions of the density matrix and hence would require state estimation. Nevertheless, future laboratory applications of quantum control, in particular in the field of quantum information sciences, will require evolution-operator control and state control, with the use of objective functionals of the types (17) and (20), respectively, together with novel state and process estimation methods [232–241].

Recently, attention has turned to problems requiring simultaneous maximization of several control objectives [242–245]. In the framework of QOCT, these optimization problems are sometimes handled through the use of a weighted-sum objective functional, such as [243, 244]

$$F_4(U(T)) = \sum_i \alpha_i \mathrm{Tr}\left[U(T)\rho_0 U^\dagger(T)\Theta_i\right] \tag{23}$$

which extends (21) to multiple quantum observables. Also, general methods of multiobjective optimization [246–248] have been recently applied to various quantum control problems [244, 245].

Another common goal in quantum control is to maximize a Lagrange-type cost functional subject to a constraint on $U(T)$ [249, 250]. For example, this type of control problem can be formulated as follows:

$$\max_{\varepsilon(\cdot)} \int_0^T G(\varepsilon(t))\, dt, \quad \text{subject to } F(U(T)) = f_0 \tag{24}$$

where $F(U(T))$ is the Mayer-type cost functional for evolution-operator, state, or observable control (as described above), and f_0 is a constant that corresponds to the target value of F. Often, the goal is to minimize the total field fluence, in which case $G(\varepsilon(t)) = -(1/2)\varepsilon^2(t)$ is used.

B. Searching for Optimal Controls

To identify optimal controls that maximize an objective functional J (of the types discussed in Section IV.A), it is convenient to define a functional $\tilde{J}$ that explicitly incorporates the dynamical constraint. For example, many QOCT studies [11, 130, 131] considered pure-state evolution of a closed quantum system, for which the dynamical constraint is satisfaction of Eq. (7). The corresponding objective functional (e.g., for observable control) $\tilde{J} = \tilde{J}[\psi(\cdot), \chi(\cdot), \varepsilon(\cdot)]$ often is taken to have the form

$$\tilde{J} = \langle\psi(T)|\Theta|\psi(T)\rangle - \int_0^T \alpha(t)\varepsilon^2(t)dt - 2\mathrm{Re}\int_0^T \langle\chi(t)|\left[\frac{d}{dt} + \frac{i}{\hbar}H(t)\right]|\psi(t)\rangle dt \tag{25}$$

Here, the first term represents the main control goal of maximizing the expectation value of the target observable Θ at the final time T; the second term is used to restrict the fluence and shape of the control field, with $\alpha(t)$ being a weight function; the third term includes an auxiliary state $|\chi(t)\rangle$ that is a Lagrange multiplier employed to enforce satisfaction of the Schrödinger equation for the pure state [Eq. (7)], and $H(t)$ is the Hamiltonian (14) that includes the time-dependent control term. More generally, satisfaction of the Schrödinger equation for the evolution operator of a closed quantum system [Eq. (5)] can be used as the dynamical

constraint for different types of objectives, including evolution-operator, state, and observable control. The corresponding general form of the objective functional $\tilde{J} = \tilde{J}[U(\cdot), V(\cdot), \varepsilon(\cdot)]$ is

$$\tilde{J} = F(U(T)) + \int_0^T G(\varepsilon(t))dt - 2\mathrm{Re}\int_0^T \mathrm{Tr}\left\{ V^\dagger(t)\left[\frac{d}{dt} + \frac{i}{\hbar}H(t)\right]U(t)\right\} dt \tag{26}$$

Here, an auxiliary operator $V(t)$ is a Lagrange multiplier employed to enforce satisfaction of Eq. (5), and, for the sake of simplicity, we assumed that G depends only on the control field.

QOCT can also be formulated for open systems with nonunitary dynamics [128, 251–258]. For example, for a quantum system coupled to a Markovian environment, the Liouville–von Neumann equation (12) must be satisfied. The corresponding objective functional (e.g., for observable control) $\tilde{J} = \tilde{J}[\rho(\cdot), \sigma(\cdot), \varepsilon(\cdot)]$ has the form

$$\tilde{J} = \mathrm{Tr}\,[\rho(T)\Theta] - \int_0^T \alpha(t)\varepsilon^2(t)dt - \int_0^T \mathrm{Tr}\left\{\sigma^\dagger(t)\left[\frac{d}{dt} + i\mathcal{L}\right]\rho(t)\right\} dt \tag{27}$$

Here, $\mathcal{L}$ is the Liouville superoperator (the generator of the dynamical semigroup), and an auxiliary density matrix $\sigma(t)$ is a Lagrange multiplier employed to enforce satisfaction of Eq. (12). Extensions of QOCT to non-Markovian open-system dynamics were also considered [256, 257, 259, 260].

Various modifications of the objective functionals (25), (26), and (27) are possible. For example, modified objective functionals can comprise additional spectral and fluence constraints on the control field [261, 262], take into account nonlinear interactions with the control field [263, 264], deal with time-dependent and time-averaged targets [258, 265–267], and include the final time as a free control parameter [268, 269]. It is also possible to formulate QOCT with time minimization as a control goal (time optimal control) [270–272]. As mentioned earlier, QOCT can also be extended to incorporate optimization of multiple objectives [242–245].

A necessary condition for a solution of the optimization problem (16) subject to the dynamical constraint (5) is that the first-order functional derivatives of the objective functional $\tilde{J}[U(\cdot), V(\cdot), \varepsilon(\cdot)]$ of Eq. (26) with respect to $V(\cdot)$, $U(\cdot)$, and $\varepsilon(\cdot)$ are equal to zero. The resulting set of Euler–Lagrange equations is given by

$$\frac{d}{dt}U(t) = -\frac{i}{\hbar}H(t)U(t), \quad U(0) = I \tag{28}$$

$$\frac{d}{dt}V(t) = -\frac{i}{\hbar}H(t)V(t), \quad V(T) = \nabla F(U(T)) \tag{29}$$

$$\frac{\partial}{\partial\varepsilon(t)}G(\varepsilon(t)) - \frac{2}{\hbar}\mathrm{Im}\left\{\mathrm{Tr}\left[V^\dagger(t)\mu U(t)\right]\right\} = 0 \tag{30}$$

where $\nabla F(U(T))$ is the gradient of F at $U(T)$ in U(N). Critical points of the objective functional, which include optimal controls, can be obtained by solving this set of equations (various algorithms employed for numerical solution are discussed below). In the special case of the objective functional $\tilde{J}[\psi(\cdot), \chi(\cdot), \varepsilon(\cdot)]$ of Eq. (25), setting the first-order functional derivatives of $\tilde{J}$ with respect to $\chi(\cdot)$, $\psi(\cdot)$, and $\varepsilon(\cdot)$ to zero results in the following Euler–Lagrange equations:

$$\frac{d}{dt}|\psi(t)\rangle = -\frac{i}{\hbar}H(t)|\psi(t)\rangle, \quad |\psi(0)\rangle = |\psi_0\rangle \tag{31}$$

$$\frac{d}{dt}|\chi(t)\rangle = -\frac{i}{\hbar}H(t)|\chi(t)\rangle, \quad |\chi(T)\rangle = \Theta|\psi(T)\rangle \tag{32}$$

$$\varepsilon(t) = -\frac{1}{\hbar\alpha(t)}\mathrm{Im}\left\{\langle\chi(t)|\mu|\psi(t)\rangle\right\} \tag{33}$$

Analogously, in the special case of the objective functional $\tilde{J}[\rho(\cdot), \sigma(\cdot), \varepsilon(\cdot)]$ of Eq. (27), setting the first-order functional derivatives of $\tilde{J}$ with respect to $\sigma(\cdot)$, $\rho(\cdot)$, and $\varepsilon(\cdot)$ to zero results in the following Euler–Lagrange equations:

$$\frac{d}{dt}\rho(t) = -i\mathcal{L}\rho(t), \quad \rho(0) = \rho_0 \tag{34}$$

$$\frac{d}{dt}\sigma(t) = -i\mathcal{L}^{\dagger}\sigma(t), \quad \sigma(T) = \Theta \tag{35}$$

$$\varepsilon(t) = -\frac{1}{\hbar\alpha(t)}\mathrm{Im}\left\{\mathrm{Tr}\left[\sigma^{\dagger}(t)\mu\rho(t)\right]\right\} \tag{36}$$

An equivalent method for deriving optimal control equations is based on applying the Pontryagin maximum principle (PMP) [249, 250, 273]. For a bilinear control system of the form (5) evolving on the unitary group, the PMP function (also referred to as the PMP Hamiltonian) is defined as

$$\begin{aligned}\mathbf{H}[U(t), V(t), \varepsilon(t)] &:= G(\varepsilon(t)) - 2\mathrm{Re}\left[\langle V(t), \frac{i}{\hbar}H(t)U(t)\rangle\right] \\ &= G(\varepsilon(t)) + \frac{2}{\hbar}\mathrm{Im}\left\{\mathrm{Tr}\left[V^{\dagger}(t)H(t)U(t)\right]\right\}\end{aligned} \tag{37}$$

where $\langle A, B\rangle = \mathrm{Tr}(A^{\dagger}B)$ is the Hilbert–Schmidt inner product. According to the PMP, all solutions to the optimization problem (16) satisfy equations

$$\frac{dU(t)}{dt} = \frac{\partial\mathbf{H}}{\partial V(t)}, \quad \frac{dV(t)}{dt} = -\frac{\partial\mathbf{H}}{\partial U(t)}, \quad \frac{\partial\mathbf{H}}{\partial\varepsilon(t)} = 0, \quad \forall t \in [0, T] \tag{38}$$

with the boundary conditions $U(0) = I$, $V(T) = \nabla F(U(T))$. It is easy to see that for the PMP function of the form (37), the conditions (38) produce Eqs. (28)–(30). Satisfaction of the first-order condition $\delta\tilde{J}/\delta\varepsilon(\cdot) = 0$ or, equivalently,

$\partial \mathbf{H}/\partial \varepsilon(t) = 0$ ($\forall t \in [0, T]$) is a necessary but not sufficient condition for optimality of a control $\varepsilon(\cdot)$. So-called Legendre conditions on the Hessian $\partial^2 \mathbf{H}/\partial \varepsilon(t')\partial \varepsilon(t)$ are also required for optimality [204, 273]. The optimality criteria are discussed in Section VII.B.

1. *Existence of Optimal Controls*

An important issue is the existence of optimal control fields (i.e., maxima of the objective functional) for realistic situations that involve practical constraints on the applied laser fields. It is important to distinguish between the existence of an optimal control field and controllability; in the former case, a field is designed, subject to particular constraints, that guides the evolution of the system toward a specified target until a maximum of the objective functional is reached, while in the latter case, the exact coincidence between the attained evolution operator (or state) and the target evolution operator (or state) is sought. The existence of optimal controls for quantum systems was analyzed in a number of studies. Peirce et al. [37] proved the existence of optimal solutions for state control in a spatially bounded quantum system that necessarily has spatially localized states and a discrete spectrum. Zhao and Rice [144] extended this analysis to a system with both discrete and continuous states and proved the existence of optimal controls over the evolution in the subspace of discrete states. Demiralp and Rabitz [145] showed that, in general, there is a denumerable infinity of solutions to a particular class of well-posed quantum control problems; the solutions can be ordered in quality according to the achieved optimal value of the objective functional. The existence of multiple control solutions has important practical consequences, suggesting that there may be broad latitude in the laboratory, even under strict experimental restrictions, for finding successful controls for well-posed quantum objectives. The existence and properties of critical points (including global optima) of objective functionals for various types of quantum control problems were further explored using the analysis of QCLs [146, 208–210, 217–221, 274] (see Section VII).

2. *Algorithms Employed in QOCT Computations*

A number of optimization algorithms have been adapted or specially developed for use in QOCT, including the conjugate gradient search method [39], the Krotov method [206, 275, 276], monotonically convergent algorithms [259, 277–282], noniterative algorithms [283], the gradient ascent pulse engineering (GRAPE) algorithm [284], a hybrid local/global algorithm [258], and homotopy-based methods [285–287]. Faster convergence of iterative QOCT algorithms was demonstrated using "mixing" strategies [288]. Also, the employment of propagation toolkits [289–291] can greatly increase the efficiency of numerical optimizations. Detailed discussions of the QOCT formalism and algorithms are available in the literature [5, 11, 130, 131].

C. Applications of QOCT

Originally, QOCT was developed to design optimal fields for manipulation of molecular systems [36–40, 124–129] and has been applied to a myriad of problems (e.g., rotational, vibrational, electronic, reactive, and other processes) [5, 11, 130]. Some recent applications include, for example, control of molecular isomerization [292–295], control of electron ring currents in chiral aromatic molecules [296], and control of heterogeneous electron transfer from surface attached molecules into semiconductor band states [297]. Beyond molecules, QOCT has been applied to various physical objectives including, for example, control of electron states in semiconductor quantum structures [298–300], control of atom transport in optical lattices [301], control of Bose–Einstein condensate transport in magnetic microtraps [302], control of a transition of ultracold atoms from the superfluid phase to a Mott insulator state [303], control of coherent population transfer in superconducting quantum interference devices [304], and control of the local electromagnetic response of nanostructured materials [305].

In the context of open-system dynamics in the presence of coupling to a Markovian environment, QOCT applications include control of unimolecular dissociation reactions in the collisional regime [128], laser cooling of molecular internal degrees of freedom coupled to a bath [252, 253, 306], control of vibrational wave packets in a model molecular system coupled to an oscillator bath at finite temperatures in the weak-field (perturbative) regime [251, 307], creation of a specified vibronic state, population inversion, wave packet shaping in the presence of dissipation in the strong-field regime [255], control of ultrafast electron transfer in donor–acceptor systems where the reaction coordinate is coupled to a reservoir of other coordinates [308], control of photodesorption of NO molecules from a metal surface in the presence of strong dissipation [309], control of excitation of intramolecular and molecule-surface vibrational modes of CO molecules adsorbed on a metal surface in the presence of dissipation to baths of substrate electrons and phonons [258, 310], and control of current flow patterns through molecular wires coupled to leads [311]. Also, QOCT was actively applied to the problem of protection of open quantum systems against environmentally induced decoherence [216, 257, 312–321].

Recently, there has been rapidly growing interest in applications of QOCT to the field of quantum information sciences. As mentioned above, one of the important problems in this field is optimal protection of quantum systems against decoherence. Applications of QOCT to quantum information processing also include optimal operation of quantum gates in closed systems [180, 205, 206, 250, 322–335] and in open systems (i.e., in the presence of decoherence) [213, 336–351] and optimal generation of entanglement [268, 269, 350, 352–354]. One particular area where QOCT methods have proved to be especially useful is design of optimal sequences of radiofrequency (RF) pulses for operation of quantum gates in

systems of coupled nuclear spins in a nuclear magnetic resonance (NMR) setup [284, 355, 356]. In a recent experiment with trapped-ion qubits, shaped pulses designed using QOCT were applied to enact single-qubit gates with enhanced robustness to noise in the control field [357]. Optimal control methods were also applied to the problem of storage and retrieval of photonic states in atomic media, including both theoretical optimization [358–360] and experimental tests [361–363].

D. Advantages and Limitations of QOCT

An advantage of QOCT relative to the laboratory execution of AFC (to be discussed in detail in Section V) is that the former can be used to optimize a well-defined objective functional of virtually any form, while the latter relies on information obtained from measurements and thus is best suited to optimize expectation values of directly measurable observables. In numerical optimizations, there is practically no difference in effort between computing the expectation value of an observable, the density matrix, or the evolution operator. In the laboratory, however, it is much more difficult to estimate a quantum state or, even more so, the evolution operator than to measure the expectation value of an observable. Moreover, state estimation error increases rapidly with the Hilbert space dimension [225, 364]. The very large number of measurements required for accurate quantum state/process tomography [229–232] renders (at least presently) the use of adaptive laboratory methods for state/evolution-operator control rather impractical.

QOCT is often used to explore new quantum phenomena in relatively simple models to gain physical insights. The realization of quantum control is ultimately performed in the laboratory, and in this context QOCT fits into what is called *open-loop control*. Generally, in open-loop control, a theoretical control design (e.g., obtained by using QOCT or another theoretical method) is implemented in the laboratory with the actual system. Unfortunately, there are not many problems for which theoretical control designs are directly applicable in the laboratory. QOCT is most useful when detailed knowledge of the system's Hamiltonian is available. Moreover, for open quantum systems, it is essential to know the details of the system–environment interaction. Therefore, the practical applicability of QOCT in the context of open-loop control is limited to very simple systems, that is, mostly to cases when a small number of degrees of freedom can be controlled separately from the remainder of the system. This may be possible when the controlled subsystem has characteristic frequencies well separated from those of other transitions and evolves on a timescale that is very different from that of the rest of the larger system. A well-known example of such a separately controllable subsystem is nuclear spins in a molecule, which can be very well controlled using RF fields without disturbing rotational, vibrational, and electronic degrees of freedom. Another example is a subset of several discrete levels in an atom or diatomic

molecule, the transitions between which frequently can be controlled in a very precise way without any significant leakage of population to other states. However, for a majority of interesting physical and chemical phenomena, controlled systems are too complex and too strongly coupled to other degrees of freedom. For such complex systems, the accuracy of control designs obtained using model-based QOCT is usually inadequate, and hence laboratory AFC is generally the preferred strategy. In these situations, QOCT may be more useful for feasibility analysis and exploration of control mechanisms, as basic features of the controlled dynamics possibly can be identified in many cases even using relatively rough models.

V. ADAPTIVE FEEDBACK CONTROL IN THE LABORATORY

Many important aspects of quantum control experiments are not fully reflected in theoretical analyses. In particular, control solutions obtained in theoretical studies strongly depend on the employed model Hamiltonian. However, for real systems controlled in the laboratory, the Hamiltonians usually are not known well (except for the simplest cases), and the Hamiltonians for the system–environment coupling are known to an even lesser degree. An additional difficulty is the computational complexity of accurately solving the optimal control equations for realistic polyatomic molecules. Another important difference between control theory and experiment arises from the difficulty of reliably implementing theoretical control designs in the laboratory owing to instrumental noise and other limitations. As a result, optimal theoretical control designs generally will not be optimal in the laboratory. Notwithstanding these comments, control simulations continue to be very valuable, and they even set forth the logic leading to practical laboratory control as explained below.

A crucial step toward selective laser control of physical and chemical phenomena on the quantum scale was the introduction of AFC (also referred to as closed-loop laboratory control or learning control). AFC was proposed and theoretically grounded by Judson and Rabitz in 1992 [132]. In AFC, a loop is closed in the laboratory (see Fig. 1), with results of measurements on the quantum system used to evaluate the success of the applied control and to refine it, until the control objective is reached as best as possible. At each cycle of the loop, the external control (e.g., a shaped laser pulse) is applied to the system (e.g., an ensemble of molecules). The signal (e.g., the yield of a particular reaction product or population in a target state) is detected and fed back to the learning algorithm (e.g., a genetic algorithm). The algorithm evaluates each control based on its measured outcome with respect to a predefined control goal and searches through the space of available controls to move toward an optimal solution.

While AFC can be simulated on the computer [132, 365–378], the important advantage of this approach lies in its ability to be directly implemented in the

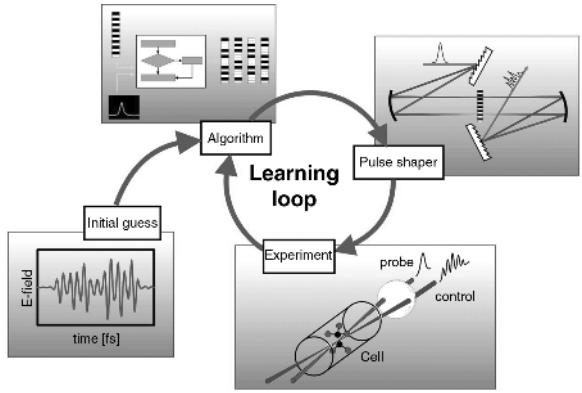

Figure 1. A schematic depiction of a closed-loop process employed in adaptive feedback control (AFC) of quantum phenomena. The input to the loop is an initial control guess which can be a design estimate or even a random field in many cases. A current design of the laser control field is created with a pulse shaper and then applied to the sample. The outcome of the control action is measured, and the results are fed back to a learning algorithm. The algorithm searches through the space of possible controls and suggests an improved field design. Excursions around the loop are repeated until a satisfactory value of the control objective is achieved. Adapted from Ref. [4]. (See the color version of this figure in Color Plates section.)

laboratory. Most important, the optimization is performed in the laboratory with the actual system and thus is independent of any model. As a result, the AFC method works remarkably well for systems even of high complexity, including, for example, large polyatomic molecules in the liquid phase, for which only very rough models are available. Second, there is no need to measure the laser field in AFC because any systematic characterization of the control "knobs" (such as pulse shaper parameters) is sufficient. This set of control "knobs" determined by the experimental apparatus defines the parameter space searched by the learning algorithm for an optimal laser shape. This procedure naturally incorporates any laboratory constraints on the control laser fields. Third, optimal controls identified in AFC are characterized by a natural degree of robustness to instrumental noise, since nonrobust solutions will be rejected by the algorithm. Fourth, in AFC, it is possible to operate at a high-duty cycle of hundreds or even thousands of experiments per second by exploiting (i) the conceptual advantage of the evolving quantum system solving its own Schrödinger equation in the fastest possible fashion and (ii) the technological advantage of high repetition rate pulsed laser systems under full automation. Fifth, in AFC, a new quantum ensemble (e.g., a new molecular sample) is used in each cycle of the loop that completely avoids the issue of back action exerted by the measurement process on a quantum system. Thus, AFC is technologically distinct from measurement-based real-time

feedback control [379–384], in which the same quantum system is manipulated until the final target objective is reached and for which measurement back action is an important effect that needs to be taken into account.

The majority of current AFC experiments employ shaped ultrafast laser pulses. In such experiments, one usually starts with a random or nearly random selection of trial shaped pulses of length $\sim 10^{-13}$ s or less. The pulses are shaped by modulating the phases and amplitudes of the spatially resolved spectral components, for example, by means of a liquid crystal modulator (LCM), an acousto-optic modulator (AOM), or a micromechanical mirror array (MMA). The experiments employ fully automated computer control of the pulse shapes guided by a learning algorithm. The shaped laser pulses produced by this method can be viewed as "photonic reagents," which interact with matter at the atomic or molecular scale to facilitate desired controlled outcomes of various physical and chemical phenomena. Femtosecond pulse-shaping technology has significantly advanced during the last two decades [7, 97–99, 385–407]. Moreover, the AFC approach itself can be used to produce optical fields with prescribed properties [408–421].

A. AFC of Photophysical Processes in Atoms

1. *AFC of Rydberg Wave Packets in Atoms*

In one of the first applications of AFC, in 1999, Bucksbaum and coworkers [422] manipulated the shape of an atomic radial wave function (a so-called Rydberg wave packet). Nonstationary Rydberg wave packets were created by irradiating cesium atoms with shaped ultrafast laser pulses. The atomic radial wave function generated by the laser pulse was reconstructed from state-selective field ionization data using a variation of the quantum holography method [423]. The distance between the measured and the target wave packet provided the feedback signal. In the linear weak-field regime, AFC equipped with a simple gradient-type algorithm was able to change the shape of the Rydberg wave packet to match the target within two iterations of the feedback control loop. If the wave packet is created in the strong-field regime, then a more sophisticated learning algorithm is generally required to implement AFC.

2. *AFC of Multiphoton Transitions in Atoms*

Control of bound-to-bound multiphoton transitions in atoms with optimally shaped femtosecond laser pulses provides a vivid illustration of the control mechanism based on multipathway quantum interference. Nonresonant multiphoton transitions involve many routes through a continuum of virtual levels. The interference pattern excited by the multiple frequency components of the control pulse can enhance or diminish the total transition probability. The interference effect depends on the spectral phase distribution of the laser pulse. A number of experiments

[424–426] used AFC to identify pulse shapes that are optimal for enhancing or canceling the probability of making a transition. Owing to the relative simplicity of the atomic systems studied, it was possible to compare the results of the AFC experiments with theoretical predictions and verify the control mechanism based on quantum interference of multiple laser-driven transition amplitudes. A related experiment [427] demonstrated that AFC-optimized shaped pulses enhance resonant multiphoton transitions significantly beyond the level achieved with transform-limited pulses, although the latter maximize the pulse's peak intensity. Another recent experiment [428] employed AFC to discover strong-field shaped laser pulses that maximize the probability of nonresonant multiphoton absorption in atomic sodium by optimally counteracting the dynamic Stark shift-induced stimulated emission. AFC with shaped femtosecond laser pulses was also applied to optimize multiphoton ionization in calcium and potassium atoms and explore underlying control mechanisms [429, 430].

3. AFC of High-Harmonic Generation

An important physical application of AFC is coherent manipulation of soft X-rays produced via high-harmonic generation (for recent reviews, see Refs. [18, 19]). In a pioneering experiment, Murnane and coworkers [431] used shaped ultrashort intense laser pulses for AFC of high-harmonic generation in atomic gases. Their results demonstrate that optimally shaped laser pulses identified by the learning algorithm can improve the efficiency of X-ray generation by an order of magnitude, manipulate the spectral characteristics of the emitted radiation, and "channel" the interaction between nonlinear processes of different orders. All these effects result from complex interferences between the quantum amplitudes of the atomic states created by the external laser field. The learning algorithm guides the pulse shaper to tailor the laser field to produce the optimal interference pattern. Several consequent AFC experiments explored various aspects of optimal high-harmonic generation in atomic gases [432–434]. Further experimental studies used AFC for optimal spatial control of high-harmonic generation in hollow fibers [435, 436], optimal control of the brilliance of high-harmonic generation in gas jet and capillary setups [437], and optimal control of the spectral shape of coherent soft X-rays [438]. The latter work [438] has been a precursor to a more recent development, in which spectrally shaped femtosecond X-ray fields were themselves used to adaptively control photofragmentation yields of SF_6 [439].

B. AFC of Electronic Excitations in Molecules

The first AFC experiment was reported in 1997 by Wilson and coworkers [440]. Femtosecond laser pulses shaped by a computer-controlled AOM were used to excite an electronic transition in molecules (laser dye IR125 in methanol solution). The measured fluorescence served as the feedback signal in AFC to optimize the

population transfer from the ground to first excited molecular electronic state. Both excitation efficiency (the ratio of the excited state population to the laser energy) and effectiveness (the total excited-state population) were optimized. Similar AFC experiments were later performed with different molecules in the liquid phase [156, 441–451]. In particular, two-photon electronic excitations in flavin mononucleotide (FMN) in aqueous solution were controlled using multiobjective optimization (a genetic algorithm was employed to simultaneously maximize the fluorescence intensity and the ratio of fluorescence and second harmonic generation intensities) [451]. Molecular electronic excitations were also optimized in AFC experiments in the solid state, with a crystal of α-perylene [449, 452].

Since these AFC experiments are performed in the condensed phase, an important issue is the degree of coherence of the controlled dynamics. This issue has been recently explored in a series of AFC experiments [156], in which the level of attained control was investigated by systematically varying properties of the environment. Specifically, AFC was applied to optimize the stimulated emission from coumarin 6 (a laser dye molecule) dissolved in cyclohexane and the recorded optimal pulse shape was used with several other solvents (linear and cyclic alkanes). The results revealed an inverse correlation between the obtained degree of control (as measured by the enhancement of stimulated emission relative to that achieved by excitation with the transform-limited pulse) and the viscosity of the solvent. This study indicates that the control mechanism involves a coherent process (i.e., based on quantum interference of coherent pathways) and that environmentally induced decoherence limits the leverage of control on the particular molecular system. Coherent control mechanisms were also identified in a number of other recent AFC experiments that optimized molecular electronic excitations in the liquid phase [157, 450].

C. AFC of Multiphoton Ionization in Molecules

The use of polarization-shaped femtosecond laser pulses can significantly enhance the level of control over multiphoton ionization in molecules. In 2004, Brixner et al. [453] demonstrated that a suitably polarization-shaped laser pulse increased the photoionization yield in K_2 beyond that obtained with an optimally shaped linearly polarized laser pulse. This effect is explained by the existence of different multiphoton ionization pathways in the molecule involving dipole transitions that are preferably excited by different polarization directions of the laser field. Suzuki et al. [454] applied AFC with polarization-shaped laser pulses to multiphoton ionization of I_2 molecules and optimized the production of oddly and evenly charged molecular ions. Weber et al. [455] performed AFC experiments with polarization-shaped laser pulses to optimize the photoionization yield in NaK molecules. Free optimization of the pulse phase, amplitude, and polarization resulted in a higher ionization yield than parameterized optimization with a train of two pulses.

Wöste and coworkers [456–461] controlled multiphoton ionization in K_2 and NaK using femtosecond laser pulses with phase and amplitude modulation, but without polarization shaping. In particular, one series of AFC experiments [459] explored the controlled dynamics by means of control pulse cleaning, which is a process of removing extraneous control field features by applying pressure in the optimization algorithm with an appropriate cost function on the spectral components of the pulse [365]. In another series of AFC experiments [460], the control mechanism of multiphoton ionization in NaK was analyzed by systematically reducing the complexity of the search space. Wöste and coworkers [457, 462–464] also demonstrated that AFC is capable of achieving isotope-selective ionization of diatomic molecules such as K_2 and NaK. They showed that differences between the dynamics of excited vibrational wave packets in distinct isotopomers can be amplified by optimally tailored control pulses. Leone and coworkers [465] applied AFC to optimize the weak-field pump-probe photoionization signal in Li_2 and used time-dependent perturbation theory to explain the control mechanism.

D. AFC of Molecular Alignment

The controlled alignment of molecules has attracted considerable attention as it can provide a well-defined sample for subsequent additional control experiments. At high laser intensities ($\sim 10^{13}$–10^{14} W cm^{-2}), dynamical variations of the molecular polarization can have a significant effect on alignment. By shaping the temporal profile of such an intense femtosecond laser pulse, it is possible to achieve control over molecular alignment. Quantum dynamics of laser-induced molecular alignment is amenable to theoretical treatment and optimization [243, 466–470] and can be successfully controlled using simple ultrafast laser pulses [471–474]. AFC provides a very effective general laboratory tool for alignment manipulation, making the best use of the laser resources. AFC of molecular alignment with intense shaped laser pulses was successfully demonstrated at room temperature for N_2 and CO [475–477].

E. AFC of Photodissociation Reactions in Molecules

A long-standing goal of photochemistry is selective control of molecular fragmentation. During the last decade, AFC employing shaped femtosecond laser pulses has achieved significant successes toward meeting this goal [8, 9, 12]. Selective quantum control of photodissociation reactions in molecules using AFC was first demonstrated by Gerber and coworkers in 1998 [478]. They studied photodissociation of an organometallic complex and employed AFC to maximize and minimize the branching ratio of two fragmentation products. The success of this AFC experiment triggered an ongoing wave of research activity in this area. In particular, Gerber's group [479–482] explored various aspects of AFC of photodissociation and photoionization reactions in polyatomic molecules in the gas phase and demonstrated that the control mechanism is not simply intensity dependent, but

rather employs the spectral phase distribution of the shaped laser pulse to steer the dynamics of the excited molecular vibrational wave packet toward the target reaction channel.

In 2001, Levis and coworkers [483] used AFC with shaped, strong-field laser pulses to demonstrate highly selective cleavage of chemical bonds in polyatomic organic molecules in the gas phase. The use of strong laser fields (with intensities of about 10^{13} W cm^{-2}) helps to effectively increase the available bandwidth, as transitions to excited molecular states are facilitated by the dynamic Stark shift. This effect opens up many reaction pathways that are inaccessible in the weak-field (perturbative) regime due to resonant spectral restrictions [12]. Although theoretical treatment of the complex strong-field molecular dynamics is extremely difficult, this complexity in no way affects employment of AFC in the laboratory, where the molecule solves its own Schrödinger equation on a femtosecond timescale. By operating at a high-duty control cycle, a learning algorithm is typically able to identify optimal laser pulses in a matter of minutes.

Selective control of molecular fragmentation in the gas phase was demonstrated in several other AFC experiments with shaped femtosecond laser pulses [484–489]. In particular, AFC of branching ratios of various photofragmentation products of dimethyl methylphosphonate was performed in the presence of a high background of a hydrocarbon and water [489]. The ability to achieve highly selective control under these conditions demonstrates that AFC may provide the means to identify complex airborne molecules. As mentioned in Section V.A.3, photofragmentation of SF_6 was controlled in an AFC experiment [439] using spectrally shaped femtosecond X-ray fields produced from intense shaped laser pulses via high-harmonic generation.

Significant attention has been devoted to the analysis of quantum dynamical processes involved in molecular photofragmentation control achieved in AFC experiments [490–498]. In particular, laboratory AFC optimizations were supplemented by theoretical *ab initio* quantum calculations to help clarify photofragmentation control mechanisms [490, 492–494]. In several other studies [495–497], a change in the basis of the control variables made it possible to reduce the dimension of the search space and thus elucidate control mechanisms of selective molecular photofragmentation. In another work [498], pump-probe spectroscopy was utilized to reveal a charge-transfer-based control mechanism in selective photofragmentation of polyatomic molecules in AFC experiments with intense shaped laser pulses.

Recently, Dantus and coworkers [499, 500] reported a study of molecular fragmentation using intense femtosecond pulses, in which they did not apply algorithm-guided AFC, but rather evaluated a large set of predetermined pulse shapes. They concluded that the yields of photofragmentation products are mainly controlled by the pulse intensity, while the details of the pulse shape (e.g., the spectral phase distribution) are not important. Levis [501] pointed out that the experimental

conditions employed by the Dantus group obscure connections to coherent processes that occur below the saturation threshold for ionization. Moreover, the search over a set of predetermined pulse shapes [499] cannot guarantee discovery of optimal controls, even if the employed set is very large. In a parameter space of the size characteristically available from a typical pulse shaper, only a dedicated optimization algorithm is capable of consistently identifying optimal control fields that commonly lie in a null space of the full search space.

F. Applications of AFC in Nonlinear Molecular Spectroscopy

Shaped femtosecond laser pulses were successfully used to enhance resolution and improve detection in several areas of nonlinear spectroscopy and microscopy [22]. Of particular interest are experiments that employ AFC to identify optimal pulse shapes. One area of nonlinear molecular spectroscopy is control of vibrational modes via stimulated Raman scattering (SRS). In the gas phase, a number of AFC experiments [502–504] manipulated molecular vibrations excited via SRS by intense ultrafast laser pulses in the impulsive regime (i.e., when the duration of the control laser pulse is shorter than the vibrational period). In the liquid phase, AFC was applied to control relative intensities of the peaks in the Raman spectrum, corresponding to the symmetric and antisymmetric C–H stretch modes of methanol [505–508]. The modes were excited via SRS in the nonimpulsive regime (i.e., the duration of the control laser pulse exceeded the vibrational period). The control pulse was shaped and the forward-scattered Raman spectrum was measured to obtain the feedback signal, with the goal of achieving selective control of the vibrational modes. However, it was argued [509, 510] that in nonimpulsive SRS, the relative peak heights in the Raman spectrum do not reflect the relative populations of the vibrational modes and that control of the spectral features demonstrated in the experiments [505–508] does not involve quantum interference of vibrational excitations, but rather is based on classical nonlinear optical effects.

Another important area of nonlinear molecular spectroscopy is control of molecular vibrational modes via coherent anti-Stokes Raman scattering (CARS). Several groups [511–518] used AFC in a CARS setup to optimally control vibrational dynamics in complex molecules. The Stokes pulse was shaped and the feedback signal was derived from the intensities observed in the CARS spectrum. In particular, AFC was applied to achieve selective enhancement or suppression of one or more vibrational modes in polymers [511] and organic molecules in the liquid phase [512–514, 516, 517]. Molecule-specific enhancement or suppression of the CARS spectral lines for a mixture of benzene and chloroform, demonstrated in a related AFC experiment [515], is an example of optimal dynamic discrimination (ODD) that will be discussed in more detail in Section V.H.

Control of molecular vibrational dynamics is possible not only through Raman-type processes, but also directly in the infrared (IR) regime. Zanni and coworkers

[519] demonstrated selective control of vibrational excitations on the ground electronic state of $W(CO)_6$ using shaped femtosecond mid-IR pulses. The spectral phase distribution of the pulse was optimized using AFC to achieve selective population of the excited vibrational levels of the T_{1u} CO stretching mode. In a related AFC experiment [520], polarization-shaped mid-IR pulses were used to selectively control vibrational excitations of the two carbonyl stretching modes in $Mn(CO)_5Br$.

G. Applications of AFC in Multiphoton Microscopy

An important application of AFC with shaped femtosecond laser pulses is in multiphoton excited fluorescence (MPEF) microscopy. For a given pulse energy, the transform-limited pulse has the maximum peak intensity, which helps to increase the fluorescence signal intensity, but unfortunately also increases the rate of photobleaching of the molecules (which is especially undesirable with samples of live cells). Use of optimally shaped pulses instead of a transform-limited pulse can reduce the bleaching rate, enhance spatial resolution, and increase contrast in biological fluorescence imaging. In a series of AFC experiments with shaped laser pulses, Midorikawa and coworkers [521–524] optimally controlled MPEF microscopy in different fluorescent biomolecules. Attenuation of photobleaching by a factor of 4 (without decreasing the fluorescence signal intensity) was demonstrated in two-photon excitation fluorescence (TPEF) from a green fluorescent protein [521]. Another AFC experiment [522] achieved selective control of two-photon and three-photon fluorescence in a mixture of two biosamples. The use of optimally tailored pulses helped to minimize the harmful three-photon fluorescence from the amino acid L-Tryptophan, without a significant loss of useful two-photon fluorescence from a green fluorescence protein. Optimally shaped supercontinuum pulses from a microstructure fiber were used in TPEF microscopy in another experimental study [523]. The pulse was shaped prior to propagation through the fiber, and AFC maximized the fluorescence signal contrast between two fluorescent proteins. A novel phase modulation technique for ultrabroadband laser pulses was developed for selective excitation of multiple fluorophores in TPEF microscopy [524]. This technique was applied to dual-color imaging of cells containing two types of fluorescent proteins, and AFC was employed to find the phase modulation that maximizes or minimizes the individual TPEF intensity from one of the fluorophores.

H. Applications of AFC for Optimal Dynamic Discrimination

Discrimination of similar systems is important for many practical problems in science and engineering. In particular, selective identification of target molecules in a mixture of structurally and spectroscopically similar compounds is a challenge

in areas such as selective excitation of multiple fluorescent proteins in microscopy of live samples, targeted component excitation in solid-state arrays, and selective transformation of chemically similar molecules. Theoretical studies [525–527] indicate that quantum systems differing even very slightly in structure may be distinguished by means of their dynamics when acted upon by a suitably tailored ultrafast control field. Such optimal dynamic discrimination can, in principle, achieve dramatic levels of control, and hence also provides a valuable test of the fundamental selectivity limits of quantum control despite noise and constrained laser resources. AFC provides a very effective laboratory means for practical implementation of ODD.

In 2001, Gerber and coworkers [528] experimentally demonstrated selective multiphoton excitation of two complex molecules in a solution. The goal was to electronically excite one molecule while simultaneously suppressing electronic excitation of the other. While these two molecules are electronically and structurally distinct, their emission ratio is practically unaffected by variations in single control parameters, such as wavelength, intensity, and linear chirp. Nevertheless, AFC was able to identify optimally shaped femtosecond laser pulses that improved the signal by approximately 50%. These results obtained in the presence of complex solvent/solute interactions aroused significant interest in ODD. In particular, AFC of photoproduct branching ratios in two very similar organometallic complexes $CpFe(CO)_2Cl$ and $CpFe(CO)_2Br$ (where $Cp = C_5H_5$) was sensitive enough to detect differences between FeCl and FeBr bonding properties [482]. This finding suggests the possibility of performing ODD of individual compounds in mixtures of chemically similar molecules. Other examples of ODD include isotope-selective ionization of diatomic molecules [457, 462–464], molecule-specific manipulation of CARS spectra from a mixture of benzene and chloroform [515], and selective excitation of multiple fluorophores in TPEF microscopy [523, 524].

A recent experimental demonstration of ODD by Roth et al. [157] achieved distinguishing excitations of two nearly identical flavin molecules in aqueous phase. The absorption spectra for flavin mononucleotide and riboflavin (RBF) are practically indistinguishable throughout the entire visible and far UV. This implementation of ODD used a shaped UV pulse centered at 400 nm and a time-delayed unshaped IR pulse centered at 800 nm. The first pulse creates a coherent vibrational wave packet on an excited electronic state, and the second pulse disrupts the wave packet motion and results in additional excitation to a higher state and consequential depletion of the recorded fluorescence signal. The effect of slight differences in the vibronic structure of the two molecules upon the dynamics of the excited wave packets is amplified by tailoring the spectral phase of the UV pulse. Since further excitation produced by the second pulse depends on the precise structure, position, and coherence of the tailored wave packet, it is possible to dynamically interrogate the two spectrally nearly identical systems and thereby produce a discriminating difference in their respective depleted fluorescence signals. Pulse

shapes that maximally discriminate between FMN and RBF were identified using AFC. The optimized depletion ratio could be changed by $\sim\pm 28\%$, despite the initially indistinguishable linear and nonlinear optical spectra. In contrast, if the UV pulse is transform limited, then the fluorescence depletion signals from the flavins are indistinguishable.

I. AFC of Photoisomerization in Complex Molecules

The control of molecular structure transformations is a coveted goal in chemistry. In particular, control of *cis–trans* isomerization has attracted much attention due to the importance of this process in chemistry and biology (e.g., it is a primary step of vision). AFC of *cis–trans* photoisomerization in cyanines (in the liquid phase) with shaped femtosecond laser pulses was first reported by Gerber and coworkers [529]. This experiment demonstrated that by using optimally shaped laser pulses it is possible to enhance or reduce isomerization efficiencies. The mechanism underlying isomerization control was discussed in a number of theoretical works [530–532]. In particular, Hunt and Robb [531] showed that the generation of the *trans* versus *cis* product is affected by the presence of an extended conical intersection seam on the PES of an excited electronic state and that photoisomerization can therefore be coherently controlled by tuning the distribution of momentum components in the photoexcited vibrational wave packet. The validity of this coherent control mechanism was corroborated in further AFC experiments by Yartsev and coworkers [533, 534] who demonstrated that optimally shaped laser pulses can be used to modify the momentum composition of the photoexcited wave packet and thus achieve significant control over the outcome of the isomerization process. Still, recent theoretical studies [535, 536] suggest that environmentally induced relaxation may affect coherent control of isomerization and other branching reactions in an excited state.

AFC of the retinal molecule in bacteriorhodopsin (from the all-*trans* to the 13-*cis* state) was demonstrated by Miller and coworkers [537]. This experiment employed both phase and amplitude modulation of femtosecond laser pulses and operated in the weak-field regime. By using optimally shaped pulses, it was possible to enhance or suppress the quantity of molecules in the 13-*cis* state by about 20%, relative to the yield observed using a transform-limited pulse with the same energy. They further explored the mechanism of coherent control of retinal photoisomerization in bacteriorhodopsin using time- and frequency-resolved pump-probe measurements [538]. Experimental data together with a theoretical analysis suggest that the isomerization yield depends on the coherent evolution of the vibrational wave packet on the excited-state PES in the presence of a conical intersection. According to this analysis, control of retinal photoisomerization is dominated by amplitude modulation of the spectral components of the excitation pulse. Gerber and coworkers [539] also demonstrated AFC of retinal

isomerization in bacteriorhodopsin. In this experiment, they pioneered the control scheme with unshaped-pump and time-delayed shaped-dump femtosecond laser pulses.

The role of quantum coherence effects in control of retinal isomerization in bacteriorhodopsin is still not fully clear, as a recent experiment by Bucksbaum and coworkers [540] found no dependence of the isomerization yield on the control pulse shape in the weak-field regime. In the strong-field regime, they found that the yield of the 13-*cis* isomer is maximized by a transform-limited pulse, which could indicate that the yield depends only on the pulse intensity, with quantum coherence not playing a significant role. These findings (especially for weak fields) apparently contradict the optimization results obtained by Miller and coworkers [537]. It is possible that these discrepancies could be explained by differences in experimental setups. In particular, Bucksbaum and coworkers [540] used only phase modulation of the control pulse, whereas Miller and coworkers [537, 538] argued that control is mainly achieved by amplitude modulation. Additional experimental and theoretical work will be needed to fully explore the mechanisms underlying condensed-phase control of photoisomerization in complex molecular systems.

Other examples of structural transformations in complex molecules include ring opening in cyclohexadiene along with isomerization as well as cyclization reactions in *cis*-stilbene. Carroll et al. [541, 542] demonstrated AFC of the photoinduced ring-opening reaction of 1,3-cyclohexadiene (CHD) to form 1,3,5-*cis*-hexatriene. Kotur et al. [543] used AFC with shaped ultrafast laser pulses in the deep UV to control the ring-opening reaction of CHD to form 1,3,5-hexatriene. Greenfield et al. [544] performed AFC of the photoisomerization and cyclization reactions in *cis*-stilbene dissolved in *n*-hexane. They employed phase-modulated 266 nm femtosecond pulses to maximize or minimize the yields of *cis*- to *trans*-stilbene isomerization, as well as *cis*-stilbene to 4*a*,4*b*-dihydrophenanthrene cyclization. In all these experiments, AFC-optimized shaped pulses significantly increased the target product yield relative to the effect of transform-limited pulses of the same energy.

J. AFC of Energy Flow in Biomolecular Complexes

Applications of quantum control to increasingly complex molecular systems have been considered. In particular, Motzkus and coworkers used AFC with shaped femtosecond laser pulses to control and analyze the energy flow pathways in the light-harvesting antenna complex LH2 of *Rhodopseudomonas acidophila* (a photosynthetic purple bacterium) [545, 546] and β-carotene [547]. They demonstrated that by shaping the spectral phase distribution of the control pulse, it is possible to manipulate the branching ratio of energy transfer between intra- and intermolecular channels in the donor–acceptor system of the LH2 complex [545]. Analysis of the transient absorption data was used to decipher the control mechanism and

identify the molecular states participating in energy transfer within LH2 [546] and β-carotene [547]. These results indicate that coherent quantum control is possible even in very complex molecular systems in a condensed-phase environment.

K. AFC of Photoinduced Electron Transfer

AFC has been applied to quantum control of intermolecular photoinduced electron transfer. Yartsev and coworkers [548] reported an AFC experiment that maximized the yield of ultrafast electron injection from the sensitizer to TiO_2 nanocrystals in the core part of a dye-sensitized solar cell. The electron transfer process was monitored using the transient absorption signal. The impulsive structure of the optimal laser pulse was observed to correlate with the coherent nuclear motion of the photoexcited dye. The pulse shape and the transient absorption kinetics were explained by an impulsive stimulated (anti-Stokes) Raman scattering process, followed by electronic excitation.

L. AFC of Nuclear Motion in Fullerenes

Fullerenes are a class of molecules of considerable interest in many areas of science. Laarmann et al. [549] employed AFC-optimized femtosecond laser pulses to coherently excite large-amplitude oscillations in C_{60} fullerene. The structure of the optimal pulses in combination with complementary two-color pump-probe data and time-dependent density functional theory calculations provided information on the underlying control mechanism. It was found that the strong laser field excites many electrons in C_{60}, and the nuclear motion is excited, in turn, due to coupling of the electron cloud to a radially symmetric breathing mode. Despite the complexity of this multiparticle system with various electronic and nuclear degrees of freedom, the optimal control fields generated essentially one-dimensional oscillatory motion for up to six cycles with an amplitude of $\sim$130% of the molecular diameter.

M. Applications of AFC in Semiconductors

Quantum control has found applications beyond atomic and molecular phenomena. In particular, it is possible to use optimal control methods to manipulate various processes in semiconductors. Kunde et al. [550, 551] demonstrated AFC of semiconductor nonlinearities using phase-modulated femtosecond laser pulses with the purpose of creating an ultrafast all-optical switch. Optimal pulse shapes discovered in this AFC experiment enhanced ultrafast semiconductor nonlinearities by almost a factor of 4. Chung and Weiner [552] employed AFC with phase-modulated femtosecond laser pulses to coherently control photocurrents in two semiconductor diodes with spectrally distinct two-photon absorption responses. AFC was able to

identify pulse shapes that maximized or minimized the photocurrent yield ratio for the two diodes.

N. AFC of Decoherence

Manipulation of quantum interference requires that the system under control remains coherent, avoiding (or at least postponing) the randomization induced by coupling to an uncontrolled environment. Therefore, the ability to manage environmentally induced decoherence would bring substantial advantages to the control of many physical and chemical phenomena. In particular, decoherence is a fundamental obstacle to quantum information processing [158], and therefore the ability to protect quantum information systems against decoherence is indispensable.

The possibility of using AFC for optimal suppression of decoherence was first proposed by Brif et al. [553] and numerical simulations in a model system were performed by Zhu and Rabitz [374]. Walmsley and coworkers [123] have recently applied AFC to extend the coherence time of molecular vibrational wave packets. The concept underlying this experiment is the use of coherent preparation of the quantum system to alter nonunitary decoherent dynamics induced by an uncontrolled environment. In this experiment, a gas-phase ensemble of K_2 at 400 °C was irradiated by a shaped femtosecond laser pulse, inducing a vibrational wave packet in the lowest excited electronic state. Decoherence of this wave packet is caused by coupling of the vibrational mode to the thermalized rotational quasi-bath. The amplitude of quantum beats in the fluorescence signal provides an estimate of the degree of wave packet localization in the phase space and therefore can be used as a coherence surrogate. The optimal pulse identified by AFC increased the quantum-beat visibility from zero to more than four times the noise level and prolonged the coherence lifetime by a factor of $\sim$2 relative to the beats produced by the transform-limited pulse.

A well-known strategy for suppressing decoherence is through application of pulse sequences designed to dynamically decouple the quantum system from the environment [554–565]. Open-loop control experiments [566–570] employed theoretically designed pulse sequences based on particular environment models. However, actual experimental environments can significantly differ from the models. To overcome this difficulty, Bollinger and coworkers [571] recently used AFC to tailor the dynamical decoupling pulse sequence to an actual noise environment. In this experiment, the system was a quantum memory realized in an array of cold $^9Be^+$ ions in a trap, with qubit states realized using a ground-state electron spin-flip transition. The main source of qubit-state decoherence is magnetic field noise. A sequence of microwave π pulses used for qubit control in this laboratory configuration is technologically quite different from shaped femtosecond optical laser pulses typically employed in molecular control experiments; however, the fundamental concept of AFC is still fully applicable. Optimal pulse sequences

discovered in this AFC experiment, without *a priori* knowledge of the noise environment, suppressed the qubit error rate by a factor of 5–10 relative to benchmark model-based sequences.

O. Future Applications of AFC

As discussed above, AFC has proved to have broad practical success as a means of achieving optimal control of quantum phenomena in the laboratory. One recognizable trend is the extension of AFC applications toward the manipulation of increasingly more complex systems and phenomena. Along this avenue, implementation of AFC could bring significant benefits to areas such as near and even remote detection of chemical compounds (first steps in this direction have recently been made [489, 572]), optimal control of molecular electronics devices, and optimal control of photoinduced phenomena in live biological samples (including nonlinear microscopy and ODD, as indicated by recent experiments performed in Midorikawa's group [521–524]).

Increasing use of AFC is also likely in optimal control of photophysical phenomena. One important area is coherent manipulation of quantum processes in solid-state systems, especially in semiconductor quantum structures [573, 574]. Another potential application is optimal storage and retrieval of photonic states in atomic vapor and solid-state quantum memories [362, 363, 575–580]. The AFC methodology may be also applicable to physical problems where, instead of laser pulses, other means (e.g., voltages applied to an array of electrodes) are used to implement the control. Examples could include optimal control of coherent electron transport in semiconductors by means of adaptively shaped electrostatic potentials [581], coherent control of charge qubits in superconducting quantum devices by gate voltages [582, 583], and coherent control of photonic qubits in integrated optical circuits via the thermo-optic effect [584]. Several types of quantum systems (e.g., flux qubits in superconducting quantum devices, hyperfine-level qubits in trapped neutral atoms and ions, electron spins of donor atoms in silicon, etc.) can be controlled by pulses of microwave radiation (e.g., AFC-optimized dynamical decoupling of trapped-ion qubits by a sequence of microwave π pulses [571], discussed in section V.N). Many possible applications of AFC could have significant implications for the progress in the field of quantum information sciences. A new domain of quantum control involves manipulation of relativistic quantum dynamics with extremely intense laser fields [585] for accelerating particles and even intervening in nuclear processes in analogy to what is happening in atomic-scale control. AFC methods could possibly become useful for optimal control of such laser-driven high-energy phenomena.

Despite significant advances achieved in the field of quantum control during the last decade, the experimental capabilities are limited by currently available laser resources. In particular, many new applications would open up, if reliable sources

of coherent laser radiation with a much wider bandwidth become available. Such resources could make possible the simultaneous manipulation of rotational, vibrational, and electronic processes in molecules in a more effective fashion, thereby achieving hitherto unattainable levels of control. Moreover, if pulse-shaping technology can be extended to coherent radiation in the attosecond regime as well as in the range of MeV photon energies, a multitude of new applications in X-ray spectroscopy, medical physics, and control of nuclear dynamics could arise.

P. Algorithmic Advances for Laboratory AFC

The learning algorithm is an important component of laboratory AFC. The majority of AFC experiments employ stochastic algorithms such as evolutionary strategies [586] and genetic algorithms [587]. Historically, genetic algorithms were characterized by the use of recombination, while evolutionary strategies primarily relied on mutation; however, modern algorithms guiding AFC experiments and simulations typically incorporate both types of genetic operations and are variably called genetic algorithms or evolutionary algorithms. These algorithms are very well suited to laboratory optimizations as they naturally match the discrete structure of control "knobs" (e.g., the pixels of a pulse shaper) and are robust to noise. Moreover, robustness to noise in AFC experiments can be enhanced by incorporating the signal-to-noise ratio into the control objective functional [365, 588]. Various aspects of evolutionary algorithms and their application to AFC of quantum phenomena were assessed [140, 589]. Evolutionary algorithms can be also used in multiobjective optimization [590, 591], and the application of this approach to quantum control problems was studied theoretically [243–245, 592] and demonstrated in AFC experiments [451, 459].

Other types of stochastic algorithms include, for example, simulated annealing [593] and ant colony optimization [594, 595]. Simulated annealing was utilized in some AFC experiments [417, 524], and it seems best suited to situations where just a few experimental parameters are optimized [596, 597]. Ant colony optimization was used in an AFC simulation [377], but it is yet to be tested in the laboratory.

As will be discussed in Section VII, the absence of local traps in QCLs (for controllable quantum systems) has important practical consequences for the optimization complexity of AFC experiments. In particular, deterministic search algorithms can be used to reach a globally optimal solution. Deterministic algorithms (e.g., the downhill simplex method) were successfully implemented in several AFC experiments [418, 544, 571]. Recently, Roslund and Rabitz [152] demonstrated the efficiency of a gradient algorithm in laboratory AFC of quantum phenomena. They implemented a robust statistical method for obtaining the gradient on a general QCL in the presence of noise. The experimentally measured gradient was utilized to climb along steepest-ascent trajectories on the landscapes of several quantum control problems. The optimization with the gradient algorithm was very

efficient, as it required approximately three times fewer experiments than needed by a standard genetic algorithm in these cases. High algorithmic efficiency is especially important for AFC of laser-driven processes in live biological samples, as damage (e.g., due to photobleaching) can be reduced by decreasing the number of trial laser pulses. Still, evolutionary or other stochastic algorithms may be preferable over deterministic algorithms in many AFC experiments due to their inherent robustness to noise. Hybrid stochastic–deterministic algorithms (e.g., derandomized evolution strategies) seem to offer the most flexibility and efficiency [153].

VI. THE ROLE OF THEORETICAL QUANTUM CONTROL DESIGNS IN THE LABORATORY

A significant portion of theoretical research in the area of quantum control is devoted to model-based computations that employ QOCT (or other similar methods) to design optimal control fields for various physical and chemical problems (see Section IV.C). Notwithstanding these extensive QOCT-based control field designs, experiments seeking optimal control of molecular processes overwhelmingly employ AFC methods as described in Section V. This raises important questions about the practical utility of open-loop control and the role of theoretical methods such as QOCT in control experiments [141]. In considering this matter, it is important to keep in mind that the AFC procedure grew out of observations from QOCT simulations and associated analyses.

As discussed in Section IV.D, the practical laboratory relevance of theoretical designs depends on the complexity of the system of interest, with simpler cases yielding theoretical models closer to reality. For example, in numerous NMR experiments employing RF fields to manipulate nuclear spins [598, 599], including NMR realizations of quantum gates [355], theoretically designed sequences of pulses (some of which were developed using QOCT [284, 356]) can function quite well. At the other extreme of system complexity are electronic and vibrational processes in polyatomic molecules whose dynamics cannot be accurately modeled at the present time. An objective assessment is that models used for polyatomic molecules in control computations are currently too simplified and computational techniques inadequate for the true levels of complexity, resulting in theoretical designs that are not directly applicable to control experiments that work with *real* systems. Optimal control is generally based on creating interference of multiple quantum pathways, which can be very sensitive to the detailed properties of the system (e.g., evolution of a laser-induced vibrational wave packet can be strongly influenced by small variations in a molecular PES, as evident from experimental ODD results [157]). Therefore, even small inaccuracies of theoretical models or associated numerical procedures may result in control designs that are not optimal for the actual systems.

These considerations lead to the conclusion that open-loop control experiments employing theoretical designs may be useful for some systems and impractical for others. The boundary between the systems for which modeling is sufficiently reliable and the systems for which it is not depends on available Hamiltonian data, numerical algorithms, and computational power. Of course, with time, better modeling will become available for more complex systems, although the exponential increase in the Hilbert space dimension with the system complexity is a fundamental feature of quantum mechanics that significantly hinders the effectiveness of numerical control designs for practical laboratory implementation. Therefore, AFC will likely continue (at least in the foreseeable future) to be much more effective for optimal manipulation of electronic and vibrational processes in molecules with four and more atoms than employment of theoretical control designs.

Notwithstanding this assessment, theoretical control studies should continue to have high significance. Theory can be especially important in exploring the feasibility of various outcomes for controlled quantum dynamics; even semiquantitative modeling may be successful for such purposes in many applications. Theoretical control simulations can provide important guidance for the selection of the experimental configuration, thereby helping to make AFC a more effective practical tool. Also, control solutions obtained via theoretical model-based computations (in particular, QOCT) should play an important role by advancing the general understanding of the character of controlled dynamics and control mechanisms.

The open-loop control procedure is not limited to the use of optimal theoretical designs generated via QOCT and similar methods. Moreover, optimality in not always required in quantum control. In the conceptually allied field of synthetic chemistry, progress has often been achieved via intuition-guided trials, leading to a gradual increase in reaction yields. Following this venerable tradition, some recent open-loop control experiments seek improvement by employing ultrafast shaped laser pulses with so-called "rational" or "judicious" control designs obtained using a combination of intuition and arguments based on some knowledge of system properties (e.g., spectral information or symmetry). This approach is popular in nonlinear spectroscopy and microscopy [22, 600–613], as well as in some other atomic [614–621], molecular [471–474, 622], and solid-state [623–626] applications. While in many situations such "rationally" designed control pulses enhance the spectroscopic resolution or increase the control yield compared to results obtained with transform-limited pulses, in general they are not optimal. Experience gained from numerous quantum control experiments indicates that intuition generally fails to discover the most effective controls (except for the simplest systems), and therefore in most cases the degree of control can be increased via closed-loop optimization employing a suitable learning algorithm. In some situations, intuition-driven control may be effective in providing a guide to initial fields for subsequent optimization under AFC.

VII. QUANTUM CONTROL LANDSCAPES

From the practical perspective, the goal of quantum control is to discover optimal solutions for manipulating quantum phenomena. Therefore, it is important not only to study general conditions under which optimal solutions exist [37, 144, 145], but also to explore the complexity of finding them. Underlying the search for optimal controls is the QCL, which specifies the physical objective as a function of the control variables. Analysis of QCLs [147] can not only establish the existence of optimal control solutions and determine their types (e.g., global versus local maxima and true maxima versus saddle points), but also make it possible to obtain necessary conditions for convergence of optimization algorithms to global maxima along with bounds on the scaling of the convergence effort. Surprisingly, these properties are independent of details of a particular Hamiltonian (provided that the system is controllable), which makes the results of landscape analysis applicable across a wide range of controlled quantum phenomena.

A. The Control Landscape and Its Critical Points

The ease of finding optimal control solutions strongly depends on the properties of the search space associated with the objective as a functional of control variables. To characterize these properties, it is convenient to express the objective functional in a form that implicitly satisfies dynamical constraints. Consider a quantum control problem with a fixed target time T for a closed system with unitary evolution. Denote by $\mathcal{U}_T : \varepsilon(\cdot) \mapsto U(T)$ the end point map from the space of control fields to the space of unitary evolution operators, induced by the Schrödinger equation (5), so that $U(T) = \mathcal{U}_T\varepsilon(\cdot)$. A Mayer-type cost functional $J = F(U(T))$ itself describes a map $\mathcal{F}$ from the space of evolution operators to the space of real-valued costs. Thus, the composition of these maps, $\mathcal{J} = \mathcal{F} \circ \mathcal{U}_T : \mathbb{K} \to \mathbb{R}$, is a map from the space of control fields to the space of real-valued costs. This map generates the functional $J[\varepsilon(\cdot)] = \mathcal{F}\mathcal{U}_T\varepsilon(\cdot) = \mathcal{J}\varepsilon(\cdot)$. The functional $J[\varepsilon(\cdot)]$ is referred to as the *quantum control landscape*. The optimal control problem may then be expressed as the unconstrained search for

$$J_{\text{opt}} = \max_{\varepsilon(\cdot)} J[\varepsilon(\cdot)] \tag{39}$$

The topology of the QCL (i.e., the character of its critical points, including local and global extrema) determines whether local search algorithms will converge to globally optimal solutions to the control problem [148]. In recent years, QCL topology studies have become an active area of research [146, 147, 169, 208–210, 217, 219–221, 627]. A model QCL with topology characteristic for state transition control (see discussion below Eq. (46)) is shown in Fig. 2.

The critical points of the QCL (also referred to as extremal controls) are defined as controls at which the first-order functional derivative of $J[\varepsilon(\cdot)]$ with respect to

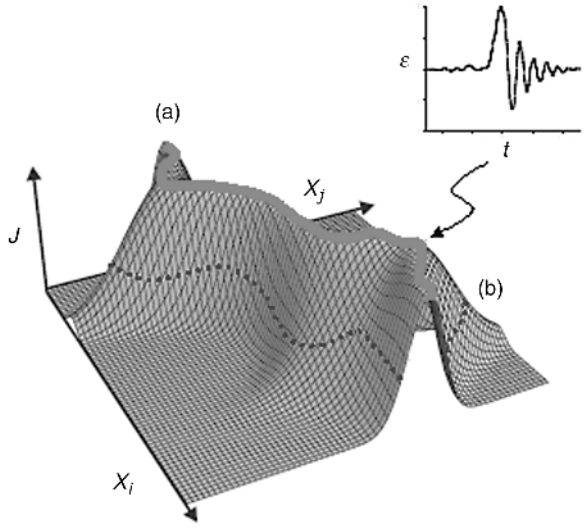

Figure 2. A model QCL. The control objective J is shown as a function of two control variables x_i and x_j out of possibly many in a realistic control experiment. The inset indicates that each point on the landscape corresponds to a particular choice of the control field $\varepsilon(\cdot)$. The topology of the depicted landscape is characteristic for the important case of state transition control, for which no local extrema exist and the global maximum is a continuous manifold, denoted in the figure by the solid curve **(a)**. The dotted line **(b)** shows a level set that is a collection of control fields that all produce the same value of the objective functional J. Adapted from Ref. [147]. (See the color version of this figure in Color Plates section.)

the control field is zero for all time, that is,

$$\frac{\delta J[\varepsilon(\cdot)]}{\delta\varepsilon(t)} = 0, \quad \forall t \in [0, T] \tag{40}$$

The critical manifold of the QCL is the collection of all critical points:

$$\mathfrak{M}(\varepsilon) := \{\varepsilon(\cdot) \mid \delta J/\delta\varepsilon(t) = 0, \quad \forall t \in [0, T]\} \tag{41}$$

1. Regular and Singular Critical Points

An important concept in landscape topology is the classification of a critical point as regular or singular [628, 629]. Using the chain rule, one obtains

$$\frac{\delta J}{\delta\varepsilon(t)} = \left\langle \nabla F(U(T)), \frac{\delta U(T)}{\delta\varepsilon(t)} \right\rangle \tag{42}$$

where $\nabla F(U(T))$ is the gradient of F at $U(T)$ and $\delta U(T)/\delta\varepsilon(t)$ is the first-order functional derivative of $U(T)$ with respect to the control field. A critical point of

$J[\varepsilon(\cdot)]$ is called *regular* if $\delta U(T)/\delta\varepsilon(t)$ is full rank and $\nabla F(U(T)) = 0$. The full rank condition on $\delta U(T)/\delta\varepsilon(t)$ is equivalent to the condition that the map $\mathcal{U}_T$ is locally surjective in the vicinity of the critical point; that is, for any local increment $\delta U(T)$ in the evolution operator there exists an increment $\delta\varepsilon(\cdot)$ in the control field such that $\mathcal{U}_T[\varepsilon(\cdot) + \delta\varepsilon(\cdot)] = \mathcal{U}_T\varepsilon(\cdot) + \delta U(T)$. Also, for the Hamiltonian of the form (14), one obtains

$$\frac{\delta U(T)}{\delta\varepsilon(t)} = \frac{i}{\hbar} U(T)\mu(t) \tag{43}$$

where

$$\mu(t) = U^{\dagger}(t)\mu U(t) \tag{44}$$

is the time-dependent dipole operator (in the Heisenberg picture). Then, for an N-level quantum system with an orthonormal basis $\{|\ell\rangle\}$, the full rank condition on $\delta U(T)/\delta\varepsilon(t)$ is equivalent to the condition that

$$\left\{ \mathrm{Re}\left[\langle\ell|\mu(t)|\ell'\rangle\right],\ \mathrm{Im}\left[\langle\ell|\mu(t)|\ell'\rangle\right] \ \middle|\ \ell = 1, \ldots, N,\ \ell' \geq \ell \right\} \tag{45}$$

is a set of N^2 linearly independent functions of time (on the interval $t \in [0, T]$) [210]. Evidence from various quantum optimal control computations shows that this condition is generally satisfied for critical points that are physically relevant control fields; however, there exist known exceptions when a critical point corresponds to a constant control field (e.g., zero field) [147]. Indeed, when a closed quantum system governed by the Hamiltonian of the form (14) is driven by a constant field, the rank of the dipole moment $\mu(t)$ is at most $N^2 - N + 1$, so that the full rank condition is not satisfied [210]. Since constant control fields are impractical in typical laboratory circumstances, theoretical studies have focused mostly on properties of regular critical points at nonconstant controls.

Note that for some particular physical objectives, the conditions for regularity of the QCL critical points can be weaker than the general condition of Eq. (45). Consider, for example, an important special case of state transition control, for which the Mayer-type cost functional $J = F_3(U(T)) = P_{\mathrm{i}\to\mathrm{f}}$ of Eq. (22) is the probability of transition between two energy levels $|\psi_{\mathrm{i}}\rangle$ and $|\psi_{\mathrm{f}}\rangle$ of the quantum system. Let $\{|\ell\rangle\}$ be the set of the eigenstates of the free Hamiltonian H_0, and denote the initial and target states as $|\psi_{\mathrm{i}}\rangle = |i\rangle$ and $|\psi_{\mathrm{f}}\rangle = |f\rangle$, respectively. Then the condition (40) for critical points becomes [221]

$$\frac{\delta J[\varepsilon(\cdot)]}{\delta\varepsilon(t)} = \frac{2}{\hbar}\mathrm{Im}\left\{ \left[\sum_{\ell \neq i} \langle i|\mu(t)|\ell\rangle\langle\ell|U^{\dagger}(T)|f\rangle \right] \langle f|U(T)|i\rangle \right\} = 0, \quad \forall t \in [0, T] \tag{46}$$

One can recognize [221] that among nonconstant controls there are only two types of critical points: (i) controls that satisfy $\langle f|U(T)|i\rangle = 0$, which implies $J = P_{\mathrm{i}\to\mathrm{f}} = 0$ (corresponding to the global minimum) and (ii) controls that satisfy $\langle \ell|U^{\dagger}(T)|f\rangle = 0$, $\forall \ell \neq i$, which implies $J = P_{\mathrm{i}\to\mathrm{f}} = 1$ (corresponding to the global maximum). In this situation, a critical point is regular if

$$\{\mathrm{Re}\,[\langle i|\mu(t)|\ell\rangle]\,,\ \mathrm{Im}\,[\langle i|\mu(t)|\ell\rangle]\ |\ \ell = 1, \ldots, N\} \tag{47}$$

is a set of $2N - 2$ linearly independent functions of time (on the interval $t \in [0, T]$) [221]. Similar to the stronger regularity condition of Eq. (45), the condition of Eq. (47) is generally satisfied for critical points that are physically relevant control fields, with known exceptions arising for some quantum systems when a critical point corresponds to a constant control field [147]. Once again, since constant control fields are not applicable in typical quantum control experiments, theoretical analyses of the state transition QCL have focused mostly on properties of regular critical points at nonconstant controls.

A critical point of $J[\varepsilon(\cdot)]$ is called *singular* if the rank of $\delta U(T)/\delta\varepsilon(t)$ is deficient that is, if the map $\mathcal{U}_T$ is not locally surjective in the point's vicinity. A critical point is called kinematic if $\nabla F(U(T)) = 0$ and nonkinematic if $\nabla F(U(T)) \neq 0$. By definition, all regular critical points are kinematic. Among singular critical points some are kinematic and some are nonkinematic (i.e., for the latter $\delta J/\delta\varepsilon(t) = 0$, whereas $\nabla F(U(T)) \neq 0$) [629]. In QCLs, the measure of regular critical points appears to be much greater than that of singular ones [629]. Therefore, attention has been focused mostly on the characterization of regular critical points, and several important results have been obtained [147]. Nevertheless, singular extremal solutions have been recently experimentally demonstrated in time optimal control of a spin-1/2 particle in a dissipative environment [630]. Singular critical points arising at constant controls (in particular, at zero field) in some special quantum systems were discussed in Ref. [147].

2. *Kinematic Critical Manifolds*

As defined above, all kinematic critical points (including all regular ones) satisfy the condition

$$\nabla F(U(T)) = 0 \tag{48}$$

Correspondingly, the manifold of kinematic critical points,

$$\mathfrak{M}(U) := \{U(T)\ |\ \nabla F(U(T)) = 0\} \tag{49}$$

is determined solely by the functional dependence of the objective $J = F(U(T))$ on the target time evolution operator (i.e., it is completely independent of the details of dynamics comprised in the system's Hamiltonian). The condition (48)

can be explored in more detail for QCLs arising from various Mayer-type cost functionals.

First, consider the case of evolution-operator control with the objective functional $J = F_1(U(T))$ of Eq. (18). Let us locally expand the evolution operator $U(T)$ to its unitary neighborhood:

$$U(T) \to U_{s,A}(T) = e^{isA}U(T), \quad s \in \mathbb{R},\ A^\dagger = A \tag{50}$$

Under this expansion, the objective is given by

$$J = \frac{1}{N}\mathrm{Re}\left\{\mathrm{Tr}\left[W^\dagger e^{isA}U(T)\right]\right\} \tag{51}$$

The condition (48) is satisfied if and only if

$$\left.\frac{dJ}{ds}\right|_{s=0} = \frac{i}{2N}\mathrm{Tr}\left\{A\left[W^\dagger U(T) - U^\dagger(T)W\right]\right\} = 0, \quad \forall A^\dagger = A \tag{52}$$

Owing to the arbitrariness of A, the condition (48) is therefore equivalent to

$$W^\dagger U(T) = U^\dagger(T)W \tag{53}$$

that is, $W^\dagger U(T)$ is required to be a Hermitian operator: $W^\dagger U(T) = [W^\dagger U(T)]^\dagger$. Since the operator $W^\dagger U(T)$ is unitary, if it is also Hermitian, then its square is the identity operator I, which means that eigenvalues of $W^\dagger U(T)$ are $+1$ and -1. Therefore, for an N-level quantum system, the condition (53) implies [208, 209]

$$W^\dagger U(T) = Y^\dagger X_k Y \tag{54}$$

where Y is an arbitrary unitary transformation,

$$X_k := -I_k \oplus I_{N-k} \tag{55}$$

I_l is the $l \times l$ identity matrix and $k = 0, 1, \ldots, N$. Correspondingly, there are $N + 1$ distinct critical submanifolds labeled by k, with critical values of J given by

$$J_k = 1 - \frac{2k}{N} \tag{56}$$

From Eq. (54), the kth critical submanifold is the orbit of X_k in $\mathrm{U}(N)$. Since X_k is invariant under the action of any operator of the form $Z_k \oplus Z_{N-k}$, where $Z_k \in \mathrm{U}(k)$, $Z_{N-k} \in \mathrm{U}(N-k)$, this orbit is diffeomorphic to the quotient space [209]

$$\mathfrak{G}_k := \frac{\mathrm{U}(N)}{\mathrm{U}(k) \times \mathrm{U}(N-k)} \tag{57}$$

which is a complex Grassmannian manifold. Thus, the kth critical submanifold can be expressed as

$$\mathfrak{M}_k(U) = \left\{ U(T) \mid W^\dagger U(T) = Y^\dagger X_k Y,\ Y \in \mathfrak{G}_k \right\} \tag{58}$$

and the entire critical manifold is

$$\mathfrak{M}(U) = \bigcup_{k=0}^{N} \mathfrak{M}_k(U) \tag{59}$$

Topologically, the critical submanifold $\mathfrak{M}_k(U)$ is equivalent to the Grassmannian manifold $\mathfrak{G}_k$, and its dimension is

$$\dim \mathfrak{M}_k(U) = \dim \mathfrak{G}_k = N^2 - k^2 - (N-k)^2 = 2k(N-k) \tag{60}$$

Thus, the global optima corresponding to $k = 0$ and $k = N$ (with $J_0 = 1$ and $J_N = -1$, respectively) are isolated points, while local extrema corresponding to $k = 1, 2, \ldots, N-1$ are smooth, compact submanifolds embedded in U(N). As we will see below, all regular local extrema are saddle-point regions.

Now consider observable control with the objective functional $J = F_3(U(T))$ of Eq. (21). Once again, we locally expand the evolution operator $U(T)$ to its unitary neighborhood as in Eq. (50). Under this expansion, the objective is given by

$$J = \mathrm{Tr}\left[e^{isA} U(T)\rho_0 U^\dagger(T) e^{-isA}\Theta\right] \tag{61}$$

The condition (48) is satisfied if and only if

$$\left.\frac{dJ}{ds}\right|_{s=0} = i\mathrm{Tr}\left\{A[U(T)\rho_0 U^\dagger(T), \Theta]\right\} = 0, \quad \forall A^\dagger = A \tag{62}$$

Owing to the arbitrariness of A, the condition (48) is therefore equivalent to

$$[U(T)\rho_0 U^\dagger(T), \Theta] = 0 \tag{63}$$

That is, the density matrix at the final time is required to commute with the target observable operator [146, 169, 217]. This condition for a kinematic critical point was studied in the context of optimization of Lagrange-type cost functionals with an end point constraint [627, 631, 632] as well as in the context of regular extremal solutions for Mayer-type cost functionals [169, 217]. The condition (63) can be further analyzed to characterize critical submanifolds for observable control of an

N-level quantum system. Let R and S denote unitary matrices that diagonalize ρ_0 and Θ, respectively, that is,

$$\tilde{\rho}_0 = R^\dagger \rho_0 R = \mathrm{diag}\{\xi_1, \ldots, \xi_1; \ldots; \xi_r, \ldots, \xi_r\} \tag{64}$$

$$\tilde{\Theta} = S^\dagger \rho_0 S = \mathrm{diag}\{\theta_1, \ldots, \theta_1; \ldots; \theta_p, \ldots, \theta_p\} \tag{65}$$

Here, $\xi_1 > \cdots > \xi_r$ are r distinct eigenvalues of ρ_0 with multiplicities $\{n_1, \ldots, n_r\}$ and $\theta_1 > \cdots > \theta_p$ are p distinct eigenvalues of Θ with multiplicities $\{m_1, \ldots, m_p\}$. Then the objective functional J can be written as

$$J = \mathrm{Tr}\left[\tilde{U}(T)\tilde{\rho}_0 \tilde{U}^\dagger(T)\tilde{\Theta}\right] \tag{66}$$

where $\tilde{U}(T) = S^\dagger U(T) R$. The condition (63) that $\rho(T)$ and Θ commute is equivalent to the condition that the matrix $\tilde{U}(T)$ is in the double coset $\mathfrak{K}_\pi$ of some permutation matrix P_π [219]:

$$\tilde{U}(T) \in \mathfrak{K}_\pi = \mathrm{U}(\mathbf{n}) P_\pi \mathrm{U}(\mathbf{m}) \tag{67}$$

Here, $\mathrm{U}(\mathbf{n})$ is the product group $\mathrm{U}(n_1) \times \cdots \times \mathrm{U}(n_r)$, where $\mathrm{U}(n_i)$ is the n_i-dimensional unitary group acting on the eigenspace of ξ_i. In the same manner, $\mathrm{U}(\mathbf{m})$ is the product group $\mathrm{U}(m_1) \times \cdots \times \mathrm{U}(m_p)$, where $\mathrm{U}(m_i)$ is the m_i-dimensional unitary group acting on the eigenspace of θ_i. Thus, each critical submanifold corresponds to a particular choice of the permutation π,

$$\mathfrak{M}_\pi(U) = \left\{ U(T) \mid S^\dagger U(T) R \in \mathfrak{K}_\pi \right\} \tag{68}$$

The entire critical manifold is

$$\mathfrak{M}(U) = \bigcup_{\pi \in \mathfrak{S}_N} \mathfrak{M}_\pi(U) = \left\{ U(T) \mid S^\dagger U(T) R \in \mathfrak{K} \right\} \tag{69}$$

where $\mathfrak{K}$ is the union of all the double cosets $\mathfrak{K}_\pi$:

$$\mathfrak{K} = \bigcup_{\pi \in \mathfrak{S}_N} \mathrm{U}(\mathbf{n}) P_\pi \mathrm{U}(\mathbf{m}) \tag{70}$$

and $\mathfrak{S}_N$ is the group of all permutations on N indices, that is, the symmetric group.

As shown by Eqs. (64) and (65), the diagonalizing matrices R and S arrange the eigenvalues of $\tilde{\rho}_0$ and $\tilde{\Theta}$, respectively, in decreasing order. Therefore, the identity permutation $\pi = (1)$ with the matrix $P_{(1)} = I_N$ corresponds to the critical submanifold that is the global maximum of J. In a similar manner, the permutation matrix $\hat{\pi}$ that rearranges the matrix elements of $\tilde{\rho}_0$ in increasing order: $P_{\hat{\pi}} \tilde{\rho}_0 P_{\hat{\pi}}^{-1} = \mathrm{diag}\{\xi_r, \ldots, \xi_r; \ldots; \xi_1, \ldots, \xi_1\}$, corresponds to the critical

submanifold that is the global minimum of J. When both ρ_0 and Θ are fully nondegenerate, one obtains

$$J_{\max} \equiv J_{(1)} = \sum_{i=1}^{N} \xi_i \theta_i, \qquad J_{\min} \equiv J_{\hat{\pi}} = \sum_{i=1}^{N} \xi_{N+1-i} \theta_i \tag{71}$$

In the case of state transition control, both $\rho_0 = |\psi_\mathrm{i}\rangle\langle\psi_\mathrm{i}|$ and $\Theta = |\psi_\mathrm{f}\rangle\langle\psi_\mathrm{f}|$ are already diagonal (in the basis of the eigenstates of H_0) and each of them has only one nonzero eigenvalue. Then, the matrices R and S are needed just to arrange the eigenvalues in decreasing order, resulting in $\tilde{\rho}_0 = \tilde{\Theta} = \mathrm{diag}\{1; 0, \ldots, 0\}$. Consequently, the identity permutation $\pi = (1)$ corresponds to the global maximum $J_{\max} \equiv J_{(1)} = 1$, while all other permutations correspond to the global minimum $J_{\min} \equiv J_{\pi \neq (1)} = 0$, and no local (intermediate) extrema exist.

Topologically, $\mathfrak{M}_\pi(U)$ is equivalent to $\mathfrak{K}_\pi$ for every π and, correspondingly, $\mathfrak{M}(U)$ is equivalent to $\mathfrak{K}$. The structure of the critical manifold depends on any degeneracies in the spectra of ρ_0 and Θ. When both ρ_0 and Θ are fully nondegenerate, then $\mathrm{U}(\mathbf{n}) = \mathrm{U}(\mathbf{m}) = [\mathrm{U}(1)]^N$, and $\mathfrak{K}$ consists of $N!$ disjoint N-dimensional tori labeled by the permutation matrices [219]. The occurrence of degeneracies in the spectra of ρ_0 and Θ will merge two or more tori together, thereby reducing the number of disjoint critical submanifolds and increasing their dimensions. In particular, for state transition control, $\mathrm{U}(\mathbf{n}) = \mathrm{U}(\mathbf{m}) = \mathrm{U}(1) \times \mathrm{U}(N-1)$, there are only two critical submanifolds corresponding to the global maximum and minimum, respectively,

$$\mathfrak{K}_{\max} \equiv \mathfrak{K}_{(1)} = [\mathrm{U}(1) \times \mathrm{U}(N-1)] I_N [\mathrm{U}(1) \times \mathrm{U}(N-1)] \tag{72}$$

$$\mathfrak{K}_{\min} \equiv \mathfrak{K}_{\{\pi \neq (1)\}} = \bigcup_{\pi \neq (1)} [\mathrm{U}(1) \times \mathrm{U}(N-1)] P_\pi [\mathrm{U}(1) \times \mathrm{U}(N-1)] \tag{73}$$

A detailed characterization of the critical submanifolds for all possible degeneracies was performed by Wu et al. [219].

B. Optimality of Control Solutions

As discussed in Section IV.B, satisfaction of the condition for a critical point (i.e., Eq. (40)) is a necessary but not sufficient condition for optimality of a control [204, 249]. For Mayer-type cost functionals, a sufficient condition for optimality is negative semidefiniteness of the Hessian of J. The characteristics of critical points (in particular, the presence or absence of local optima) are important for the convergence properties of search algorithms [147]. To classify critical points as global maxima and minima, local maxima and minima, and saddle points, we examine the second-order variation in J for an arbitrary control variation $\delta\varepsilon(\cdot)$.

For Mayer-type cost functionals $J = F(U(T))$, this second-order variation can be written as

$$\delta^2 J = \mathcal{Q}_F(\delta U(T), \delta U(T)) + \langle \nabla F(U(T)), \delta^2 U(T) \rangle \tag{74}$$

where $\delta U(T)$ and $\delta^2 U(T)$ are the first- and second-order variations, respectively, of $U(T)$ caused by a control variation $\delta\varepsilon(\cdot)$ over $[0, T]$, and $\mathcal{Q}_F$ is the Hessian quadratic form (HQF) of $F(U)$. Assuming that the critical point $\varepsilon(\cdot)$ is regular (i.e., that the gradient of $F(U)$ is zero), we obtain

$$\delta^2 J = \mathcal{Q}_F(\delta U(T), \delta U(T)) \tag{75}$$

This HQF was studied for evolution-operator control [208–210] and observable control [148, 218–220]. The optimality of regular critical points can be determined by inspecting the number of positive, negative, and null eigenvalues of the Hessian or, equivalently, the coefficients of the HQF when written in a diagonal basis. An issue of special interest is to determine whether any of the regular extremal controls are local maxima (frequently referred to as local traps due to their ability to halt searches guided by gradient algorithms before reaching the global maximum). A detailed analysis for evolution-operator control and observable control reveals [147, 148, 208–210, 218–220] that for controllable closed quantum systems all regular optima are global, that is, no local traps exist. Except for the global maximum and minimum, the remainder of regular extrema are saddle points. Moreover, a recent numerical study [629] indicated that none of the identified singular critical points are local traps. The basic steps in the derivations of these important results are presented below.

To analyze the kinematic structure of the landscape (i.e., the dependence of J on $U(T)$) in the vicinity of a regular critical point, it is convenient to use the local expansion of the evolution operator to its unitary neighborhood: $U(T) \to e^{isA}U(T)$, as in Eq. (50). The second-order variation in J of Eq. (75) is then given by

$$\delta^2 J(A) = \left. \frac{d^2 J}{ds^2} \right|_{s=0} \tag{76}$$

where the Hermitian operator A serves as a kinematic variable on the landscape.

For evolution-operator control, using J of the form (51) and Eq. (76), one obtains

$$\delta^2 J(A) = -\frac{1}{N} \mathrm{Re}\left\{ \mathrm{Tr}\left[A^2 W^\dagger U(T) \right] \right\} \tag{77}$$

Using Eq. (58), the HQF at the kth critical submanifold can be expressed as

$$\delta^2 J_k(A) = -\frac{1}{N}\mathrm{Re}\{\mathrm{Tr}[\tilde{A}^2 X_k]\} \tag{78}$$

where the operator X_k is given by Eq. (55) and $\tilde{A} = YAY^\dagger$, $Y \in \mathfrak{G}_k$. Using an orthonormal basis $\{|\ell\rangle\}$, Eq. (78) can be expressed as

$$\delta^2 J_k(A) = -\frac{1}{N}\sum_{\ell=1}^{N} x_{k,\ell}\langle\ell|\tilde{A}^2|\ell\rangle, \qquad x_{k,\ell} = \begin{cases} -1, & \ell \le k \\ +1, & \ell > k \end{cases} \tag{79}$$

For $k = 0$, the critical point $J_0 = 1$ is the global maximum; indeed, $X_0 = I_N$ has only positive eigenvalues, and the HQF at this point is always negative. For $k = N$, the critical point $J_N = -1$ is the global minimum; indeed, $X_N = -I_N$ has only negative eigenvalues, and the HQF at this point is always positive. For critical submanifolds corresponding to $k = 1, 2, \ldots, N-1$, the operator X_k has both positive and negative eigenvalues, and therefore $\delta^2 J_k(A)$ has both positive and negative diagonal coefficients. This result proves that all regular local extrema are saddle points.

The Hessian of J can be also expressed in the dynamic picture of the QCL (i.e., when J is considered as a functional of $\varepsilon(\cdot)$). For the Hamiltonian of the form (14), it can be shown that [148]

$$\frac{\delta U(t)}{\delta\varepsilon(t')} = \frac{i}{\hbar}U(t)\mu(t') \tag{80}$$

$$\frac{\delta\mu(t)}{\delta\varepsilon(t')} = \frac{i}{\hbar}[\mu(t), \mu(t')] \tag{81}$$

for $t \ge t'$. Using these results, the Hessian

$$\mathrm{H}(t, t') := \frac{\delta^2 J}{\delta\varepsilon(t')\delta\varepsilon(t)} \tag{82}$$

can be expressed as [210]

$$\mathrm{H}(t, t') = -\frac{1}{\hbar^2 N}\mathrm{Re}\{\mathrm{Tr}[W^\dagger U(T)\mu(t)\mu(t')]\} \tag{83}$$

Correspondingly, at the critical submanifold $\mathfrak{M}_k(U)$, the Hessian is given by

$$\mathrm{H}_k(t, t') = -\frac{1}{\hbar^2 N}\mathrm{Re}\{\mathrm{Tr}\,[X_k\tilde{\mu}(t)\tilde{\mu}(t')]\,\} \tag{84}$$

where $\tilde{\mu}(t) = Y\mu(t)Y^\dagger$, $Y \in \mathfrak{G}_k$. The bounds on the Hessian as well as its ranks and signatures at the critical submanifolds were obtained by Ho et al. [210].

A similar analysis of the HQF can also be performed for observable control. Using J of the form (61), Eq. (76), and condition (63) for kinematic critical points, one obtains:

$$\delta^2 J(A) = 2\mathrm{Tr}\left[AU(T)\rho_0 U^\dagger(T)A\Theta - A^2 U(T)\rho_0 U^\dagger(T)\Theta\right] \tag{85}$$

At a critical submanifold $\mathfrak{M}_\pi(U)$ corresponding to a permutation π, the HQF is

$$\delta^2 J_\pi(A) = 2\mathrm{Tr}\left[\tilde{A}P_\pi\tilde{\rho}_0 P_\pi^{-1}\tilde{A}\tilde{\Theta} - \tilde{A}^2 P_\pi\tilde{\rho}_0 P_\pi^{-1}\tilde{\Theta}\right] \tag{86}$$

where $\tilde{\rho}_0 = R^\dagger\rho R$, $\tilde{\Theta} = S^\dagger\Theta S$, $\tilde{A} = S^\dagger A S$, and R and S are unitary matrices defined by Eqs. (64) and (65). Based on Eq. (86), it can be shown [219, 220] that, besides the two submanifolds corresponding to the global maximum and minimum of J, the HQF at any other critical submanifold has both positive and negative diagonal coefficients; that is, all regular local extrema are saddle points. In the special case of state transition control, the HQF at the global maximum and minimum manifolds is given by

$$\delta^2 J_{\max}(A) = -\delta^2 J_{\min}(A) = -\sum_{\ell \neq 1} |\tilde{A}_{\ell 1}|^2 \tag{87}$$

where $\{\tilde{A}_{\ell\ell'}\}$ are matrix elements of $\tilde{A}$ in the same basis as the diagonal representation of $\tilde{\rho}_0$ and $\tilde{\Theta}$.

An expression for the Hessian of J in the dynamic picture of the QCL, for the Hamiltonian of the form (14), was obtained by Ho and Rabitz [148]:

$$\mathrm{H}(t,t') = -\frac{1}{\hbar^2}\mathrm{Tr}\left\{[[\Theta(T),\mu(t')],\mu(t)]\rho_0\right\} \tag{88}$$

where $\Theta(T) = U^\dagger(T)\Theta U(T)$ is the target observable in the Heisenberg picture at the final time. They also obtained bounds on the Hessian, computed its ranks at the critical submanifolds, and used the expression (88) to prove the absence of local traps among regular critical points in the QCL for observable control [148].

Analysis of the Hessian of the objective functional was also extended (in the kinematic picture) to the QCL for observable control of finite-dimensional open quantum systems with Kraus-map dynamics [274]. The QCL topology of such systems has the same basic characteristics as that of closed quantum systems described above; that is, all regular critical submanifolds, except for the global maximum and minimum, consist of saddle points. The underlying assumption of this analysis is Kraus-map controllability (see Section III). Also, it was recently shown [633] that the evolution of a quantum system undergoing real-time feedback control (RTFC), including effects of measurements, feedback actions, and interactions with auxiliary quantum systems, can be generally represented by a Kraus

map. Therefore, open-loop control, AFC, and RTFC, despite the operational and technological differences between them, have a common fundamental property, as they all share the same QCL topology, characterized by the absence of local traps under the assumption of Kraus-map controllability.

C. Pareto Optimality for Multiobjective Control

Many practical quantum control problems seek to optimize multiple, often competing, objectives. In such situations, the usual notion of optimality is replaced by that of Pareto optimality. The *Pareto front* of a multiobjective control problem is the set of all controls such that all other controls have a lower value for at least one of the objectives [246–248]. The analysis of the Pareto front reveals the nature of conflicts and trade-offs between different control objectives. The structure of the landscape for multiobservable control is of interest and follows directly from that of single-observable control [244]. Of particular relevance to many chemical and physical applications is the problem of simultaneous maximization of the expectation values of multiple observables. Such simultaneous maximization is possible if the intersection $\bigcap_i \mathfrak{M}_i^{(\max)}$ (where $\mathfrak{M}_i^{(\max)}$ is the maximum submanifold of the ith objective) is nonempty and a point in the intersection can be reached under some control $\varepsilon(\cdot)$; in this regard, the dimension of the intersection manifold $\bigcap_i \mathfrak{M}_i^{(\max)}$ has been analyzed [245]. It has been shown that the common QOCT technique of running many independent maximizations of a cost functional such as (23) (using different weight coefficients $\{\alpha_i\}$) is incapable of sampling many regions of the Pareto front [245]. Alternative methods for Pareto front sampling are discussed further below.

D. Landscape Exploration via Homotopy Trajectory Control

The absence of local traps in QCLs for observable control and evolution-operator control has important implications for the design of optimization algorithms. Many practical applications require algorithms capable of searching QCLs for optimal solutions that satisfy additional criteria, such as minimization of the field fluence or maximization of the robustness to laser noise. So-called *homotopy trajectory control* algorithms (in particular, diffeomorphic modulation under observable-response-preserving homotopy (D-MORPH)) [285–287] can follow paths to the global maximum of a Mayer-type cost functional, exploiting the trap-free nature of the QCL, while locally optimizing auxiliary costs. The essential prerequisite for successful use of these algorithms is the existence of a connected path between initial and target controls under the posed conditions. Homotopy trajectory control is closely related to the notion of a level set that is defined as the collection of controls that all produce the same value of the cost functional J. Theoretical analysis [147, 286, 287] predicts that for controllable quantum systems in the kinematic picture, each level set is a continuous manifold. A homotopy trajectory algorithm

is able to move on such a manifold exploring different control solutions that result in the same value of the cost functional, but may differ in other properties (e.g., the field fluence or robustness). A version of the D-MORPH algorithm was also developed for evolution-operator control of closed quantum systems; this algorithm was able to identify optimal controls generating a target unitary transformation up to machine precision [328].

Homotopy trajectory algorithms are also very useful for exploring QCLs for multiple objectives. For example, in order to traverse the space of expectation values of multiple observables while locally minimizing a Lagrange-type cost, a special control algorithm was developed [244]. This algorithm is also applicable to a general class of Pareto quantum optimal control problems [245]. The algorithm can traverse the Pareto front to identify admissible trade-offs in optimization of multiple control objectives (e.g., maximization of multiple observable expectation values). This method can continuously sample the Pareto front during the course of one optimization run [245] and thus can be more efficient than the use of standard QOCT with cost functionals of the form (23).

E. Practical Importance of Control Landscape Analysis

The absence of local traps in QCLs of controllable quantum systems has very important implications for the feasibility of AFC experiments (see Section V). The relationship between the QCL structure and the optimization complexity of algorithms used in AFC has been the subject of recent theoretical analyses [147, 149–151]. The results of these studies support the vast empirical evidence [148], indicating that the favorable QCL topology strongly correlates with fast mean convergence times to the global optimum. The trap-free QCL topology also ensures convergence of gradient-based optimization algorithms to the global maximum. These algorithms can be used to search for optimal solutions to a variety of quantum control problems. In addition to theoretical studies (mostly using QOCT), gradient algorithms are also applicable in quantum control experiments [152], provided that measurement of the gradient is sufficiently robust to laser and detection noise (see Section V.P).

The theory of QCLs was also used to explain a dramatic degree of inherent robustness to laser-field noise, observed in many AFC experiments involving strong-field control of nonlinear photophysical and photochemical processes (e.g., high-harmonic generation (see Section V.A.3), multiphoton ionization (see Section V.C), and molecular fragmentation (see Section V.E)). This behavior can be understood in terms of an extensive null space of the Hessian at the top of the QCL, implying a very gentle slope near the global maximum [218, 221]. This characteristic of the QCL makes it possible to tolerate much of the laser noise while maintaining a high control yield. Such robustness is expected to be a key attractive feature of observable control across virtually all quantum phenomena.

Significant efforts have been recently devoted to experimental observation of QCLs, aiming both at testing the predictions of the theoretical analysis and at obtaining a better understanding of control mechanisms. Roslund et al. [634] observed quantum control level sets (for maximization of nonresonant two-photon absorption in a molecule and second harmonic generation in a nonlinear crystal) and found them to be continuous manifolds (closed surfaces) in the QCL. A diverse family of control mechanisms was encountered, as each of the multiple control fields forming a level set preserves the observable value by exciting a distinct pattern of constructive and destructive quantum interferences.

Wollenhaupt, Baumert, and coworkers [635, 636] employed parameterized pulse shapes to reduce the dimensionality of the optimization problem (maximization of the Autler–Townes contrast in strong-field ionization of potassium atoms) and observed the corresponding two-dimensional QCL. To better understand the performance of AFC, the evolution of different optimization procedures was visualized by means of trajectories on the surface of the measured QCL. Marquetand et al. [637] observed a two-dimensional QCL (for maximization of the retinal photoisomerization yield in bacteriorhodopsin) and used it to elucidate the properties of molecular wave packet evolution on the excited-state PES. It is important to note that the theoretical analysis of QCL topology has been carried out with no constraints placed on the controls (see Sections VII.A and VII.B). A main conclusion from these studies is the inherent lack of local traps on the QCLs. However, significant constraints on the controls can distort and isolate portions of the erstwhile trap-free landscape to produce apparent (i.e., false) traps. Such structure has been seen in some experimental studies [635–637] in which the number of control variables was artificially reduced.

VIII. CONCLUSIONS

This chapter reviewed several important topics in the field of quantum control, including controllability of closed and open quantum systems, the formalism of QOCT, AFC of quantum phenomena in the laboratory, and the theory of QCLs. We also attempted to emphasize the synergistic connection between the theoretical and experimental advances, which has been of central importance for the recent development of the field. There are many aspects of quantum control that we are unable to discuss here in sufficient detail. We refer the interested reader to thematic reviews available on many topics, including single-parameter control methods [3, 5, 6, 20, 61, 62, 82, 83], controllability of quantum dynamics [10], the formalism and applications of QOCT [10, 11, 130, 131], femtosecond pulse-shaping technology [7, 97–99], applications of laboratory AFC [8, 9, 12, 13, 17–19, 133, 135, 138, 638], quantum control experiments with "rational" control designs [14, 22, 23], and the formalism of QCLs [147].

Among theoretical advances made in the last few years in the general area of quantum control, the introduction of QCLs is of special note. The analysis of the QCL topology provides the basis for understanding the complexity of optimizing different types of control objectives in the laboratory. In turn, this understanding can help identify the most suitable optimization algorithms for various theoretical and experimental applications of quantum control (see Sections VII.D, VII.E, and V.P). In addition, the landscape analysis may be extended to the study of quantum control problems involving simultaneous optimization of multiple objectives (see sections VII.C and VII.D). This research area is still at an early stage of development with much remaining to be investigated. In particular, an open issue that deserves significant attention is the effect of field constraints (e.g., due to limited laboratory resources) on the accessible regions of QCLs.

There are several additional research directions for which exploration of the QCL features may provide important insights. One ubiquitous problem with wide-ranging implications is evaluation of the robustness of control solutions to noise and imperfections, which depends on the degree of flatness of the QCL around an optimal solution. The landscape-assisted robustness analysis may have important implications for design of various systems and processes, from chemical reactions to quantum computers. Another interesting issue is related to a phenomenon discovered for observable control of an open quantum system prepared in a mixed state and coupled to a thermal environment [274]. Specifically, the range of the QCL (i.e., the difference between maximum and minimum expectation values of the target observable) decreases when the temperature of the environment rises. Therefore, an important application of the QCL analysis would be determination of the fundamental thermodynamic limits on the control yield for open quantum systems.

Quantum optimal control may facilitate future advances in many new areas of research. In particular, the ability to steer quantum evolution in an optimal fashion should be useful for acquiring better knowledge of the structure and dynamical behavior of quantum systems, as well as the mechanisms by which physical and chemical phenomena can be managed. For example, in many AFC experiments, the characteristics of the resultant optimal control fields were used (often in combination with additional measurements and simulations) to decipher physical mechanisms responsible for the achieved control [446–450, 452, 460, 476, 479, 480, 490, 492–498, 502, 503, 515, 517, 519, 533, 534, 538, 542–544]. However, much additional theoretical and experimental work is still needed to better understand the controlled dynamics of complex systems.

A challenging problem of particular importance is to clarify the role of coherent quantum effects in the control of photophysical and photochemical phenomena in the condensed phase. In a related area, recent experimental studies reported manifestations of long-lived electronic quantum coherence in energy transfer processes in photosynthetic systems [639–643]. Evidence of long-lived electronic and

vibrational quantum coherence was also found in intrachain energy transfer in a conjugated polymer [644, 645]. These findings have attracted significant attention [646–649] to the possible role of quantum coherence in efficient biological light-harvesting and other phenomena involving energy transfer at the macromolecular level. A number of theoretical models [650–670] were developed to explain the existence of quantum transport in the presence of strong coupling to a thermal environment. An important open issue of immediate relevance is the possibility of using quantum control methods to optimally manipulate and explore the dynamics of energy transfer and other photoinduced processes in complex chemical and biological systems.

Hamiltonian identification is another potentially important application of quantum control aimed at revealing detailed information about physical systems. Extraction of the Hamiltonian from measured data is an inverse problem that generally suffers from ill-posedness due to inevitable incompleteness of the data used for inversion. Recent attempts to address this challenging problem include Hamiltonian identification via inversion of time-dependent data (instead of traditional use of time-independent spectroscopic data) [671–676] and application of global, nonlinear, map-facilitated inversion procedures [677, 678]. In this context, it appears that suitable controls can be used to significantly increase the information content of the measured data. For example, it may be possible to control the motion of a molecular wave packet to gain more information on interatomic forces in selected regions of a PES [130]. An interesting proposal that may further advance this concept is *optimal Hamiltonian identification* [679, 680], which aims to employ coherent control of quantum dynamics to minimize the uncertainty in the extracted Hamiltonian despite finite data resolution and noise.

Control of quantum phenomena is a thriving research field characterized by a remarkable growing breadth of applications. As virtually all atomic and molecular dynamical processes should be amenable to control, the field is still young in its development, notwithstanding the many major advances made in recent years. We hope that this perspective on the many important directions of theoretical and experimental quantum control research will contribute to facilitating future progress in the field.

Acknowledgments

This work was supported by DOE, NSF, ARO, and Lockheed Martin.

References

1. P. Brumer and M. Shapiro, *Annu. Rev. Phys. Chem.*, **43**, 257–282 (1992).
2. W. S. Warren, H. Rabitz, and M. Dahleh, *Science*, **259**, 1581–1589 (1993).
3. R. J. Gordon and S. A. Rice, *Annu. Rev. Phys. Chem.*, **48**, 601–641 (1997).
4. H. Rabitz, R. de Vivie-Riedle, M. Motzkus, and K. Kompa, *Science*, **288**, 824–828 (2000).

5. S. A. Rice and M. Zhao, *Optical Control of Molecular Dynamics*, Wiley, New York, 2000.
6. P. Brumer and M. Shapiro, *Principles of the Quantum Control of Molecular Processes*, Wiley-Interscience, Hoboken, NJ, 2003.
7. D. Goswami, *Phys. Rep.*, **374**, 385–481 (2003).
8. T. Brixner and G. Gerber, *ChemPhysChem*, **4**, 418–438 (2003).
9. P. Nuernberger, G. Vogt, T. Brixner, and G. Gerber, *Phys. Chem. Chem. Phys.*, **9**, 2470–2497 (2007).
10. D. D'Alessandro, *Introduction to Quantum Control and Dynamics*, Chapman & Hall/CRC, Boca Raton, FL, 2007.
11. G. G. Balint-Kurti, S. Zou, and A. Brown, in *Advances in Chemical Physics*, Vol. 138, S. A. Rice, ed., Wiley, New York, 2008, pp. 43–94.
12. R. J. Levis and H. A. Rabitz, *J. Phys. Chem. A*, **106**, 6427–6444 (2002).
13. T. C. Weinacht and P. H. Bucksbaum, *J. Opt. B Quantum Semiclassical Opt.*, **4**, R35–R52 (2002).
14. M. Dantus and V. V. Lozovoy, *Chem. Rev.*, **104**, 1813–1860 (2004).
15. R. E. Carley, E. Heesel, and H. H. Fielding, *Chem. Soc. Rev.*, **34**, 949–969 (2005).
16. M. Wollenhaupt, V. Engel, and T. Baumert, *Annu. Rev. Phys. Chem.*, **56**, 25–56 (2005).
17. W. Wohlleben, T. Buckup, J. L. Herek, and M. Motzkus, *ChemPhysChem*, **6**, 850–857 (2005).
18. T. Pfeifer, C. Spielmann, and G. Gerber, *Rep. Prog. Phys.*, **69**, 443–505 (2006).
19. C. Winterfeldt, C. Spielmann, and G. Gerber, *Rev. Mod. Phys.*, **80**, 117–140 (2008).
20. K. Ohmori, *Annu. Rev. Phys. Chem.*, **60**, 487–511 (2009).
21. L. G. C. Rego, L. F. Santos, and V. S. Batista, *Annu. Rev. Phys. Chem.*, **60**, 293–320 (2009).
22. Y. Silberberg, *Annu. Rev. Phys. Chem.*, **60**, 277–292 (2009).
23. F. Krausz and M. Ivanov, *Rev. Mod. Phys.*, **81**, 163–234 (2009).
24. V. S. Letokhov, *Phys. Today*, **30**, 23–32 (1977).
25. N. Bloembergen and E. Yablonovitch, *Phys. Today*, **31**, 23–30 (1978).
26. A. H. Zewail, *Phys. Today*, **33**, 25–33 (1980).
27. N. Bloembergen and A. H. Zewail, *J. Phys. Chem.*, **88**, 5459–5465 (1984).
28. T. Elsaesser and W. Kaiser, *Annu. Rev. Phys. Chem.*, **42**, 83–107 (1991).
29. A. H. Zewail, *J. Phys. Chem.*, **100**, 12701–12724 (1996).
30. P. Brumer and M. Shapiro, *Chem. Phys. Lett.*, **126**, 541–546 (1986).
31. P. Brumer and M. Shapiro, *Faraday Discuss. Chem. Soc.*, **82**, 177–185 (1986).
32. M. Shapiro, J. W. Hepburn, and P. Brumer, *Chem. Phys. Lett.*, **149**, 451–454 (1988).
33. P. Brumer and M. Shapiro, *Acc. Chem. Res.*, **22**, 407–413 (1989).
34. D. J. Tannor and S. A. Rice, *J. Chem. Phys.*, **83**, 5013–5018 (1985).
35. D. J. Tannor, R. Kosloff, and S. A. Rice, *J. Chem. Phys.*, **85**, 5805–5820 (1986).
36. S. Shi, A. Woody, and H. Rabitz, *J. Chem. Phys.*, **88**, 6870–6883 (1988).
37. A. P. Peirce, M. A. Dahleh, and H. Rabitz, *Phys. Rev. A*, **37**, 4950–4964 (1988).
38. S. Shi and H. Rabitz, *Chem. Phys.*, **139**, 185–199 (1989).
39. R. Kosloff, S. A. Rice, P. Gaspard, S. Tersigni, and D. J. Tannor, *Chem. Phys.*, **139**, 201–220 (1989).
40. W. Jakubetz, J. Manz, and H.-J. Schreier, *Chem. Phys. Lett.*, **165**, 100–106 (1990).
41. C. K. Chan, P. Brumer, and M. Shapiro, *J. Chem. Phys.*, **94**, 2688–2696 (1991).

42. Z. Chen, P. Brumer, and M. Shapiro, *J. Chem. Phys.*, **98**, 6843–6852 (1993).
43. S. Lee, *J. Chem. Phys.*, **108**, 3903–3908 (1998).
44. C. Chen, Y.-Y. Yin, and D. S. Elliott, *Phys. Rev. Lett.*, **64**, 507–510 (1990).
45. C. Chen and D. S. Elliott, *Phys. Rev. Lett.*, **65**, 1737–1740 (1990).
46. S. M. Park, S.-P. Lu, and R. J. Gordon, *J. Chem. Phys.*, **94**, 8622–8624 (1991).
47. S.-P. Lu, S. M. Park, Y. Xie, and R. J. Gordon, *J. Chem. Phys.*, **96**, 6613–6620 (1992).
48. G. Xing, X. Wang, X. Huang, R. Bersohn, and B. Katz, *J. Chem. Phys.*, **104**, 826–831 (1996).
49. X. Wang, R. Bersohn, K. Takahashi, M. Kawasaki, and H. L. Kim, *J. Chem. Phys.*, **105**, 2992–2997 (1996).
50. H. G. Muller, P. H. Bucksbaum, D. W. Schumacher, and A. Zavriyev, *J. Phys. B At. Mol. Opt. Phys.*, **23**, 2761–2769 (1990).
51. D. W. Schumacher, F. Weihe, H. G. Muller, and P. H. Bucksbaum, *Phys. Rev. Lett.*, **73**, 1344–1347 (1994).
52. Y.-Y. Yin, C. Chen, D. S. Elliott, and A. V. Smith, *Phys. Rev. Lett.*, **69**, 2353–2356 (1992).
53. Y.-Y. Yin, D. S. Elliott, R. Shehadeh, and E. R. Grant, *Chem. Phys. Lett.*, **241**, 591–596 (1995).
54. B. Sheehy, B. Walker, and L. F. DiMauro, *Phys. Rev. Lett.*, **74**, 4799–4802 (1995).
55. V. D. Kleiman, L. Zhu, X. Li, and R. J. Gordon, *J. Chem. Phys.*, **102**, 5863–5866 (1995).
56. V. D. Kleiman, L. Zhu, J. Allen, and R. J. Gordon, *J. Chem. Phys.*, **103**, 10800–10803 (1995).
57. L. Zhu, V. Kleiman, X. Li, S.-P. Lu, K. Trentelman, and R. J. Gordon, *Science*, **270**, 77–80 (1995).
58. E. Dupont, P. B. Corkum, H. C. Liu, M. Buchanan, and Z. R. Wasilewski, *Phys. Rev. Lett.*, **74**, 3596–3599 (1995).
59. A. Haché, Y. Kostoulas, R. Atanasov, J. L. P. Hughes, J. E. Sipe, and H. M. van Driel, *Phys. Rev. Lett.*, **78**, 306–309 (1997).
60. C. Chen and D. S. Elliott, *Phys. Rev. A*, **53**, 272–279 (1996).
61. M. Shapiro and P. Brumer, *J. Chem. Soc., Faraday Trans.*, **93**, 1263–1277 (1997).
62. M. Shapiro and P. Brumer, *Rep. Prog. Phys.*, **66**, 859–942 (2003).
63. T. Baumert, M. Grosser, R. Thalweiser, and G. Gerber, *Phys. Rev. Lett.*, **67**, 3753–3756 (1991).
64. T. Baumert, B. Bühler, M. Grosser, R. Thalweiser, V. Weiss, E. Wiedenmann, and G. Gerber, *J. Phys. Chem.*, **95**, 8103–8110 (1991).
65. T. Baumert and G. Gerber, *Isr. J. Chem.*, **34**, 103–114 (1994).
66. E. D. Potter, J. L. Herek, S. Pedersen, Q. Liu, and A. H. Zewail, *Nature*, **355**, 66–68 (1992).
67. J. L. Herek, A. Materny, and A. H. Zewail, *Chem. Phys. Lett.*, **228**, 15–25 (1994).
68. F. Gai, J. C. McDonald, and P. A. Anfinrud, *J. Am. Chem. Soc.*, **119**, 6201–6202 (1997).
69. S. L. Logunov, V. V. Volkov, M. Braun, and M. A. El-Sayed, *Proc. Natl. Acad. Sci. USA*, **98**, 8475–8479 (2001).
70. S. Ruhman, B. Hou, N. Friedman, M. Ottolenghi, and M. Sheves, *J. Am. Chem. Soc.*, **124**, 8854–8858 (2002).
71. D. S. Larsen, M. Vengris, I. H. van Stokkum, M. A. van der Horst, F. L. de Weerd, K. J. Hellingwerf, and R. van Grondelle, *Biophys. J.*, **86**, 2538–2550 (2004).
72. D. S. Larsen, I. H. van Stokkum, M. Vengris, M. A. van der Horst, F. L. de Weerd, K. J. Hellingwerf, and R. van Grondelle, *Biophys. J.*, **87**, 1858–1872 (2004).
73. D. S. Larsen and R. van Grondelle, *ChemPhysChem*, **6**, 828–837 (2005).
74. M. Vengris, D. S. Larsen, M. A. van der Horst, O. F. A. Larsen, K. J. Hellingwerf, and R. van Grondelle, *J. Phys. Chem. B*, **109**, 4197–4208 (2005).

75. M. Vengris, I. H. M. van Stokkum, X. He, A. F. Bell, P. J. Tonge, R. van Grondelle, and D. S. Larsen, *J. Phys. Chem. A,* **108**, 4587–4598 (2004).
76. U. Gaubatz, P. Rudecki, M. Becker, S. Schiemann, M. Külz, and K. Bergmann, *Chem. Phys. Lett.*, **149**, 463–468 (1988).
77. J. R. Kuklinski, U. Gaubatz, F. T. Hioe, and K. Bergmann, *Phys. Rev. A*, **40**, 6741–6744 (1989).
78. U. Gaubatz, P. Rudecki, S. Schiemann, and K. Bergmann, *J. Chem. Phys.*, **92**, 5363–5376 (1990).
79. B. W. Shore, K. Bergmann, J. Oreg, and S. Rosenwaks, *Phys. Rev. A*, **44**, 7442–7447 (1991).
80. M. N. Kobrak and S. A. Rice, *Phys. Rev. A*, **57**, 2885–2894 (1998).
81. M. Demirplak and S. A. Rice, *J. Chem. Phys.*, **116**, 8028–8035 (2002).
82. K. Bergmann, H. Theuer, and B. W. Shore, *Rev. Mod. Phys.*, **70**, 1003–1025 (1998).
83. N. V. Vitanov, T. Halfmann, B. W. Shore, and K. Bergmann, *Annu. Rev. Phys. Chem.*, **52**, 763–809 (2001).
84. L. D. Noordam, D. I. Duncan, and T. F. Gallagher, *Phys. Rev. A*, **45**, 4734–4737 (1992).
85. R. R. Jones, C. S. Raman, D. W. Schumacher, and P. H. Bucksbaum, *Phys. Rev. Lett.*, **71**, 2575–2578 (1993).
86. R. R. Jones, D. W. Schumacher, T. F. Gallagher, and P. H. Bucksbaum, *J. Phys. B At. Mol. Opt. Phys.*, **28**, L405–L411 (1995).
87. V. Blanchet, C. Nicole, M.-A. Bouchene, and B. Girard, *Phys. Rev. Lett.*, **78**, 2716–2719 (1997).
88. M.-A. Bouchene, V. Blanchet, C. Nicole, N. Melikechi, B. Girard, H. Ruppe, S. Rutz, E. Schreiber, and L. Wöste, *Eur. Phys. J. D*, **2**, 131–141 (1998).
89. N. F. Scherer, R. J. Carlson, A. Matro, M. Du, A. J. Ruggiero, V. Romero-Rochin, J. A. Cina, G. R. Fleming, and S. A. Rice, *J. Chem. Phys.*, **95**, 1487–1511 (1991).
90. N. F. Scherer, A. Matro, L. D. Ziegler, M. Du, R. J. Carlson, J. A. Cina, and G. R. Fleming, *J. Chem. Phys.*, **96**, 4180–4194 (1992).
91. V. Blanchet, M. A. Bouchène, and B. Girard, *J. Chem. Phys.*, **108**, 4862–4876 (1998).
92. C. Doulé, E. Hertz, L. Berguiga, R. Chaux, B. Lavorel, and O. Faucher, *J. Phys. B At. Mol. Opt. Phys.*, **34**, 1133–1142 (2001).
93. K. Ohmori, Y. Sato, E. E. Nikitin, and S. A. Rice, *Phys. Rev. Lett.*, **91**, 243003 (2003).
94. E. Hertz, O. Faucher, B. Lavorel, and R. Chaux, *J. Chem. Phys.*, **113**, 6132–6138 (2000).
95. N. H. Bonadeo, J. Erland, D. Gammon, D. Park, D. S. Katzer, and D. G. Steel, *Science*, **282**, 1473–1476 (1998).
96. T. Flissikowski, A. Betke, I. A. Akimov, and F. Henneberger, *Phys. Rev. Lett.*, **92**, 227401 (2004).
97. H. Kawashima, M. M. Wefers, and K. A. Nelson, *Annu. Rev. Phys. Chem.*, **46**, 627–656 (1995).
98. A. M. Weiner, *Prog. Quantum Electron.*, **19**, 161–237 (1995).
99. A. M. Weiner, *Rev. Sci. Instrum.*, **71**, 1929–1960 (2000).
100. C. J. Bardeen, Q. Wang, and C. V. Shank, *Phys. Rev. Lett.*, **75**, 3410–3413 (1995).
101. B. Kohler, V. V. Yakovlev, J. Che, J. L. Krause, M. Messina, K. R. Wilson, N. Schwentner, R. M. Whitnell, and Y. Yan, *Phys. Rev. Lett.*, **74**, 3360–3363 (1995).
102. C. J. Bardeen, J. Che, K. R. Wilson, V. V. Yakovlev, V. A. Apkarian, C. C. Martens, R. Zadoyan, B. Kohler, and M. Messina, *J. Chem. Phys.*, **106**, 8486–8503 (1997).
103. C. J. Bardeen, J. Che, K. R. Wilson, V. V. Yakovlev, P. Cong, B. Kohler, J. L. Krause, and M. Messina, *J. Phys. Chem. A*, **101**, 3815–3822 (1997).
104. C. J. Bardeen, Q. Wang, and C. V. Shank, *J. Phys. Chem. A*, **102**, 2759–2766 (1998).
105. K. Misawa and T. Kobayashi, *J. Chem. Phys.*, **113**, 7546–7553 (2000).

106. S. Malkmus, R. Dürr, C. Sobotta, H. Pulvermacher, W. Zinth, and M. Braun, *J. Phys. Chem. A*, **109**, 10488–10492 (2005).

107. J. S. Melinger, S. R. Gandhi, A. Hariharan, J. X. Tull, and W. S. Warren, *Phys. Rev. Lett.*, **68**, 2000–2003 (1992).

108. B. Broers, H. B. van Linden van den Heuvell, and L. D. Noordam, *Phys. Rev. Lett.*, **69**, 2062–2065 (1992).

109. P. Balling, D. J. Maas, and L. D. Noordam, *Phys. Rev. A*, **50**, 4276–4285 (1994).

110. V. D. Kleiman, S. M. Arrivo, J. S. Melinger, and E. J. Heilweil, *Chem. Phys.*, **233**, 207–216 (1998).

111. T. Witte, T. Hornung, L. Windhorn, D. Proch, R. de Vivie-Riedle, M. Motzkus, and K. L. Kompa, *J. Chem. Phys.*, **118**, 2021–2024 (2003).

112. T. Witte, J. S. Yeston, M. Motzkus, E. J. Heilweil, and K.-L. Kompa, *Chem. Phys. Lett.*, **392**, 156–161 (2004).

113. A. Assion, T. Baumert, J. Helbing, V. Seyfried, and G. Gerber, *Chem. Phys. Lett.*, **259**, 488–494 (1996).

114. G. Cerullo, C. J. Bardeen, Q. Wang, and C. V. Shank, *Chem. Phys. Lett.*, **262**, 362–368 (1996).

115. C. J. Bardeen, V. V. Yakovlev, J. A. Squier, and K. R. Wilson, *J. Am. Chem. Soc.*, **120**, 13023–13027 (1998).

116. G. J. Brakenhoff, A. H. Buist, M. Müller, J. A. Squier, C. J. Bardeen, V. V. Yakovlev, and K. R. Wilson, *Proc. SPIE*, **3605**, 40–47 (1999).

117. G. Vogt, P. Nuernberger, R. Selle, F. Dimler, T. Brixner, and G. Gerber, *Phys. Rev. A*, **74**, 033413 (2006).

118. T. Chen, A. Vierheilig, P. Waltner, M. Heid, W. Kiefer, and A. Materny, *Chem. Phys. Lett.*, **326**, 375–382 (2000).

119. T. Hellerer, A. M. Enejder, and A. Zumbusch, *Appl. Phys. Lett.*, **85**, 25–27 (2004).

120. K. P. Knutsen, J. C. Johnson, A. E. Miller, P. B. Petersen, and R. J. Saykally, *Chem. Phys. Lett.*, **387**, 436–441 (2004).

121. M. Wollenhaupt, A. Präkelt, C. Sarpe-Tudoran, D. Liese, and T. Baumert, *Appl. Phys. B*, **82**, 183–188 (2006).

122. M. Krug, T. Bayer, M. Wollenhaupt, C. Sarpe-Tudoran, T. Baumert, S. S. Ivanov, and N. V. Vitanov, *New J. Phys.*, **11**, 105051 (2009).

123. M. P. A. Branderhorst, P. Londero, P. Wasylczyk, C. Brif, R. L. Kosut, H. Rabitz, and I. A. Walmsley, *Science*, **320**, 638–643 (2008).

124. S. Shi and H. Rabitz, *J. Chem. Phys.*, **92**, 364–376 (1990).

125. S. Shi and H. Rabitz, *J. Chem. Phys.*, **92**, 2927–2937 (1990).

126. M. Dahleh, A. P. Peirce, and H. Rabitz, *Phys. Rev. A*, **42**, 1065–1079 (1990).

127. S. Shi and H. Rabitz, *Comput. Phys. Commun.*, **63**, 71–83 (1991).

128. P. Gross, D. Neuhauser, and H. Rabitz, *J. Chem. Phys.*, **94**, 1158–1166 (1991).

129. M. Sugawara and Y. Fujimura, *J. Chem. Phys.*, **100**, 5646–5655 (1994).

130. H. Rabitz and W. S. Zhu, *Acc. Chem. Res.*, **33**, 572–578 (2000).

131. J. Werschnik and E. K. U. Gross, *J. Phys. B At. Mol. Opt. Phys.*, **40**, R175–R211 (2007).

132. R. S. Judson and H. Rabitz, *Phys. Rev. Lett.*, **68**, 1500–1503 (1992).

133. T. Brixner, N. Damrauer, and G. Gerber, in *Advances in Atomic, Molecular, and Optical Physics*, Vol. 46, B. Bederson and H. Walther, eds., Academic Press, San Diego, 2001, pp. 1–54.

134. C. Brif and H. Rabitz, in *Fundamentals of Chemistry*, S. Carra, ed., Vol. 6 of *Encyclopedia of Life Support Systems*, EOLSS Publishers, Oxford, 2003.
135. T. Brixner, N. H. Damrauer, G. Krampert, P. Niklaus, and G. Gerber, *J. Mod. Opt.*, **50**, 539–560 (2003).
136. I. Walmsley and H. Rabitz, *Phys. Today*, **56**, 43–49 (2003).
137. T. Brixner and G. Gerber, *Phys. Scr.*, **T110**, 101–107 (2004).
138. T. Brixner, T. Pfeifer, G. Gerber, M. Wollenhaupt, and T. Baumert, in *Femtosecond Laser Spectroscopy*, P. Hannaford, ed., Springer, New York, 2005, chapter 9.
139. E. Brown and H. Rabitz, *J. Math. Chem.*, **31**, 17–63 (2002).
140. D. Zeidler, S. Frey, K.-L. Kompa, and M. Motzkus, *Phys. Rev. A*, **64**, 023420 (2001).
141. H. Rabitz, *Theor. Chem. Acc.*, **109**, 64–70 (2003).
142. G. M. Huang, T. J. Tarn, and J. W. Clark, *J. Math. Phys.*, **24**, 2608–2618 (1983).
143. V. Ramakrishna, M. V. Salapaka, M. Dahleh, H. Rabitz, and A. Peirce, *Phys. Rev. A*, **51**, 960–966 (1995).
144. M. Zhao and S. A. Rice, *J. Chem. Phys.*, **95**, 2465–2472 (1991).
145. M. Demiralp and H. Rabitz, *Phys. Rev. A*, **47**, 809–816 (1993).
146. H. Rabitz, M. Hsieh, and C. Rosenthal, *Science*, **303**, 1998–2001 (2004).
147. R. Chakrabarti and H. Rabitz, *Int. Rev. Phys. Chem.*, **26**, 671–735 (2007).
148. T.-S. Ho and H. Rabitz, *J. Photochem. Photobiol. A*, **180**, 226–240 (2006).
149. R. Chakrabarti, R. B. Wu, and H. Rabitz, arXiv:0708.3513 (2008).
150. K. Moore, M. Hsieh, and H. Rabitz, *J. Chem. Phys.*, **128**, 154117 (2008).
151. A. Oza, A. Pechen, J. Dominy, V. Beltrani, K. Moore, and H. Rabitz, *J. Phys. A Math. Theor.*, **42**, 205305 (2009).
152. J. Roslund and H. Rabitz, *Phys. Rev. A*, **79**, 053417 (2009).
153. J. Roslund, O. M. Shir, T. Bäck, and H. Rabitz, *Phys. Rev. A*, **80**, 043415 (2009).
154. H.-P. Breuer and F. Petruccione, *The Theory of Open Quantum Systems*, Oxford University Press, New York, 2002.
155. C. W. Gardiner and P. Zoller, *Quantum Noise: A Handbook of Markovian and Non-Markovian Quantum Stochastic Methods with Applications to Quantum Optics*, Springer, Berlin, 2004.
156. P. van der Walle, M. T. W. Milder, L. Kuipers, and J. L. Herek, *Proc. Natl. Acad. Sci. USA*, **106**, 7714–7717 (2009).
157. M. Roth, L. Guyon, J. Roslund, V. Boutou, F. Courvoisier, J.-P. Wolf, and H. Rabitz, *Phys. Rev. Lett.*, **102**, 253001 (2009).
158. M. A. Nielsen and I. L. Chuang, *Quantum Computation and Quantum Information*, Cambridge University Press, Cambridge, 2000.
159. K. Kraus, *States, Effects and Operations: Fundamental Notions of Quantum Theory*, Vol. 190 of *Lecture Notes in Physics*, Springer, Berlin, 1983.
160. R. Alicki and K. Lendi, *Quantum Dynamical Semigroups and Applications*, Vol. 717 of *Lecture Notes in Physics*, Springer, Berlin, 2007.
161. M.-D. Choi, *Linear Algebra Appl.*, **10**, 285–290 (1975).
162. G. Lindblad, *Commun. Math. Phys.*, **48**, 119–130 (1976).
163. G. Turinici and H. Rabitz, *Chem. Phys.*, **267**, 1–9 (2001).
164. G. Turinici and H. Rabitz, *J. Phys. A Math. Gen.*, **36**, 2565–2576 (2003).

165. F. Albertini and D. D'Alessandro, in *Proceedings of the 40th IEEE Conference on Decision and Control*, Vol. 2, pp. 1589–1594, 2001.
166. H. Fu, S. G. Schirmer, and A. I. Solomon, *J. Phys. A Math. Gen.*, **34**, 1679–1690 (2001).
167. S. G. Schirmer, H. Fu, and A. I. Solomon, *Phys. Rev. A*, **63**, 063410 (2001).
168. C. Altafini, *J. Math. Phys.*, **43**, 2051–2062 (2002).
169. M. D. Girardeau, S. G. Schirmer, J. V. Leahy, and R. M. Koch, *Phys. Rev. A*, **58**, 2684–2689 (1998).
170. S. G. Schirmer and J. V. Leahy, *Phys. Rev. A*, **63**, 025403 (2001).
171. S. G. Schirmer, A. I. Solomon, and J. V. Leahy, *J. Phys. A Math. Gen.*, **35**, 4125–4141 (2002).
172. S. G. Schirmer, A. I. Solomon, and J. V. Leahy, *J. Phys. A Math. Gen.*, **35**, 8551–8562 (2002).
173. A. Albertini and D. D'Alessandro, *IEEE Trans. Autom. Control*, **48**, 1399–1403 (2003).
174. S. P. Shah, D. J. Tannor, and S. A. Rice, *Phys. Rev. A*, **66**, 033405 (2002).
175. J. Gong and S. A. Rice, *Phys. Rev. A*, **69**, 063410 (2004).
176. S. G. Schirmer, I. C. H. Pullen, and A. I. Solomon, *J. Opt. B Quantum Semiclassical Opt.*, **7**, S293–S299 (2005).
177. G. Turinici and H. Rabitz, *J. Phys. A Math. Theor.*, **43**, 105303 (2010).
178. J. W. Clark, D. G. Lucarelli, and T. J. Tarn, *Int. J. Mod. Phys. B*, **17**, 5397–5411 (2003).
179. R. B. Wu, T. J. Tarn, and C. W. Li, *Phys. Rev. A*, **73**, 012719 (2006).
180. R. B. Wu, R. Chakrabarti, and H. Rabitz, *Phys. Rev. A*, **77**, 052303 (2008).
181. S. Lloyd and L. Viola, *Phys. Rev. A*, **65**, 010101 (2001).
182. A. I. Solomon and S. G. Schirmer, arXiv:quant-ph/0401094 (2004).
183. C. Altafini, *J. Math. Phys.*, **44**, 2357–2372 (2003).
184. C. Altafini, *Phys. Rev. A*, **70**, 062321 (2004).
185. R. Romano, *J. Phys. A Math. Gen.*, **38**, 9105–9114 (2005).
186. R. Wu, A. Pechen, C. Brif, and H. Rabitz, *J. Phys. A Math. Theor.*, **40**, 5681–5693 (2007).
187. R. Vilela Mendes, *Phys. Lett. A*, **373**, 2529–2532 (2009).
188. G. Dirr, U. Helmke, I. Kurniawan, and T. Schulte-Herbrüggen, *Rep. Math. Phys.*, **64**, 93–121 (2009).
189. A. Pechen and H. Rabitz, *Phys. Rev. A*, **73**, 062102 (2006).
190. H. M. Wiseman and G. J. Milburn, *Phys. Rev. A*, **49**, 4110–4125 (1994).
191. S. Lloyd, *Phys. Rev. A*, **62**, 022108 (2000).
192. R. J. Nelson, Y. Weinstein, D. Cory, and S. Lloyd, *Phys. Rev. Lett.*, **85**, 3045–3048 (2000).
193. H. Mabuchi, *Phys. Rev. A*, **78**, 032323 (2008).
194. M. Yanagisawa and H. Kimura, *IEEE Trans. Autom. Control*, **48**, 2107–2120 (2003).
195. M. Yanagisawa and H. Kimura, *IEEE Trans. Autom. Control*, **48**, 2121–2132 (2003).
196. R. Romano and D. D'Alessandro, *Phys. Rev. A*, **73**, 022323 (2006).
197. J. Nie, H. C. Fu, and X. X. Yi, *Quant. Inf. Comp.*, **10**, 87–96 (2010).
198. R. Vilela Mendes and V. I. Man'ko, *Phys. Rev. A*, **67**, 053404 (2003).
199. A. Pechen, N. Il'in, F. Shuang, and H. Rabitz, *Phys. Rev. A*, **74**, 052102 (2006).
200. F. Shuang, A. Pechen, T.-S. Ho, and H. Rabitz, *J. Chem. Phys.*, **126**, 134303 (2007).
201. F. Shuang, M. Zhou, A. Pechen, R. Wu, O. M. Shir, and H. Rabitz, *Phys. Rev. A*, **78**, 063422 (2008).

202. D. Dong, C. Zhang, H. Rabitz, A. Pechen, and T.-J. Tarn, *J. Chem. Phys.*, **129**, 154103 (2008).
203. K. Jacobs, *New J. Phys.*, **12**, 043005 (2010).
204. R. F. Stengel, *Optimal Control and Estimation*, Dover, Mineola, NY, 1994.
205. J. P. Palao and R. Kosloff, *Phys. Rev. Lett.*, **89**, 188301 (2002).
206. J. P. Palao and R. Kosloff, *Phys. Rev. A*, **68**, 062308 (2003).
207. R. A. Horn and C. R. Johnson, *Matrix Analysis*, Cambridge University Press, Cambridge, 1990.
208. H. Rabitz, M. Hsieh, and C. Rosenthal, *Phys. Rev. A*, **72**, 052337 (2005).
209. M. Hsieh and H. Rabitz, *Phys. Rev. A*, **77**, 042306 (2008).
210. T.-S. Ho, J. Dominy, and H. Rabitz, *Phys. Rev. A*, **79**, 013422 (2009).
211. A. Gilchrist, N. K. Langford, and M. A. Nielsen, *Phys. Rev. A*, **71**, 062310 (2005).
212. R. L. Kosut, M. Grace, C. Brif, and H. Rabitz, arXiv:quant-ph/0606064 (2006).
213. M. D. Grace, J. Dominy, R. L. Kosut, C. Brif, and H. Rabitz, *New J. Phys.*, **12**, 015001 (2010).
214. R. Jozsa, *J. Mod. Opt.*, **41**, 2315–2323 (1994).
215. C. A. Fuchs and J. van de Graaf, *IEEE Trans. Inf. Theory*, **45**, 1216–1227 (1999).
216. H. Jirari and W. Pötz, *Phys. Rev. A*, **72**, 013409 (2005).
217. H. Rabitz, M. Hsieh, and C. Rosenthal, *J. Chem. Phys.*, **124**, 204107 (2006).
218. Z. Shen, M. Hsieh, and H. Rabitz, *J. Chem. Phys.*, **124**, 204106 (2006).
219. R. B. Wu, H. Rabitz, and M. Hsieh, *J. Phys. A Math. Theor.*, **41**, 015006 (2008).
220. M. Hsieh, R. B. Wu, and H. Rabitz, *J. Chem. Phys.*, **130**, 104109 (2009).
221. H. Rabitz, T.-S. Ho, M. Hsieh, R. Kosut, and M. Demiralp, *Phys. Rev. A*, **74**, 012721 (2006).
222. J. Bertrand and P. Bertrand, *Found. Phys.*, **17**, 397–405 (1987).
223. K. Vogel and H. Risken, *Phys. Rev. A*, **40**, 2847–2849 (1989).
224. U. Leonhardt, *Measuring the Quantum State of Light*, Cambridge University Press, Cambridge, 1997.
225. V. Bužek, R. Derka, G. Adam, and P. L. Knight, *Annu. Phys.*, **266**, 454–496 (1998).
226. C. Brif and A. Mann, *Phys. Rev. A*, **59**, 971–987 (1999).
227. C. Brif and A. Mann, *J. Opt. B Quantum Semiclassical Opt.*, **2**, 245–251 (2000).
228. J. Řeháček, D. Mogilevtsev, and Z. Hradil, *New J. Phys.*, **10**, 043022 (2008).
229. G. M. D'Ariano and P. Lo Presti, *Phys. Rev. Lett.*, **86**, 4195–4198 (2001).
230. R. Kosut, I. A. Walmsley, and H. Rabitz, arXiv:quant-ph/0411093 (2004).
231. M. P. A. Branderhorst, I. A. Walmsley, R. L. Kosut, and H. Rabitz, *J. Phys. B At. Mol. Opt. Phys.*, **41**, 074004 (2008).
232. M. Mohseni, A. T. Rezakhani, and D. A. Lidar, *Phys. Rev. A*, **77**, 032322 (2008).
233. K. C. Young, M. Sarovar, R. Kosut, and K. B. Whaley, *Phys. Rev. A*, **79**, 062301 (2009).
234. J. Emerson, M. Silva, O. Moussa, C. Ryan, M. Laforest, J. Baugh, D. G. Cory, and R. Laflamme, *Science*, **317**, 1893–1896 (2007).
235. R. L. Kosut, arXiv:0812.4323 (2009).
236. M. P. A. Branderhorst, J. Nunn, I. A. Walmsley, and R. L. Kosut, *New J. Phys.*, **11**, 115010 (2009).
237. A. Shabani, R. L. Kosut, M. Mohseni, H. Rabitz, M. A. Broome, M. P. Almeida, A. Fedrizzi, and A. G. White, *Phys. Rev. Lett.*, **106**, 100401 (2011).
238. A. Bendersky, F. Pastawski, and J. P. Paz, *Phys. Rev. Lett.*, **100**, 190403 (2008).
239. C. T. Schmiegelow, M. A. Larotonda, and J. P. Paz, arXiv:1002.4436 (2010).

240. M. Cramer and M. B. Plenio, arXiv:1002.3780 (2010).
241. S. T. Flammia, D. Gross, S. D. Bartlett, and R. Somma, arXiv:1002.3839 (2010).
242. Y. Ohtsuki, K. Nakagami, Y. Fujimura, W. S. Zhu, and H. Rabitz, *J. Chem. Phys.*, **114**, 8867–8876 (2001).
243. O. M. Shir, M. Emmerich, T. Bäck, and M. J. J. Vrakking, in *Proceedings of IEEE Congress on Evolutionary Computation (CEC 2007)*, pp. 4108–4115, 2007.
244. R. Chakrabarti, R. B. Wu, and H. Rabitz, *Phys. Rev. A*, **77**, 063425 (2008).
245. R. Chakrabarti, R. B. Wu, and H. Rabitz, *Phys. Rev. A*, **78**, 033414 (2008).
246. V. Chankong and Y. Y. Haimes, *Multiobjective Decision Making Theory and Methodology*, North-Holland, New York, 1983.
247. R. E. Steuer, *Multiple Criteria Optimization: Theory, Computation and Application*, Wiley, New York, 1986.
248. K. M. Miettinen, *Nonlinear Multiobjective Optimization*, Kluwer, Norwell, MA, 1998.
249. V. Jurdjevic, *Geometric Control Theory*, Cambridge University Press, Cambridge, 1997.
250. D. D'Alessandro and M. Dahleh, *IEEE Trans. Autom. Control*, **46**, 866–876 (2001).
251. Y. J. Yan, R. E. Gillilan, R. M. Whitnell, K. R. Wilson, and S. Mukamel, *J. Phys. Chem.*, **97**, 2320–2333 (1993).
252. A. Bartana, R. Kosloff, and D. J. Tannor, *J. Chem. Phys.*, **99**, 196–210 (1993).
253. A. Bartana, R. Kosloff, and D. J. Tannor, *J. Chem. Phys.*, **106**, 1435–1448 (1997).
254. Y. Ohtsuki, W. S. Zhu, and H. Rabitz, *J. Chem. Phys.*, **110**, 9825–9832 (1999).
255. Y. Ohtsuki, K. Nakagami, W. S. Zhu, and H. Rabitz, *Chem. Phys.*, **287**, 197–216 (2003).
256. R. Xu, Y.-J. Yan, Y. Ohtsuki, Y. Fujimura, and H. Rabitz, *J. Chem. Phys.*, **120**, 6600–6608 (2004).
257. W. Cui, Z. R. Xi, and Y. Pan, *Phys. Rev. A*, **77**, 032117 (2008).
258. S. Beyvers and P. Saalfrank, *J. Chem. Phys.*, **128**, 074104 (2008).
259. Y. Ohtsuki, Y. Teranishi, P. Saalfrank, G. Turinici, and H. Rabitz, *Phys. Rev. A*, **75**, 033407 (2007).
260. M. Mohseni and A. T. Rezakhani, *Phys. Rev. A*, **80**, 010101 (2009).
261. J. Werschnik and E. K. U. Gross, *J. Opt. B Quantum Semiclassical Opt.*, **7**, S300–S312 (2005).
262. M. Lapert, R. Tehini, G. Turinici, and D. Sugny, *Phys. Rev. A*, **79**, 063411 (2009).
263. M. Lapert, R. Tehini, G. Turinici, and D. Sugny, *Phys. Rev. A*, **78**, 023408 (2008).
264. Y. Ohtsuki and K. Nakagami, *Phys. Rev. A*, **77**, 033414 (2008).
265. I. Serban, J. Werschnik, and E. K. U. Gross, *Phys. Rev. A*, **71**, 053810 (2005).
266. A. Kaiser and V. May, *J. Chem. Phys.*, **121**, 2528–2535 (2004).
267. I. Grigorenko, M. E. Garcia, and K. H. Bennemann, *Phys. Rev. Lett.*, **89**, 233003 (2002).
268. K. Mishima and K. Yamashita, *J. Chem. Phys.*, **130**, 034108 (2009).
269. K. Mishima and K. Yamashita, *J. Chem. Phys.*, **131**, 014109 (2009).
270. N. Khaneja, R. Brockett, and S. J. Glaser, *Phys. Rev. A*, **63**, 032308 (2001).
271. N. Khaneja, S. J. Glaser, and R. Brockett, *Phys. Rev. A*, **65**, 032301 (2002).
272. T. O. Reiss, N. Khaneja, and S. J. Glaser, *J. Magn. Reson.*, **154**, 192–195 (2002).
273. A. E. Bryson and Y.-C. Ho, *Applied Optimal Control: Optimization, Estimation and Control*, Taylor & Francis, Boca Raton, FL, 1975.
274. R. B. Wu, A. Pechen, H. Rabitz, M. Hsieh, and B. Tsou, *J. Math. Phys.*, **49**, 022108 (2008).
275. D. J. Tannor, V. Kazakov, and V. Orlov, in *Time Dependent Quantum Molecular Dynamics*, J. Broeckhove and L. Lathouwers, eds., Plenum Press, New York, 1992, pp. 347–360.

276. J. Somlói, V. A. Kazakov, and D. J. Tannor, *Chem. Phys.*, **172**, 85–98 (1993).
277. W. S. Zhu, J. Botina, and H. Rabitz, *J. Chem. Phys.*, **108**, 1953–1963 (1998).
278. W. S. Zhu and H. Rabitz, *J. Chem. Phys.*, **109**, 385–391 (1998).
279. G. Maday and G. Turinici, *J. Chem. Phys.*, **118**, 8191–8196 (2003).
280. Y. Ohtsuki, G. Turinici, and H. Rabitz, *J. Chem. Phys.*, **120**, 5509–5517 (2004).
281. A. Borzì, J. Salomon, and S. Volkwein, *J. Comput. Appl. Math.*, **216**, 170–197 (2008).
282. P. Ditz and A. Borzì, *Comput. Phys. Commun.*, **178**, 393–399 (2008).
283. W. S. Zhu and H. Rabitz, *J. Chem. Phys.*, **110**, 7142–7152 (1999).
284. N. Khaneja, T. Reiss, C. Kehlet, T. Schulte-Herbrüggen, and S. J. Glaser, *J. Magn. Reson.*, **172**, 296–305 (2005).
285. C. Hillermeier, *Nonlinear Multiobjective Optimization: A Generalized Homotopy Approach*, Birkhäuser, Basel, 2001.
286. A. Rothman, T.-S. Ho, and H. Rabitz, *J. Chem. Phys.*, **123**, 134104 (2005).
287. A. Rothman, T.-S. Ho, and H. Rabitz, *Phys. Rev. A*, **73**, 053401 (2006).
288. A. Castro and E. K. U. Gross, *Phys. Rev. E*, **79**, 056704 (2009).
289. F. Yip, D. Mazziotti, and H. Rabitz, *J. Chem. Phys.*, **118**, 8168–8172 (2003).
290. G. G. Balint-Kurti, F. R. Manby, Q. Ren, M. Artamonov, T.-S. Ho, and H. Rabitz, *J. Chem. Phys.*, **122**, 084110 (2005).
291. M. Hsieh and H. Rabitz, *Phys. Rev. E*, **77**, 037701 (2008).
292. M. Artamonov, T.-S. Ho, and H. Rabitz, *Chem. Phys.*, **305**, 213–222 (2004).
293. M. Artamonov, T.-S. Ho, and H. Rabitz, *Chem. Phys.*, **328**, 147–155 (2006).
294. M. Artamonov, T.-S. Ho, and H. Rabitz, *J. Chem. Phys.*, **124**, 064306 (2006).
295. Y. Kurosaki, M. Artamonov, T.-S. Ho, and H. Rabitz, *J. Chem. Phys.*, **131**, 044306 (2009).
296. M. Kanno, K. Hoki, H. Kono, and Y. Fujimura, *J. Chem. Phys.*, **127**, 204314 (2007).
297. L. Wang and V. May, *Chem. Phys.*, **361**, 1–8 (2009).
298. S. G. Kosionis, A. F. Terzis, and E. Paspalakis, *Phys. Rev. B*, **75**, 193305 (2007).
299. E. Räsänen, A. Castro, J. Werschnik, A. Rubio, and E. K. U. Gross, *Phys. Rev. Lett.*, **98**, 157404 (2007).
300. E. Räsänen, A. Castro, J. Werschnik, A. Rubio, and E. K. U. Gross, *Phys. Rev. B*, **77**, 085324 (2008).
301. G. D. Chiara, T. Calarco, M. Anderlini, S. Montangero, P. J. Lee, B. L. Brown, W. D. Phillips, and J. V. Porto, *Phys. Rev. A*, **77**, 052333 (2008).
302. U. Hohenester, P. K. Rekdal, A. Borzì, and J. Schmiedmayer, *Phys. Rev. A*, **75**, 023602 (2007).
303. P. Doria, T. Calarco, and S. Montangero, *Phys. Rev. Lett.*, **106**, 190501 (2011).
304. H. Jirari, F. W. J. Hekking, and O. Buisson, *Europhys. Lett.*, **87**, 28004 (2009).
305. I. Grigorenko and H. Rabitz, *Appl. Phys. Lett.*, **94**, 253107 (2009).
306. A. Bartana, R. Kosloff, and D. J. Tannor, *Chem. Phys.*, **267**, 195–207 (2001).
307. J. Cao, M. Messina, and K. R. Wilson, *J. Chem. Phys.*, **106**, 5239–5248 (1997).
308. T. Mančal, U. Kleinekathöfer, and V. May, *J. Chem. Phys.*, **117**, 636–646 (2002).
309. K. Nakagami, Y. Ohtsuki, and Y. Fujimura, *Chem. Phys. Lett.*, **360**, 91–98 (2002).
310. S. Beyvers, Y. Ohtsuki, and P. Saalfrank, *J. Chem. Phys.*, **124**, 234706 (2006).
311. G. Q. Li, S. Welack, M. Schreiber, and U. Kleinekathöfer, *Phys. Rev. B*, **77**, 075321 (2008).
312. U. Hohenester and G. Stadler, *Phys. Rev. Lett.*, **92**, 196801 (2004).

313. S. E. Sklarz, D. J. Tannor, and N. Khaneja, *Phys. Rev. A*, **69**, 053408 (2004).
314. I. A. Grigorenko and D. V. Khveshchenko, *Phys. Rev. Lett.*, **94**, 040506 (2005).
315. H. Jirari and W. Pötz, *Phys. Rev. A*, **74**, 022306 (2006).
316. M. Wenin and W. Pötz, *Phys. Rev. A*, **74**, 022319 (2006).
317. W. Pötz, *J. Comput. Electron.*, **6**, 171–174 (2007).
318. A. Pelzer, S. Ramakrishna, and T. Seideman, *J. Chem. Phys.*, **129**, 134301 (2008).
319. J. P. Palao, R. Kosloff, and C. P. Koch, *Phys. Rev. A*, **77**, 063412 (2008).
320. H. Jirari, *Europhys. Lett.*, **87**, 40003 (2009).
321. G. Gordon, *J. Phys. B At. Mol. Opt. Phys.*, **42**, 223001 (2009).
322. G. D. Sanders, K. W. Kim, and W. C. Holton, *Phys. Rev. A*, **59**, 1098–1101 (1999).
323. S. E. Sklarz and D. J. Tannor, arXiv:quant-ph/0404081 (2004).
324. S. E. Sklarz and D. J. Tannor, *Chem. Phys.*, **322**, 87–97 (2006).
325. T. Schulte-Herbrüggen, A. Spörl, N. Khaneja, and S. J. Glaser, *Phys. Rev. A*, **72**, 042331 (2005).
326. A. Spörl, T. Schulte-Herbrüggen, S. J. Glaser, V. Bergholm, M. J. Storcz, J. Ferber, and F. K. Wilhelm, *Phys. Rev. A*, **75**, 012302 (2007).
327. R. de Vivie-Riedle and U. Troppmann, *Chem. Rev.*, **107**, 5082–5100 (2007).
328. J. Dominy and H. Rabitz, *J. Phys. A Math. Theor.*, **41**, 205305 (2008).
329. M. Schröder and A. Brown, *J. Chem. Phys.*, **131**, 034101 (2009).
330. V. Nebendahl, H. Häffner, and C. F. Roos, *Phys. Rev. A*, **79**, 012312 (2009).
331. S. Schirmer, *J. Mod. Opt.*, **56**, 831–839 (2009).
332. R. Nigmatullin and S. G. Schirmer, *New J. Phys.*, **11**, 105032 (2009).
333. R. Fisher, F. Helmer, S. J. Glaser, F. Marquardt, and T. Schulte-Herbrüggen, *Phys. Rev. B*, **81**, 085328 (2010).
334. C. Gollub, M. Kowalewski, and R. de Vivie-Riedle, *Phys. Rev. Lett.*, **101**, 073002 (2008).
335. M. Schröder and A. Brown, *New J. Phys.*, **11**, 105031 (2009).
336. I. A. Grigorenko and D. V. Khveshchenko, *Phys. Rev. Lett.*, **95**, 110501 (2005).
337. T. Schulte-Herbrüggen, A. Spörl, N. Khaneja, and S. J. Glaser, *J. Phys. B At. Mol. Opt. Phys.*, **44**, 154013 (2011).
338. U. Hohenester, *Phys. Rev. B*, **74**, 161307 (2006).
339. S. Montangero, T. Calarco, and R. Fazio, *Phys. Rev. Lett.*, **99**, 170501 (2007).
340. M. Grace, C. Brif, H. Rabitz, I. A. Walmsley, R. L. Kosut, and D. A. Lidar, *J. Phys. B At. Mol. Opt. Phys.*, **40**, S103–S125 (2007).
341. M. D. Grace, C. Brif, H. Rabitz, D. A. Lidar, I. A. Walmsley, and R. L. Kosut, *J. Mod. Opt.*, **54**, 2339–2349 (2007).
342. M. Wenin and W. Pötz, *Phys. Rev. A*, **78**, 012358 (2008).
343. M. Wenin and W. Pötz, *Phys. Rev. B*, **78**, 165118 (2008).
344. P. Rebentrost, I. Serban, T. Schulte-Herbrüggen, and F. K. Wilhelm, *Phys. Rev. Lett.*, **102**, 090401 (2009).
345. P. Rebentrost and F. K. Wilhelm, *Phys. Rev. B*, **79**, 060507 (2009).
346. F. Motzoi, J. M. Gambetta, P. Rebentrost, and F. K. Wilhelm, *Phys. Rev. Lett.*, **103**, 110501 (2009).
347. S. Safaei, S. Montangero, F. Taddei, and R. Fazio, *Phys. Rev. B*, **79**, 064524 (2009).
348. R. Roloff and W. Pötz, *Phys. Rev. B*, **79**, 224516 (2009).
349. M. Wenin, R. Roloff, and W. Pötz, *J. Appl. Phys.*, **105**, 084504 (2009).

350. R. Roloff, M. Wenin, and W. Pötz, *J. Comput. Electron.*, **8**, 29–34 (2009).
351. R. Roloff, M. Wenin, and W. Pötz, *J. Comput. Theor. Nanosci.*, **6**, 1837–1863 (2009).
352. F. Galve and E. Lutz, *Phys. Rev. A*, **79**, 032327 (2009).
353. R. Fisher, H. Yuan, A. Spörl, and S. Glaser, *Phys. Rev. A*, **79**, 042304 (2009).
354. X. Wang and S. G. Schirmer, *Phys. Rev. A*, **80**, 042305 (2009).
355. L. M. K. Vandersypen and I. L. Chuang, *Rev. Mod. Phys.*, **76**, 1037–1069 (2005).
356. C. A. Ryan, C. Negrevergne, M. Laforest, E. Knill, and R. Laflamme, *Phys. Rev. A*, **78**, 012328 (2008).
357. N. Timoney, V. Elman, S. Glaser, C. Weiss, M. Johanning, W. Neuhauser, and C. Wunderlich, *Phys. Rev. A*, **77**, 052334 (2008).
358. J. Nunn, I. A. Walmsley, M. G. Raymer, K. Surmacz, F. C. Waldermann, Z. Wang, and D. Jaksch, *Phys. Rev. A*, **75**, 011401 (2007).
359. A. V. Gorshkov, A. André, M. Fleischhauer, A. S. Sørensen, and M. D. Lukin, *Phys. Rev. Lett.*, **98**, 123601 (2007).
360. A. V. Gorshkov, T. Calarco, M. D. Lukin, and A. S. Sørensen, *Phys. Rev. A*, **77**, 043806 (2008).
361. I. Novikova, A. V. Gorshkov, D. F. Phillips, A. S. Sørensen, M. D. Lukin, and R. L. Walsworth, *Phys. Rev. Lett.*, **98**, 243602 (2007).
362. I. Novikova, N. B. Phillips, and A. V. Gorshkov, *Phys. Rev. A*, **78**, 021802 (2008).
363. N. B. Phillips, A. V. Gorshkov, and I. Novikova, *Phys. Rev. A*, **78**, 023801 (2008).
364. R. Chakrabarti and A. Ghosh, arXiv:0904.1628 (2009).
365. J. M. Geremia, W. S. Zhu, and H. Rabitz, *J. Chem. Phys.*, **113**, 10841–10848 (2000).
366. F. G. Omenetto, B. P. Luce, and A. J. Taylor, *J. Opt. Soc. Am. B*, **16**, 2005–2009 (1999).
367. T. Brixner, F. J. García de Abajo, J. Schneider, and W. Pfeiffer, *Phys. Rev. Lett.*, **95**, 093901 (2005).
368. T. Brixner, F. J. G. de Abajo, J. Schneider, C. Spindler, and W. Pfeiffer, *Phys. Rev. B*, **73**, 125437 (2006).
369. T. Brixner, F. García de Abajo, C. Spindler, and W. Pfeiffer, *Appl. Phys. B*, **84**, 89–95 (2006).
370. E. Hertz, A. Rouzée, S. Guérin, B. Lavorel, and O. Faucher, *Phys. Rev. A*, **75**, 031403 (2007).
371. D. Voronine, D. Abramavicius, and S. Mukamel, *J. Chem. Phys.*, **124**, 034104 (2006).
372. D. V. Voronine, D. Abramavicius, and S. Mukamel, *J. Chem. Phys.*, **126**, 044508 (2007).
373. P. Tuchscherer, C. Rewitz, D. V. Voronine, F. J. García de Abajo, W. Pfeiffer, and T. Brixner, *Opt. Express*, **17**, 14235–14259 (2009).
374. W. S. Zhu and H. Rabitz, *J. Chem. Phys.*, **118**, 6751–6757 (2003).
375. M. Grace, C. Brif, H. Rabitz, I. Walmsley, R. Kosut, and D. Lidar, *New J. Phys.*, **8**, 35 (2006).
376. C. Gollub and R. de Vivie-Riedle, *Phys. Rev. A*, **78**, 033424 (2008).
377. C. Gollub and R. de Vivie-Riedle, *Phys. Rev. A*, **79**, 021401 (2009).
378. R. R. Zaari and A. Brown, *J. Chem. Phys.*, **132**, 014307 (2010).
379. V. P. Belavkin, *Autom. Remote Control*, **44**, 178–188 (1983).
380. H. M. Wiseman and G. J. Milburn, *Phys. Rev. Lett.*, **70**, 548–551 (1993).
381. H. M. Wiseman, *Phys. Rev. A*, **49**, 2133–2150 (1994).
382. A. C. Doherty, S. Habib, K. Jacobs, H. Mabuchi, and S. M. Tan, *Phys. Rev. A*, **62**, 012105 (2000).
383. A. Doherty, J. Doyle, H. Mabuchi, K. Jacobs, and S. Habib, in *Proceedings of the 39th IEEE Conference on Decision and Control*, vol. 1, pp. 949–954, 2000.

384. H. M. Wiseman and G. J. Milburn, *Quantum Measurement and Control*, Cambridge University Press, Cambridge, 2010.

385. A. M. Weiner, D. E. Leaird, J. S. Patel, and J. R. Wullert, *Opt. Lett.*, **15**, 326 (1990).

386. M. M. Wefers and K. A. Nelson, *Opt. Lett.*, **18**, 2032–2034 (1993).

387. M. M. Wefers and K. A. Nelson, *Opt. Lett.*, **20**, 1047 (1995).

388. C. W. Hillegas, J. X. Tull, D. Goswami, D. Strickland, and W. S. Warren, *Opt. Lett.*, **19**, 737–739 (1994).

389. G. Stobrawa, M. Hacker, T. Feurer, D. Zeidler, M. Motzkus, and F. Reichel, *Appl. Phys. B*, **72**, 627–630 (2001).

390. A. Monmayrant and B. Chatel, *Rev. Sci. Instrum.*, **75**, 2668–2671 (2004).

391. A. Präkelt, M. Wollenhaupt, A. Assion, C. Horn, C. Sarpe-Tudoran, M. Winter, and T. Baumert, *Rev. Sci. Instrum.*, **74**, 4950–4953 (2003).

392. E. Frumker, E. Tal, Y. Silberberg, and D. Majer, *Opt. Lett.*, **30**, 2796–2798 (2005).

393. Z. Jiang, C.-B. Huang, D. E. Leaird, and A. M. Weiner, *Nat. Photonics*, **1**, 463–467 (2007).

394. Z. Jiang, C.-B. Huang, D. E. Leaird, and A. M. Weiner, *J. Opt. Soc. Am. B*, **24**, 2124–2128 (2007).

395. T. Brixner and G. Gerber, *Opt. Lett.*, **26**, 557–559 (2001).

396. T. Brixner, G. Krampert, P. Niklaus, and G. Gerber, *Appl. Phys. B*, **74**, S133–S144 (2002).

397. L. Polachek, D. Oron, and Y. Silberberg, *Opt. Lett.*, **31**, 631–633 (2006).

398. M. Plewicki, F. Weise, S. M. Weber, and A. Lindinger, *Appl. Opt.*, **45**, 8354–8359 (2006).

399. M. Ninck, A. Galler, T. Feurer, and T. Brixner, *Opt. Lett.*, **32**, 3379–3381 (2007).

400. O. Masihzadeh, P. Schlup, and R. A. Bartels, *Opt. Express*, **15**, 18025–18032 (2007).

401. M. Plewicki, S. M. Weber, F. Weise, and A. Lindinger, *Appl. Phys. B*, **86**, 259–263 (2007).

402. F. Weise and A. Lindinger, *Opt. Lett.*, **34**, 1258–1260 (2009).

403. D. Kupka, P. Schlup, and R. A. Bartels, *Rev. Sci. Instrum.*, **80**, 053110 (2009).

404. P. Nuernberger, G. Vogt, R. Selle, S. Fechner, T. Brixner, and G. Gerber, *Appl. Phys. B*, **88**, 519–526 (2007).

405. D. S. N. Parker, A. D. G. Nunn, R. S. Minns, and H. H. Fielding, *Appl. Phys. B*, **94**, 181–186 (2009).

406. R. Selle, P. Nuernberger, F. Langhojer, F. Dimler, S. Fechner, G. Gerber, and T. Brixner, *Opt. Lett.*, **33**, 803–805 (2008).

407. P. Nuernberger, R. Selle, F. Langhojer, F. Dimler, S. Fechner, G. Gerber, and T. Brixner, *J. Opt. A Pure Appl. Opt.*, **11**, 085202 (2009).

408. T. Baumert, T. Brixner, V. Seyfried, M. Strehle, and G. Gerber, *Appl. Phys. B*, **65**, 779–782 (1997).

409. D. Yelin, D. Meshulach, and Y. Silberberg, *Opt. Lett.*, **22**, 1793–1795 (1997).

410. T. Brixner, M. Strehle, and G. Gerber, *Appl. Phys. B*, **68**, 281–284 (1999).

411. E. Zeek, K. Maginnis, S. Backus, U. Russek, M. Murnane, G. Mourou, H. Kapteyn, and G. Vdovin, *Opt. Lett.*, **24**, 493–495 (1999).

412. E. Zeek, R. Bartels, M. M. Murnane, H. C. Kapteyn, S. Backus, and G. Vdovin, *Opt. Lett.*, **25**, 587–589 (2000).

413. D. Zeidler, T. Hornung, D. Proch, and M. Motzkus, *Appl. Phys. B*, **70**, S125–S131 (2000).

414. U. Siegner, M. Haiml, J. Kunde, and U. Keller, *Opt. Lett.*, **27**, 315–317 (2002).

415. A. Efimov, M. D. Moores, N. M. Beach, J. L. Krause, and D. H. Reitze, *Opt. Lett.*, **23**, 1915–1917 (1998).

416. A. Efimov, M. D. Moores, B. Mei, J. L. Krause, C. W. Siders, and D. H. Reitze, *Appl. Phys. B*, **70**, S133–S141 (2000).

417. D. Meshulach, D. Yelin, and Y. Silberberg, *J. Opt. Soc. Am. B*, **15**, 1615–1619 (1998).

418. T. Brixner, A. Oehrlein, M. Strehle, and G. Gerber, *Appl. Phys. B*, **70**, S119–S124 (2000).

419. T. Brixner, N. H. Damrauer, G. Krampert, P. Niklaus, and G. Gerber, *J. Opt. Soc. Am. B*, **20**, 878–881 (2003).

420. T. Suzuki, S. Minemoto, and H. Sakai, *Appl. Opt.*, **43**, 6047–6050 (2004).

421. M. Aeschlimann, M. Bauer, D. Bayer, T. Brixner, F. J. García de Abajo, W. Pfeiffer, M. Rohmer, C. Spindler, and F. Steeb, *Nature*, **446**, 301–304 (2007).

422. T. C. Weinacht, J. Ahn, and P. H. Bucksbaum, *Nature*, **397**, 233–235 (1999).

423. C. Leichtle, W. P. Schleich, I. S. Averbukh, and M. Shapiro, *Phys. Rev. Lett.*, **80**, 1418–1421 (1998).

424. D. Meshulach and Y. Silberberg, *Nature*, **396**, 239–242 (1998).

425. D. Meshulach and Y. Silberberg, *Phys. Rev. A*, **60**, 1287–1292 (1999).

426. T. Hornung, R. Meier, D. Zeidler, K.-L. Kompa, D. Proch, and M. Motzkus, *Appl. Phys. B*, **71**, 277–284 (2000).

427. N. Dudovich, B. Dayan, S. M. Gallagher Faeder, and Y. Silberberg, *Phys. Rev. Lett.*, **86**, 47–50 (2001).

428. C. Trallero-Herrero, J. L. Cohen, and T. Weinacht, *Phys. Rev. Lett.*, **96**, 063603 (2006).

429. E. Papastathopoulos, M. Strehle, and G. Gerber, *Chem. Phys. Lett.*, **408**, 65–70 (2005).

430. M. Wollenhaupt, A. Präkelt, C. Sarpe-Tudoran, D. Liese, and T. Baumert, *J. Opt. B Quantum Semiclassical Opt.*, **7**, S270–S276 (2005).

431. R. Bartels, S. Backus, E. Zeek, L. Misoguti, G. Vdovin, I. P. Christov, M. M. Murnane, and H. C. Kapteyn, *Nature*, **406**, 164–166 (2000).

432. R. Bartels, S. Backus, I. Christov, H. Kapteyn, and M. Murnane, *Chem. Phys.*, **267**, 277–289 (2001).

433. R. A. Bartels, M. M. Murnane, H. C. Kapteyn, I. Christov, and H. Rabitz, *Phys. Rev. A*, **70**, 043404 (2004).

434. D. H. Reitze, S. Kazamias, F. Weihe, G. Mullot, D. Douillet, F. Augé, O. Albert, V. Ramanathan, J. P. Chambaret, D. Hulin, and P. Balcou, *Opt. Lett.*, **29**, 86–88 (2004).

435. T. Pfeifer, R. Kemmer, R. Spitzenpfeil, D. Walter, C. Winterfeldt, G. Gerber, and C. Spielmann, *Opt. Lett.*, **30**, 1497–1499 (2005).

436. D. Walter, T. Pfeifer, C. Winterfeldt, R. Kemmer, R. Spitzenpfeil, G. Gerber, and C. Spielmann, *Opt. Express*, **14**, 3433–3442 (2006).

437. R. Spitzenpfeil, S. Eyring, C. Kern, C. Ott, J. Lohbreier, J. Henneberger, N. Franke, S. Jung, D. Walter, M. Weger, C. Winterfeldt, T. Pfeifer, and C. Spielmann, *Appl. Phys. A*, **96**, 69–81 (2009).

438. T. Pfeifer, D. Walter, C. Winterfeldt, C. Spielmann, and G. Gerber, *Appl. Phys. B*, **80**, 277–280 (2005).

439. T. Pfeifer, R. Spitzenpfeil, D. Walter, C. Winterfeldt, F. Dimler, G. Gerber, and C. Spielmann, *Opt. Express*, **15**, 3409–3416 (2007).

440. C. J. Bardeen, V. V. Yakovlev, K. R. Wilson, S. D. Carpenter, P. M. Weber, and W. S. Warren, *Chem. Phys. Lett.*, **280**, 151–158 (1997).

441. O. Nahmias, O. Bismuth, O. Shoshana, and S. Ruhman, *J. Phys. Chem. A*, **109**, 8246–8253 (2005).

442. S.-H. Lee, K.-H. Jung, J. H. Sung, K.-H. Hong, and C. H. Nam, *J. Chem. Phys.*, **117**, 9858–9861 (2002).

443. V. I. Prokhorenko, A. M. Nagy, and R. J. D. Miller, *J. Chem. Phys.*, **122**, 184502 (2005).

444. S. Zhang, Z. Sun, X. Zhang, Y. Xu, Z. Wang, Z. Xu, and R. Li, *Chem. Phys. Lett.*, **415**, 346–350 (2005).

445. T. Brixner, N. H. Damrauer, B. Kiefer, and G. Gerber, *J. Chem. Phys.*, **118**, 3692–3701 (2003).

446. M. A. Montgomery, R. R. Meglen, and N. H. Damrauer, *J. Phys. Chem. A*, **110**, 6391–6394 (2006).

447. M. A. Montgomery, R. R. Meglen, and N. H. Damrauer, *J. Phys. Chem. A*, **111**, 5126–5129 (2007).

448. M. A. Montgomery and N. H. Damrauer, *J. Phys. Chem. A*, **111**, 1426–1433 (2007).

449. I. Otake, S. S. Kano, and A. Wada, *J. Chem. Phys.*, **124**, 014501 (2006).

450. D. G. Kuroda, C. P. Singh, Z. Peng, and V. D. Kleiman, *Science*, **326**, 263–267 (2009).

451. L. Bonacina, J. Extermann, A. Rondi, V. Boutou, and J.-P. Wolf, *Phys. Rev. A*, **76**, 023408 (2007).

452. T. Okada, I. Otake, R. Mizoguchi, K. Onda, S. S. Kano, and A. Wada, *J. Chem. Phys.*, **121**, 6386–6391 (2004).

453. T. Brixner, G. Krampert, T. Pfeifer, R. Selle, G. Gerber, M. Wollenhaupt, O. Graefe, C. Horn, D. Liese, and T. Baumert, *Phys. Rev. Lett.*, **92**, 208301 (2004).

454. T. Suzuki, S. Minemoto, T. Kanai, and H. Sakai, *Phys. Rev. Lett.*, **92**, 133005 (2004).

455. S. M. Weber, M. Plewicki, F. Weise, and A. Lindinger, *J. Chem. Phys.*, **128**, 174306 (2008).

456. C. Lupulescu, A. Lindinger, M. Plewicki, A. Merli, S. M. Weber, and L. Wöste, *Chem. Phys.*, **296**, 63–69 (2004).

457. S. M. Weber, A. Lindinger, M. Plewicki, C. Lupulescu, F. Vetter, and L. Wöste, *Chem. Phys.*, **306**, 287–293 (2004).

458. B. Schäfer-Bung, R. Mitrić, V. Bonačić-Koutecký, A. Bartelt, C. Lupulescu, A. Lindinger, Š. Vajda, S. M. Weber, and L. Wöste, *J. Phys. Chem. A*, **108**, 4175–4179 (2004).

459. A. Lindinger, S. M. Weber, C. Lupulescu, F. Vetter, M. Plewicki, A. Merli, L. Wöste, A. F. Bartelt, and H. Rabitz, *Phys. Rev. A*, **71**, 013419 (2005).

460. A. F. Bartelt, T. Feurer, and L. Wöste, *Chem. Phys.*, **318**, 207–216 (2005).

461. A. Lindinger, S. M. Weber, A. Merli, F. Sauer, M. Plewicki, and L. Wöste, *J. Photochem. Photobiol. A*, **180**, 256–261 (2006).

462. A. Lindinger, F. Vetter, C. Lupulescu, M. Plewicki, S. M. Weber, A. Merli, and L. Wöste, *Chem. Phys. Lett.*, **397**, 123–127 (2004).

463. A. Lindinger, C. Lupulescu, M. Plewicki, F. Vetter, A. Merli, S. M. Weber, and L. Wöste, *Phys. Rev. Lett.*, **93**, 033001 (2004).

464. A. Lindinger, C. Lupulescu, F. Vetter, M. Plewicki, S. M. Weber, A. Merli, and L. Wöste, *J. Chem. Phys.*, **122**, 024312 (2005).

465. J. B. Ballard, H. U. Stauffer, Z. Amitay, and S. R. Leone, *J. Chem. Phys.*, **116**, 1350–1360 (2002).

466. C. Siedschlag, O. M. Shir, T. Bäck, and M. J. J. Vrakking, *Opt. Commun.*, **264**, 511–518 (2006).

467. O. M. Shir, V. Beltrani, T. Bäck, H. Rabitz, and M. J. J. Vrakking, *J. Phys. B At. Mol. Opt. Phys.*, **41**, 074021 (2008).

468. A. Rouzée, A. Gijsbertsen, O. Ghafur, O. M. Shir, T. Bäck, S. Stolte, and M. J. J. Vrakking, *New J. Phys.*, **11**, 105040 (2009).

469. M. Leibscher, I. S. Averbukh, and H. Rabitz, *Phys. Rev. Lett.*, **90**, 213001 (2003).

470. M. Leibscher, I. S. Averbukh, and H. Rabitz, *Phys. Rev. A*, **69**, 013402 (2004).

471. H. Stapelfeldt and T. Seideman, *Rev. Mod. Phys.*, **75**, 543–557 (2003).

472. C. Z. Bisgaard, M. D. Poulsen, E. Péronne, S. S. Viftrup, and H. Stapelfeldt, *Phys. Rev. Lett.*, **92**, 173004 (2004).

473. M. Renard, E. Hertz, B. Lavorel, and O. Faucher, *Phys. Rev. A*, **69**, 043401 (2004).

474. M. Renard, E. Hertz, S. Guérin, H. R. Jauslin, B. Lavorel, and O. Faucher, *Phys. Rev. A*, **72**, 025401 (2005).

475. C. Horn, M. Wollenhaupt, M. Krug, T. Baumert, R. de Nalda, and L. Bañares, *Phys. Rev. A*, **73**, 031401 (2006).

476. R. de Nalda, C. Horn, M. Wollenhaupt, M. Krug, L. Bañares, and T. Baumert, *J. Raman Spectrosc.*, **38**, 543–550 (2007).

477. D. Pinkham, K. E. Mooney, and R. R. Jones, *Phys. Rev. A*, **75**, 013422 (2007).

478. A. Assion, T. Baumert, M. Bergt, T. Brixner, B. Kiefer, V. Seyfried, M. Strehle, and G. Gerber, *Science*, **282**, 919–922 (1998).

479. M. Bergt, T. Brixner, B. Kiefer, M. Strehle, and G. Gerber, *J. Phys. Chem. A*, **103**, 10381–10387 (1999).

480. T. Brixner, B. Kiefer, and G. Gerber, *Chem. Phys.*, **267**, 241–246 (2001).

481. N. H. Damrauer, C. Dietl, G. Krampert, S.-H. Lee, K.-H. Jung, and G. Gerber, *Eur. Phys. J. D*, **20**, 71–76 (2002).

482. M. Bergt, T. Brixner, C. Dietl, B. Kiefer, and G. Gerber, *J. Organomet. Chem.*, **661**, 199–209 (2002).

483. R. J. Levis, G. M. Menkir, and H. Rabitz, *Science*, **292**, 709–713 (2001).

484. Š. Vajda, A. Bartelt, E.-C. Kaposta, T. Leisner, C. Lupulescu, S. Minemoto, P. Rosendo-Francisco, and L. Wöste, *Chem. Phys.*, **267**, 231–239 (2001).

485. A. Bartelt, S. Minemoto, C. Lupulescu, Š. Vajda, and L. Wöste, *Eur. Phys. J. D*, **16**, 127–131 (2001).

486. A. Lindinger, C. Lupulescu, A. Bartelt, Š. Vajda, and L. Wöste, *Spectrochim. Acta B At. Spectrosc.*, **58**, 1109–1124 (2003).

487. A. Bartelt, A. Lindinger, C. Lupulescu, Š. Vajda, and L. Wöste, *Phys. Chem. Chem. Phys.*, **6**, 1679–1686 (2004).

488. E. Wells, K. J. Betsch, C. W. S. Conover, M. J. DeWitt, D. Pinkham, and R. R. Jones, *Phys. Rev. A*, **72**, 063406 (2005).

489. L. Palliyaguru, J. Sloss, H. Rabitz, and R. J. Levis, *J. Mod. Opt.*, **55**, 177–185 (2008).

490. C. Daniel, J. Full, L. González, C. Kaposta, M. Krenz, C. Lupulescu, J. Manz, S. Minemoto, M. Oppel, P. Rosendo-Francisco, Š. Vajda, and L. Wöste, *Chem. Phys.*, **267**, 247–260 (2001).

491. Š. Vajda, P. Rosendo-Francisco, C. Kaposta, M. Krenz, C. Lupulescu, and L. Wöste, *Eur. Phys. J. D*, **16**, 161–164 (2001).

492. C. Daniel, J. Full, L. González, C. Lupulescu, J. Manz, A. Merli, Š. Vajda, and L. Wöste, *Science*, **299**, 536–539 (2003).

493. D. Cardoza, M. Baertschy, and T. Weinacht, *J. Chem. Phys.*, **123**, 074315 (2005).

494. D. Cardoza, M. Baertschy, and T. Weinacht, *Chem. Phys. Lett.*, **411**, 311–315 (2005).

495. D. Cardoza, F. Langhojer, C. Trallero-Herrero, O. L. A. Monti, and T. Weinacht, *Phys. Rev. A*, **70**, 053406 (2004).

496. F. Langhojer, D. Cardoza, M. Baertschy, and T. Weinacht, *J. Chem. Phys.*, **122**, 014102 (2005).

497. D. Cardoza, C. Trallero-Herrero, F. Langhojer, H. Rabitz, and T. Weinacht, *J. Chem. Phys.*, **122**, 124306 (2005).

498. D. Cardoza, B. J. Pearson, M. Baertschy, and T. Weinacht, *J. Photochem. Photobiol A*, **180**, 277–281 (2006).

499. V. V. Lozovoy, X. Zhu, T. C. Gunaratne, D. A. Harris, J. C. Shane, and M. Dantus, *J. Phys. Chem. A*, **112**, 3789–3812 (2008).

500. X. Zhu, T. C. Gunaratne, V. V. Lozovoy, and M. Dantus, *J. Phys. Chem. A*, **113**, 5264–5266 (2009).

501. R. J. Levis, *J. Phys. Chem. A*, **113**, 5267–5268 (2009).

502. T. Hornung, R. Meier, and M. Motzkus, *Chem. Phys. Lett.*, **326**, 445–453 (2000).

503. T. C. Weinacht, R. Bartels, S. Backus, P. H. Bucksbaum, B. Pearson, J. M. Geremia, H. Rabitz, H. C. Kapteyn, and M. M. Murnane, *Chem. Phys. Lett.*, **344**, 333–338 (2001).

504. R. A. Bartels, T. C. Weinacht, S. R. Leone, H. C. Kapteyn, and M. M. Murnane, *Phys. Rev. Lett.*, **88**, 033001 (2002).

505. T. C. Weinacht, J. L. White, and P. H. Bucksbaum, *J. Phys. Chem. A*, **103**, 10166–10168 (1999).

506. B. J. Pearson, J. L. White, T. C. Weinacht, and P. H. Bucksbaum, *Phys. Rev. A*, **63**, 063412 (2001).

507. J. L. White, B. J. Pearson, and P. H. Bucksbaum, *J. Phys. B At. Mol. Opt. Phys.*, **37**, L399–L405 (2004).

508. B. J. Pearson and P. H. Bucksbaum, *Phys. Rev. Lett.*, **92**, 243003 (2004).

509. M. Spanner and P. Brumer, *Phys. Rev. A*, **73**, 023809 (2006).

510. M. Spanner and P. Brumer, *Phys. Rev. A*, **73**, 023810 (2006).

511. D. Zeidler, S. Frey, W. Wohlleben, M. Motzkus, F. Busch, T. Chen, W. Kiefer, and A. Materny, *J. Chem. Phys.*, **116**, 5231–5235 (2002).

512. J. Konradi, A. K. Singh, and A. Materny, *Phys. Chem. Chem. Phys.*, **7**, 3574–3579 (2005).

513. J. Konradi, A. Scaria, V. Namboodiri, and A. Materny, *J. Raman Spectrosc.*, **38**, 1006–1021 (2007).

514. J. Konradi, A. K. Singh, A. V. Scaria, and A. Materny, *J. Raman Spectrosc.*, **37**, 697–704 (2006).

515. J. Konradi, A. K. Singh, and A. Materny, *J. Photochem. Photobiol. A*, **180**, 289–299 (2006).

516. A. Scaria, J. Konradi, V. Namboodiri, and A. Materny, *J. Raman Spectrosc.*, **39**, 739–749 (2008).

517. S. Zhang, L. Zhang, X. Zhang, L. Ding, G. Chen, Z. Sun, and Z. Wang, *Chem. Phys. Lett.*, **433**, 416–421 (2007).

518. B. von Vacano, W. Wohlleben, and M. Motzkus, *Opt. Lett.*, **31**, 413–415 (2006).

519. D. B. Strasfeld, S.-H. Shim, and M. T. Zanni, *Phys. Rev. Lett.*, **99**, 038102 (2007).

520. D. B. Strasfeld, C. T. Middleton, and M. T. Zanni, *New J. Phys.*, **11**, 105046 (2009).

521. H. Kawano, Y. Nabekawa, A. Suda, Y. Oishi, H. Mizuno, A. Miyawaki, and K. Midorikawa, *Biochem. Biophys. Res. Commun.*, **311**, 592–596 (2003).

522. J. Chen, H. Kawano, Y. Nabekawa, H. Mizuno, A. Miyawaki, T. Tanabe, F. Kannari, and K. Midorikawa, *Opt. Express.*, **12**, 3408–3414 (2004).

523. J. Tada, T. Kono, A. Suda, H. Mizuno, A. Miyawaki, K. Midorikawa, and F. Kannari, *Appl. Opt.*, **46**, 3023–3030 (2007).

524. K. Isobe, A. Suda, M. Tanaka, F. Kannari, H. Kawano, H. Mizuno, A. Miyawaki, and K. Midorikawa, *Opt. Express.*, **17**, 13737–13746 (2009).

525. B. Q. Li, G. Turinici, V. Ramakrishna, and H. Rabitz, *J. Phys. Chem. B*, **106**, 8125–8131 (2002).
526. G. Turinici, V. Ramakhrishna, B. Q. Li, and H. Rabitz, *J. Phys. A Math. Gen.*, **37**, 273–282 (2004).
527. B. Q. Li, W. S. Zhu, and H. Rabitz, *J. Chem. Phys.*, **124**, 024101 (2006).
528. T. Brixner, N. H. Damrauer, P. Niklaus, and G. Gerber, *Nature*, **414**, 57–60 (2001).
529. G. Vogt, G. Krampert, P. Niklaus, P. Nuernberger, and G. Gerber, *Phys. Rev. Lett.*, **94**, 068305 (2005).
530. K. Hoki and P. Brumer, *Phys. Rev. Lett.*, **95**, 168305 (2005).
531. P. A. Hunt and M. A. Robb, *J. Am. Chem. Soc.*, **127**, 5720–5726 (2005).
532. R. Improta and F. Santoro, *J. Chem. Theory Comput.*, **1**, 215–229 (2005).
533. B. Dietzek, B. Brüggemann, T. Pascher, and A. Yartsev, *Phys. Rev. Lett.*, **97**, 258301 (2006).
534. B. Dietzek, B. Brüggemann, T. Pascher, and A. Yartsev, *J. Am. Chem. Soc.*, **129**, 13014–13021 (2007).
535. K. Hoki and P. Brumer, *Chem. Phys. Lett.*, **468**, 23–27 (2009).
536. G. Katz, M. A. Ratner, and R. Kosloff, *New J. Phys.*, **12**, 015003 (2010).
537. V. I. Prokhorenko, A. M. Nagy, S. A. Waschuk, L. S. Brown, R. R. Birge, and R. J. D. Miller, *Science*, **313**, 1257–1261 (2006).
538. V. I. Prokhorenko, A. M. Nagy, L. S. Brown, and R. J. D. Miller, *Chem. Phys.*, **341**, 296–309 (2007).
539. G. Vogt, P. Nuernberger, T. Brixner, and G. Gerber, *Chem. Phys. Lett.*, **433**, 211–215 (2006).
540. A. C. Florean, D. Cardoza, J. L. White, J. K. Lanyi, R. J. Sension, and P. H. Bucksbaum, *Proc. Natl. Acad. Sci. USA*, **106**, 10896–10900 (2009).
541. E. C. Carroll, B. J. Pearson, A. C. Florean, P. H. Bucksbaum, and R. J. Sension, *J. Chem. Phys.*, **124**, 114506 (2006).
542. E. C. Carroll, J. L. White, A. C. Florean, P. H. Bucksbaum, and R. J. Sension, *J. Phys. Chem. A*, **112**, 6811–6822 (2008).
543. M. Kotur, T. Weinacht, B. J. Pearson, and S. Matsika, *J. Chem. Phys.*, **130**, 134311 (2009).
544. M. Greenfield, S. D. McGrane, and D. S. Moore, *J. Phys. Chem. A*, **113**, 2333–2339 (2009).
545. J. L. Herek, W. Wohlleben, R. J. Cogdell, D. Zeidler, and M. Motzkus, *Nature*, **417**, 533–535 (2002).
546. W. Wohlleben, T. Buckup, J. L. Herek, R. J. Cogdell, and M. Motzkus, *Biophys. J.*, **85**, 442–450 (2003).
547. T. Buckup, T. Lebold, A. Weigel, W. Wohlleben, and M. Motzkus, *J. Photochem. Photobiol. A*, **180**, 314–321 (2006).
548. B. Brüggemann, J. A. Organero, T. Pascher, T. Pullerits, and A. Yartsev, *Phys. Rev. Lett.*, **97**, 208301 (2006).
549. T. Laarmann, I. Shchatsinin, A. Stalmashonak, M. Boyle, N. Zhavoronkov, J. Handt, R. Schmidt, C. P. Schulz, and I. V. Hertel, *Phys. Rev. Lett.*, **98**, 058302 (2007).
550. J. Kunde, B. Baumann, S. Arlt, F. Morier-Genoud, U. Siegner, and U. Keller, *Appl. Phys. Lett.*, **77**, 924–926 (2000).
551. J. Kunde, B. Baumann, S. Arlt, F. Morier-Genoud, U. Siegner, and U. Keller, *J. Opt. Soc. Am. B*, **18**, 872–881 (2001).
552. J.-H. Chung and A. Weiner, *IEEE J. Sel. Top. Quantum Electron.*, **12**, 297–306 (2006).
553. C. Brif, H. Rabitz, S. Wallentowitz, and I. A. Walmsley, *Phys. Rev. A*, **63**, 063404 (2001).
554. U. Haeberlen, *High Resolution NMR in Solids*, Academic Press, New York, 1976.

555. L. Viola and S. Lloyd, *Phys. Rev. A*, **58**, 2733–2744 (1998).
556. L. Viola, E. Knill, and S. Lloyd, *Phys. Rev. Lett.*, **82**, 2417–2421 (1999).
557. P. Zanardi, *Phys. Lett. A*, **258**, 77–82 (1999).
558. D. Vitali and P. Tombesi, *Phys. Rev. A*, **59**, 4178–4186 (1999).
559. D. Vitali and P. Tombesi, *Phys. Rev. A*, **65**, 012305 (2001).
560. M. S. Byrd and D. A. Lidar, *Phys. Rev. A*, **67**, 012324 (2003).
561. K. Khodjasteh and D. A. Lidar, *Phys. Rev. Lett.*, **95**, 180501 (2005).
562. P. Facchi, S. Tasaki, S. Pascazio, H. Nakazato, A. Tokuse, and D. A. Lidar, *Phys. Rev. A*, **71**, 022302 (2005).
563. L. Viola and E. Knill, *Phys. Rev. Lett.*, **94**, 060502 (2005).
564. G. S. Uhrig, *Phys. Rev. Lett.*, **98**, 100504 (2007).
565. S. Pasini and G. S. Uhrig, *Phys. Rev. A*, **81**, 012309 (2010).
566. E. Fraval, M. J. Sellars, and J. J. Longdell, *Phys. Rev. Lett.*, **95**, 030506 (2005).
567. J. J. L. Morton, A. M. Tyryshkin, A. Ardavan, S. C. Benjamin, K. Porfyrakis, S. A. Lyon, and G. A. D. Briggs, *Nat. Phys.*, **2**, 40–43 (2006).
568. J. J. L. Morton, A. M. Tyryshkin, R. M. Brown, S. Shankar, B. W. Lovett, A. Ardavan, T. Schenkel, E. E. Haller, J. W. Ager, and S. A. Lyon, *Nature*, **455**, 1085–1088 (2008).
569. S. Damodarakurup, M. Lucamarini, G. Di Giuseppe, D. Vitali, and P. Tombesi, *Phys. Rev. Lett.*, **103**, 040502 (2009).
570. Y. Sagi, I. Almog, and N. Davidson, arXiv:0905.0286 (2009).
571. M. J. Biercuk, H. Uys, A. P. VanDevender, N. Shiga, W. M. Itano, and J. J. Bollinger, *Nature*, **458**, 996–1000 (2009).
572. S. D. McGrane, R. J. Scharff, M. Greenfield, and D. S. Moore, *New J. Phys.*, **11**, 105047 (2009).
573. F. Rossi and T. Kuhn, *Rev. Mod. Phys.*, **74**, 895–950 (2002).
574. R. Hanson, L. P. Kouwenhoven, J. R. Petta, S. Tarucha, and L. M. K. Vandersypen, *Rev. Mod. Phys.*, **79**, 1217 (2007).
575. J. Appel, E. Figueroa, D. Korystov, M. Lobino, and A. I. Lvovsky, *Phys. Rev. Lett.*, **100**, 093602 (2008).
576. K. S. Choi, H. Deng, J. Laurat, and H. J. Kimble, *Nature*, **452**, 67–71 (2008).
577. M. U. Staudt, S. R. Hastings-Simon, M. Nilsson, M. Afzelius, V. Scarani, R. Ricken, H. Suche, W. Sohler, W. Tittel, and N. Gisin, *Phys. Rev. Lett.*, **98**, 113601 (2007).
578. K. F. Reim, J. Nunn, V. O. Lorenz, B. J. Sussman, K. Lee, N. K. Langford, D. Jaksch, and I. A. Walmsley, *Nat. Photonics*, **4**, 218–221 (2010).
579. A. I. Lvovsky, B. C. Sanders, and W. Tittel, *Nat. Photonics*, **3**, 706–714 (2009).
580. C. Simon, M. Afzelius, J. Appel, A. B. de la Giroday, S. J. Dewhurst, N. Gisin, C. Y. Hu, F. Jelezko, S. Kroll, J. H. Muller, J. Nunn, E. Polzik, J. Rarity, H. de Riedmatten, W. Rosenfeld, A. J. Shields, N. Skold, R. M. Stevenson, R. Thew, I. Walmsley, M. Weber, H. Weinfurter, J. Wrachtrup, and R. J. Young, *Eur. Phys. J. D*, **58**, 1–22 (2010).
581. F. Solas, J. M. Ashton, A. Markmann, and H. A. Rabitz, *J. Chem. Phys.*, **130**, 214702 (2009).
582. Y. Makhlin, G. Schön, and A. Shnirman, *Rev. Mod. Phys.*, **73**, 357–400 (2001).
583. J. Clarke and F. K. Wilhelm, *Nature*, **453**, 1031–1042 (2008).
584. I. A. Walmsley, private communication (2009).
585. C. Liu, M. C. Kohler, K. Z. Hatsagortsyan, C. Muller, and C. H. Keitel, *New J. Phys.*, **11**, 105045 (2009).

586. H.-P. Schwefel, *Evolution and Optimum Seeking*, Wiley, New York, 1995.
587. D. E. Goldberg, *Genetic Algorithms in Search, Optimization, and Machine Learning*, Addison-Wesley, Reading, MA, 2007.
588. A. F. Bartelt, M. Roth, M. Mehendale, and H. Rabitz, *Phys. Rev. A*, **71**, 063806 (2005).
589. O. M. Shir, C. Siedschlag, T. Bäck, and M. J. J. Vrakking, *Artificial Evolution*, Vol. 3871 of *Lecture Notes in Computer Science*, Springer, Berlin, 2006, pp. 85–96.
590. C. M. Fonseca and P. J. Fleming, *Evol. Comput.*, **3**, 1–16 (1995).
591. K. Deb, *Evol. Comput.*, **7**, 205–230 (1999).
592. C. Gollub and R. de Vivie-Riedle, *New J. Phys.*, **11**, 013019 (2009).
593. S. Kirkpatrick, J. Gelatt, C. D., and M. P. Vecchi, *Science*, **220**, 671–680 (1983).
594. M. Dorigo, V. Maniezzo, and A. Colorni, *IEEE Trans. Syst. Man Cybern. B*, **26**, 29–41 (1996).
595. E. Bonabeau, M. Dorigo, and G. Theraulaz, *Nature*, **406**, 39–42 (2000).
596. T. Feurer, *Appl. Phys. B*, **68**, 55–60 (1999).
597. A. Glaß, T. Rozgonyi, T. Feurer, R. Sauerbrey, and G. Szabó, *Appl. Phys. B*, **71**, 267–276 (2000).
598. R. R. Ernst, *Principles of Nuclear Magnetic Resonance in One and Two Dimensions*, Oxford University Press, Oxford, 1990.
599. M. H. Levitt, *Spin Dynamics*, Wiley, New York, 2001.
600. N. Dudovich, D. Oron, and Y. Silberberg, *Nature*, **418**, 512–514 (2002).
601. D. Oron, N. Dudovich, D. Yelin, and Y. Silberberg, *Phys. Rev. Lett.*, **88**, 063004 (2002).
602. D. Oron, N. Dudovich, and Y. Silberberg, *Phys. Rev. Lett.*, **89**, 273001 (2002).
603. D. Oron, N. Dudovich, D. Yelin, and Y. Silberberg, *Phys. Rev. A*, **65**, 043408 (2002).
604. N. Dudovich, D. Oron, and Y. Silberberg, *J. Chem. Phys.*, **118**, 9208–9215 (2003).
605. D. Oron, N. Dudovich, and Y. Silberberg, *Phys. Rev. Lett.*, **90**, 213902 (2003).
606. E. Gershgoren, R. A. Bartels, J. T. Fourkas, R. Tobey, M. M. Murnane, and H. C. Kapteyn, *Opt. Lett.*, **28**, 361–363 (2003).
607. I. Pastirk, J. D. Cruz, K. Walowicz, V. Lozovoy, and M. Dantus, *Opt. Express*, **11**, 1695–1701 (2003).
608. S.-H. Lim, A. G. Caster, and S. R. Leone, *Phys. Rev. A*, **72**, 041803 (2005).
609. J. P. Ogilvie, D. Débarre, X. Solinas, J.-L. Martin, E. Beaurepaire, and M. Joffre, *Opt. Express*, **14**, 759–766 (2006).
610. B. von Vacano and M. Motzkus, *J. Chem. Phys.*, **127**, 144514 (2007).
611. D. Pestov, X. Wang, R. K. Murawski, G. O. Ariunbold, V. A. Sautenkov, and A. V. Sokolov, *J. Opt. Soc. Am. B*, **25**, 768–772 (2008).
612. S. Postma, A. C. W. van Rhijn, J. P. Korterik, P. Gross, J. L. Herek, and H. L. Offerhaus, *Opt. Express*, **16**, 7985–7996 (2008).
613. K. Isobe, A. Suda, M. Tanaka, H. Hashimoto, F. Kannari, H. Kawano, H. Mizuno, A. Miyawaki, and K. Midorikawa, *Opt. Express*, **17**, 11259–11266 (2009).
614. N. Dudovich, D. Oron, and Y. Silberberg, *Phys. Rev. Lett.*, **92**, 103003 (2004).
615. M. Wollenhaupt, M. Krug, J. Köhler, T. Bayer, C. Sarpe-Tudoran, and T. Baumert, *Appl. Phys. B*, **95**, 245–259 (2009).
616. A. Präkelt, M. Wollenhaupt, C. Sarpe-Tudoran, and T. Baumert, *Phys. Rev. A*, **70**, 063407 (2004).
617. H. G. Barros, W. Lozano B., S. S. Vianna, and L. H. Acioli, *Opt. Lett.*, **30**, 3081–3083 (2005).

618. H. G. Barros, J. Ferraz, W. Lozano B., L. H. Acioli, and S. S. Vianna, *Phys. Rev. A*, **74**, 055402 (2006).

619. M. Wollenhaupt, A. Präkelt, C. Sarpe-Tudoran, D. Liese, T. Bayer, and T. Baumert, *Phys. Rev. A*, **73**, 063409 (2006).

620. N. Dudovich, T. Polack, A. Pe'er, and Y. Silberberg, *Phys. Rev. Lett.*, **94**, 083002 (2005).

621. Z. Amitay, A. Gandman, L. Chuntonov, and L. Rybak, *Phys. Rev. Lett.*, **100**, 193002 (2008).

622. H. Ibrahim, M. Héjjas, M. Fushitani, and N. Schwentner, *J. Phys. Chem. A*, **113**, 7439–7450 (2009).

623. Y. Nakamura, Y. A. Pashkin, and J. S. Tsai, *Nature*, **398**, 786–788 (1999).

624. T. Feurer, J. C. Vaughan, and K. A. Nelson, *Science*, **299**, 374–377 (2003).

625. R. Fanciulli, A. M. Weiner, M. M. Dignam, D. Meinhold, and K. Leo, *Phys. Rev. B*, **71**, 153304 (2005).

626. B. Golan, Z. Fradkin, G. Kopnov, D. Oron, and R. Naaman, *J. Chem. Phys.*, **130**, 064705 (2009).

627. S. J. Glaser, T. Schulte-Herbrüggen, M. Sieveking, O. Schedletzky, N. C. Nielsen, O. W. Sørensen, and C. Griesinger, *Science*, **280**, 421–424 (1998).

628. B. Bonnard and M. Chyba, *Singular Trajectories and Their Role in Control Theory*, Springer, Berlin, 2003.

629. R. B. Wu, J. Dominy, T.-S. Ho, and H. Rabitz, arXiv:0907.2354 (2009).

630. M. Lapert, Y. Zhang, M. Braun, S. J. Glaser, and D. Sugny, *Phys. Rev. Lett.*, **104**, 083001 (2010).

631. R. W. Brockett, *Linear Algebra Appl.*, **146**, 79–91 (1991).

632. J. von Neumann, *Tomsk Univ. Rev.*, **1**, 286–300 (1937).

633. A. Pechen, C. Brif, R. B. Wu, R. Chakrabarti, and H. Rabitz, *Phys. Rev. A*, **82**, 030101 (2010).

634. J. Roslund, M. Roth, and H. Rabitz, *Phys. Rev. A*, **74**, 043414 (2006).

635. M. Wollenhaupt, A. Präkelt, C. Sarpe-Tudoran, D. Liese, and T. Baumert, *J. Mod. Opt.*, **52**, 2187–2195 (2005).

636. T. Bayer, M. Wollenhaupt, and T. Baumert, *J. Phys. B At. Mol. Opt. Phys.*, **41**, 074007 (2008).

637. P. Marquetand, P. Nuernberger, G. Vogt, T. Brixner, and V. Engel, *Europhys. Lett.*, **80**, 53001 (2007).

638. C. Brif, R. Chakrabarti, and H. Rabitz, *New J. Phys.*, **12**, 075008 (2010).

639. G. S. Engel, T. R. Calhoun, E. L. Read, T.-K. Ahn, T. Mančal, Y.-C. Cheng, R. E. Blankenship, and G. R. Fleming, *Nature*, **446**, 782–786 (2007).

640. H. Lee, Y.-C. Cheng, and G. R. Fleming, *Science*, **316**, 1462–1465 (2007).

641. I. P. Mercer, Y. C. El-Taha, N. Kajumba, J. P. Marangos, J. W. G. Tisch, M. Gabrielsen, R. J. Cogdell, E. Springate, and E. Turcu, *Phys. Rev. Lett.*, **102**, 057402 (2009).

642. E. Collini, C. Y. Wong, K. E. Wilk, P. M. G. Curmi, P. Brumer, and G. D. Scholes, *Nature*, **463**, 644–647 (2010).

643. G. Panitchayangkoon, D. Hayes, K. A. Fransted, J. R. Caram, E. Harel, J. Wen, R. E. Blankenship, and G. S. Engel, arXiv:1001.5108 (2010).

644. E. Collini and G. D. Scholes, *Science*, **323**, 369–373 (2009).

645. E. Collini and G. D. Scholes, *J. Phys. Chem. A*, **113**, 4223–4241 (2009).

646. Y.-C. Cheng and G. R. Fleming, *Annu. Rev. Phys. Chem.*, **60**, 241–262 (2009).

647. D. Beljonne, C. Curutchet, G. D. Scholes, and R. J. Silbey, *J. Phys. Chem. B*, **113**, 6583–6599 (2009).

648. D. Abramavicius, B. Palmieri, D. V. Voronine, F. Šanda, and S. Mukamel, *Chem. Rev.*, **109**, 2350–2408 (2009).
649. M. Arndt, T. Juffmann, and V. Vedral, *HFSP J.*, **3**, 386–400 (2009).
650. Y.-C. Cheng and G. R. Fleming, *J. Phys. Chem. A*, **112**, 4254–4260 (2008).
651. A. Ishizaki and G. R. Fleming, *Proc. Natl. Acad. Sci. USA*, **106**, 17255–17260 (2009).
652. A. Ishizaki and G. R. Fleming, *J. Chem. Phys.*, **130**, 234110 (2009).
653. A. Ishizaki and G. R. Fleming, *J. Chem. Phys.*, **130**, 234111 (2009).
654. A. Olaya-Castro, C. F. Lee, F. F. Olsen, and N. F. Johnson, *Phys. Rev. B*, **78**, 085115 (2008).
655. Z. G. Yu, M. A. Berding, and H. Wang, *Phys. Rev. E*, **78**, 050902 (2008).
656. S. Jang, Y.-C. Cheng, D. R. Reichman, and J. D. Eaves, *J. Chem. Phys.*, **129**, 101104 (2008).
657. S. Jang, *J. Chem. Phys.*, **131**, 164101 (2009).
658. M. Mohseni, P. Rebentrost, S. Lloyd, and A. Aspuru-Guzik, *J. Chem. Phys.*, **129**, 174106 (2008).
659. P. Rebentrost, M. Mohseni, I. Kassal, S. Lloyd, and A. Aspuru-Guzik, *New J. Phys.*, **11**, 033003 (2009).
660. P. Rebentrost, M. Mohseni, and A. Aspuru-Guzik, *J. Phys. Chem. B*, **113**, 9942–9947 (2009).
661. P. Rebentrost, R. Chakraborty, and A. Aspuru-Guzik, *J. Chem. Phys.*, **131**, 184102 (2009).
662. M. B. Plenio and S. F. Huelga, *New J. Phys.*, **10**, 113019 (2008).
663. F. Caruso, A. W. Chin, A. Datta, S. F. Huelga, and M. B. Plenio, *J. Chem. Phys.*, **131**, 105106 (2009).
664. B. Palmieri, D. Abramavicius, and S. Mukamel, *J. Chem. Phys.*, **130**, 204512 (2009).
665. M. Thorwart, J. Eckel, J. Reina, P. Nalbach, and S. Weiss, *Chem. Phys. Lett.*, **478**, 234–237 (2009).
666. A. Nazir, *Phys. Rev. Lett.*, **103**, 146404 (2009).
667. F. Caruso, A. W. Chin, A. Datta, S. F. Huelga, and M. B. Plenio, arXiv:0912.0122 (2009).
668. K. Brádler, M. M. Wilde, S. Vinjanampathy, and D. B. Uskov, arXiv:0912.5112 (2009).
669. A. Perdomo, L. Vogt, A. Najmaie, and A. Aspuru-Guzik, arXiv:1001.2602 (2010).
670. F. Fassioli and A. Olaya-Castro, arXiv:1003.3610 (2010).
671. Z.-M. Lu and H. Rabitz, *Phys. Rev. A*, **52**, 1961–1967 (1995).
672. Z.-M. Lu and H. Rabitz, *J. Phys. Chem.*, **99**, 13731–13735 (1995).
673. W. S. Zhu and H. Rabitz, *J. Chem. Phys.*, **111**, 472–480 (1999).
674. W. S. Zhu and H. Rabitz, *J. Phys. Chem. A*, **103**, 10187–10193 (1999).
675. C. Brif and H. Rabitz, *J. Phys. B At. Mol. Opt. Phys.*, **33**, L519–L525 (2000).
676. L. Kurtz, H. Rabitz, and R. de Vivie-Riedle, *Phys. Rev. A*, **65**, 032514 (2002).
677. J. M. Geremia and H. Rabitz, *J. Chem. Phys.*, **115**, 8899–8912 (2001).
678. J. M. Geremia and H. A. Rabitz, *Phys. Rev. A*, **70**, 023804 (2004).
679. J. M. Geremia and H. Rabitz, *Phys. Rev. Lett.*, **89**, 263902 (2002).
680. J. M. Geremia and H. Rabitz, *J. Chem. Phys.*, **118**, 5369–5382 (2003).